

Low Magnitude Loading of the Spine:

In-vivo and In-vitro Studies

by

Jack Patrick Callaghan

A thesis

presented to the University of Waterloo

in fulfilment of the degree of

Doctor of Philosophy

in

Kinesiology

Waterloo, Ontario, Canada, 1999

© Jack Patrick Callaghan 1999



National Library
of Canada

Acquisitions and
Bibliographic Services

395 Wellington Street
Ottawa ON K1A 0N4
Canada

Bibliothèque nationale
du Canada

Acquisitions et
services bibliographiques

395, rue Wellington
Ottawa ON K1A 0N4
Canada

Your file Votre référence

Our file Notre référence

The author has granted a non-exclusive licence allowing the National Library of Canada to reproduce, loan, distribute or sell copies of this thesis in microform, paper or electronic formats.

The author retains ownership of the copyright in this thesis. Neither the thesis nor substantial extracts from it may be printed or otherwise reproduced without the author's permission.

L'auteur a accordé une licence non exclusive permettant à la Bibliothèque nationale du Canada de reproduire, prêter, distribuer ou vendre des copies de cette thèse sous la forme de microfiche/film, de reproduction sur papier ou sur format électronique.

L'auteur conserve la propriété du droit d'auteur qui protège cette thèse. Ni la thèse ni des extraits substantiels de celle-ci ne doivent être imprimés ou autrement reproduits sans son autorisation.

0-612-38228-1

The University of Waterloo requires the signatures of all persons using or photocopying this thesis. Please sign below, and give address and date.

ABSTRACT

LOW MAGNITUDE LOADING OF THE SPINE:

IN-VIVO AND IN-VITRO STUDIES

Low magnitude loading on the body has become an important issue with the occurrence of injuries that have been attributed to repetitive loading of tissue at magnitudes of forces and motions that are below the known maximum strength of the tissues in question. The general purpose of this thesis was to explore the in vivo low level static and dynamic loading on the spine and determine if these loading parameters could generate injuries when similar low magnitude parameters were tested in vitro. In vivo activities (walking, sitting, standing, and back extensor exercises) were examined to quantify the magnitude of low back joint loads, motions, and muscular activations levels required. In vitro highly repetitive loading was performed at modest flexion/extension moments or angular rotations combined with low magnitude axial compressive forces.

Walking was found to be a highly dynamic/cyclic activity with moderate spine loads and small lumbar spine angular motions. The back extensor exercises produced a range of joint loads from low loads for exercises such as single leg extension to loads exceeding spinal compression limits for contraindicated trunk extension exercises. Sitting and standing both resulted in low magnitude joint forces and muscular activity levels. Standing exhibited very small and static ranges of spine postures whereas sitting resulted in a range of postures from 30% to 80% of the lumbar spines flexion range of motion.

The in vitro highly repetitive testing of porcine cervical spine motion segments at low magnitude compressive loads and modest flexion/extension motions and moments resulted in

intervertebral disc herniations. The angular stiffness of specimens increased throughout the testing cycle and increased magnitudes of axial compressive loads resulted in increased probability and severity of disc damage.

This research documents the magnitude of lumbar spine joint forces, spinal motions, and muscular activation levels during common in vivo activities and demonstrates that low level repetitive loading scenarios can result in spinal injuries.

ACKNOWLEDGEMENTS

I wish to thank my supervisor, mentor, and friend, Stuart M. McGill Ph.D. for freely giving of his time and ideas. I appreciated the professional and personal guidance he provided as well as an unsurpassed enthusiasm for his work.

I thank my committee members Dr. J. Medley, Dr. R.W. Norman, and Dr. R.P. Wells. I would also like to thank my external member Dr. I. A. F. Stokes for attending my defense and for his encouraging words.

I would like to acknowledge the Natural Sciences and Engineering Research Council of Canada for funding the Spine laboratory where these studies took place. I would also like to recognize the Ontario Graduate Scholarship that helped to fund my Ph.D. studies.

Help from the following people was greatly appreciated for various aspects of producing the papers in this thesis: Cathy Silcher, Shirley Rietdyk, and Milad Ishac for the paper examining gait; Brenda R. Santos for assistance with the sitting study; Jennifer L. Gunning who played a large role in the back exercise study; Jim Baleshta's aid on the test apparatus design for the in vitro repetitive loading study; finally, to Wendell Prime who was both a friend and constant source of information.

To my parents, Bill and Lois Callaghan, I want to thank you for all of the support and love you have given me through a long educational adventure. It was reassuring to know you always believed in me.

Two of the many friends who I worked, played, and consoled with deserve special recognition. Vanessa you made me laugh at times when I didn't think I had it in me. Dave, one of the best things that happened at Waterloo was developing such a strong and supportive

friendship with you. You both were willing to listen and not judge, and were both there when I really needed a friend - Thank you!

Finally I would like to thank my best friend and love, Lisa Brereton. You have given more than you ever asked. Your smile lifts my heart, your energy is infectious, and your never ending optimism is endearing. You enabled me to see the light when it was darkest.

DEDICATION

To Family and Friends

No distance of place or lapse of time can lessen the friendship
of those who are thoroughly persuaded of each other's worth.

--Robert Southey

TABLE OF CONTENTS

ABSTRACT	iv
ACKNOWLEDGEMENTS	vi
DEDICATION	viii
LIST OF TABLES	xii
LIST OF ILLUSTRATIONS	xiii
Reader's Guide to this Thesis	1

Chapter I

Introduction	3
MAJOR PHILOSOPHICAL ISSUES RELATED TO THIS BODY OF WORK, SUPPORTING EVIDENCE, AND THEIR PRACTICAL IMPLICATIONS .	6
OVERVIEW OF GENERAL IN-VIVO METHODS	16
Electromyography	16
Lumbar Spine Kinematics	17
Modeling Techniques	18

Chapter II

Low Back Three-Dimensional Joint Forces, Kinematics, and Kinetics During Walking	22
ABSTRACT	22
INTRODUCTION	24
METHODS	27
Participants	27
Instrumentation	27
Data Collection	29
Data Processing	30
RESULTS	32
Forces and Moments	33
Lumbar Kinematics	40
Trunk EMG	43
Arm Swing Effects	47
DISCUSSION	47

Chapter III

Low Back Joint Loading and Kinematics During Standing and Unsupported Sitting	55
ABSTRACT	55
INTRODUCTION	56
METHODS	58
Participants	58
Instrumentation	58
Data Collection/Reduction	60
RESULTS	62
DISCUSSION	70
CONCLUSIONS	73

Chapter IV

The Relationship Between Lumbar Spine Load and Muscular Activity During Extensor Exercise	74
ABSTRACT	74
INTRODUCTION	75
METHODS	77
Participants	77
Instrumentation	77
Data Collection	79
Data Reduction:	80
RESULTS	86
DISCUSSION	91
CONCLUSION	93

Chapter V

Studies on Disc Damage from Highly Repetitive Flexion/Extension Motions with Compressive Force	94
ABSTRACT	94
INTRODUCTION	96
MATERIALS AND METHODS	99
RESULTS	105
DISCUSSION	113

Chapter VI

Summary	119
---------------	-----

APPENDIX A

The Porcine Cervical Spine as a Model of the Human Lumbar Spine:	
An Anatomical, Geometrical and Functional Comparison	124
ABSTRACT	124
INTRODUCTION	125
Geometrical Measurements	127
Mechanical Properties	129
RESULTS	131
DISCUSSION	140

APPENDIX B

Analysis of the loads transferred loads to the spinal motion segment during in vitro testing	145
REFERENCES	152

LIST OF TABLES

Table 2.1:	Anthropometric measurements and normal walking cadence of the 5 participants.	27
Table 2.2:	Minimum and maximum joint forces (L4/5), calculated using an EMG driven model, for five participants at three walking speeds and two arm conditions. Forces are normalized to percent body weight ((Joint Force/body weight)*100)	35
Table 2.3:	Joint reaction force, normalized to percent body weight ((Joint Force/body weight)*100), minimums and maximums calculated using an inverse rigid link model.	36
Table 2.4:	Joint moments at L4/5 (minimum and maximum) for all five participants and six conditions (3 walking speeds by 2 arm conditions). The moments are normalized to percent of the product of body weight and height (Joint Moment / (body weight * height))*100.	39
Table 2.5:	Minimum and maximums of lumbar spine motion (degrees) for the three walking speeds and two arm conditions. The measures are expressed relative to a normal upright standing posture.	42
Table 2.6:	Peak activation levels for each of the seven surface EMG sites. The activation has been normalized to maximum voluntary contraction (%MVC).	46
Table 3.1:	Mean and one standard deviation of peak lumbar spine flexion range of motion tests (n =8) expressed as a percent of the initial test (test 1).	63
Table 3.2:	Muscle and ligament forces from the EMG driven model for subject 1 in standing trial 1 and sitting posture 2 (62% of lumbar spine flexion) and each fascicles active and passive contribution to joint compression and shear.	68
Table 4.1:	Mean activation (SD) levels of the 14 EMG channels for the thirteen participants expressed as a percentage of MVC (100%).	88
Table 5.1:	Specimen Data means (and 1 standard deviation). Rotational measures used the following convention: positive values indicate flexion, negative values indicate extension.	109
Table 6.1:	A comparison of the compressive forces and flexion angles used for the in-vitro testing with the magnitudes that were calculated from the in-vivo studies of this thesis.	121
Table A.1:	Human - Porcine comparison of vertebral body dimensions, mean (sd)	132
Table A.2:	Comparison of upper endplate area (UEA) and lower endplate area (LEA) using both the formula of an ellipse and simograph, mean (sd).	133
Table A.3:	Human - Porcine comparison of the posterior elements and the spinal canal dimensions, mean (sd).	135
Table A.4:	Comparison of the mechanical properties of the human and porcine motion segments under shear loading, mean (sd)	136
Table A.5:	Comparison of the mechanical properties of the human and porcine motion segments under compressive loading, mean (sd)	138

LIST OF ILLUSTRATIONS

Figure 2.1:	Joint forces at L4/L5 (normalized to percent body weight) for one participant for three walking cadences with normal arm swing. The curves are normalized for one stride (RHC to RHC) with toe off occurring at 61% (fast),63% (normal), and 65% (slow) of stride. 1a Joint compression force at L4/L5. 1b Net Anterior posterior joint shear force with positive indicating forward shear of the trunk with respect to the pelvis. 1c Net lateral joint shear force with a positive value indicating right shear of the trunk with respect to the pelvis. 34	34
Figure 2.2:	Joint moments at L4/L5 (normalized to percent body weight * height) calculated using an EMG driven model for one participant for three walking cadences with normal arm swing. The curves are normalized for one stride (RHC to RHC) with toe off occurring at 62% (fast),64% (normal), and 65% (slow) of stride. 1a Joint flexion extension moment. 1b Lateral bend moment. 1c Axial twist moment. 38	38
Figure 2.3:	Relative lumbar spine motion with respect to the pelvis. The ensembled data for one participant for three walking cadences with normal arm swing are shown. The curves are normalized for one stride (RHC to RHC) with toe off occurring at 61% (fast),63% (normal), and 65% (slow) of stride. 1a Lumbar spine flexion extension, positive indicates an extension of the trunk with respect to the pelvis. 1b Lateral bend of the trunk with respect to the pelvis. A positive value indicates right lateral bend of the trunk with respect to the pelvis. 1c Positive axial twist movement was defined as left twisting of the trunk with respect to the pelvis. 41	41
Figure 2.4:	The fourteen EMG channels used for the gait analysis. Ensembled data for one participant for three walking cadences with normal arm swing are shown. The right (R-) data was the collected signals with the left (L-) channels being calculated based on symmetrical gait. The curves are normalized for one stride (RHC to RHC) with toe off occurring at 61% (fast),63% (normal), and 65% (slow) of stride. The seven channels recorded were: rectus abdominis (RA), external oblique (EO), internal oblique (IO), latissimus dorsi (LD), thoracic erector spinae (TES), lumbar erector spinae (LES), and multifidus (MULT). 45	45
Figure 3.1:	The time line of the testing protocol for the 8 subjects. The sitting period was for 2 hours with the standing prior to and following sitting having a duration of 3 minutes. The lumbar spine range of motion tests (ROM) were completed before and after every major task. 60	60
Figure 3.2:	An APDF of a static lumbar spine posture adopted by one subject for the duration of a 2 hour period of sitting. 64	64
Figure 3.3:	An APDF of one subject who adopted "dynamic" lumbar spine postures that varied over a wide range for the 2 hour period of sitting. There are 3 clear postures in which the individual equally divided the sitting period. 64	64

Figure 3.4:	Mean and ± 1 SD (n = 8) of the postures assumed during the sitting and standing tasks.	65
Figure 3.5:	The L4/L5 joint compression forces calculated using a three-dimensional EMG driven model for the primary postures adopted while sitting. A representative posture/s for each subject (numbered 1 through 8) was selected based on the APDF of their lumbar spine kinematics.	67
Figure 3.6:	Low back joint compression forces (L4/L5) calculated during 3 minutes of standing before and after sitting for 2 hours.	67
Figure 3.7:	Average muscle activation APDFs across 8 subjects for the 2 hour sitting period and the 2 standing periods. (RUES: Right Upper Erector Spinae; RLES: Right Lower Erector Spinae; LUES: Left Upper Erector Spinae; LLES: Left Lower Erector Spinae).	69
Figure 4.1:	Exercise one and two involved extension of the leg to horizontal. The exercise was performed for both legs (Right Leg (RL) and Left Leg (LL)). The posture shown was chosen as representing the most challenging instant.	81
Figure 4.2:	Extension of the contralateral arm combined with leg extension constituted exercises three and four. The posture shown was used to represent the instant of peak loading. Both sides of the body were exercised (Right Leg - Left Arm (RL&LA) and Left Leg - Right Arm (LL&RA)).	81
Figure 4.3:	Active trunk extension combined with leg extension was the fifth exercise (T&L). The exercise was initiated from a prone posture on the floor, the participants performed active trunk and leg extension (maximum comfortable) and returned to the prone position.	82
Figure 4.4:	Exercise six involved a large range of motion. The start position was a fully flexed posture, followed by active extension until the trunk was horizontal to the ground (T), which corresponded to the peak loading posture (shown here). . .	82
Figure 4.5:	EMG model predictions of joint compression, mean and standard deviation for all trials and across all participants.	87
Figure 4.6:	Anterior - posterior joint shear forces (mean and standard deviation) calculated by the EMG driven model. A positive shear value indicates a net anterior shear of the trunk with respect to the pelvis.	89
Figure 4.7:	Mean and standard deviation of medial - lateral joint shear forces from the EMG driven model. A positive value indicates the trunk is shearing to the participants right with respect to the pelvis.	89
Figure 4.8:	Lumbar sagittal plane spine posture (mean and one standard deviation) for all participants in the peak load position. A positive posture indicates trunk (T12 level) extension with respect to the sacrum, a negative represents lumbar spine flexion.	90
Figure 5.1:	Frontal (a) and sagittal (b) views of the test apparatus used to apply coupled axial compressive load and pure flexion moments to produce repeated flexion extension motions. The X-Y table permitted translations as opposed to artificially constraining each end.	101

Figure 5.2:	Range of motion test for one specimen tested with a compressive load of 260N. The point where the curve deviates from the superimposed line (arrow) indicates either the torque or angular position employed for the repeated dynamic test. 102
Figure 5.3:	An x-ray for one specimen prior to (a) and following (b) repeated testing. The arrow indicates the posterior tracking of the radio-opaque dye indicating a herniation. 106
Figure 5.4:	a) The posterior extrusion of blue dye was evident when the neural arch was removed. b) A transverse section through the intervertebral disc reveals the posterior herniation as well as delamination of the annulus. c) An intervertebral disc from the 267N group loaded for 86,400 cycles with the nucleus pulposus still intact. 107
Figure 5.5:	The total range (flexion peak - extension peak) of the angular position and torque control groups. Beginning versus end comparisons were significant for both torque and angular positional control ($P < 0.0001$). Comparisons of axial compressive load that were different within each control method ($P < 0.05$) are indicated with the same symbol. 110
Figure 5.6:	Time series for two specimens. Upper) Torque control specimen loaded at +11 and -5 N*m with a compressive load of 1472N showing the decreased angular rotations with a constant torque application. Lower) Angular positional control specimen loaded at +14° and -2.5° with a compressive load of 1472N showing the increased torque required to maintain the same angular rotations. 111
Figure 5.7:	Mean rotational stiffness (+ 1SD). Beginning versus end comparisons were significant for both torque and angular positional control ($P < 0.0001$). Comparisons of axial compressive load that were different within each control method ($P < 0.05$) are indicated with the same symbol. 111
Figure 5.8:	The flexion and extension moments from the range of motion test. Only the pre-post comparison of extension moments within angular positional control were significant ($P < 0.014$). Comparisons of axial compressive load that were different within each control method ($P < 0.05$) are indicated with the same symbol. 112
Figure A.1:	Schematic top and side view of a human lumbar vertebra illustrating the measured parameters: width and depth of both upper and lower endplates (UEW, LEW, UED, LED, pedicle width (PEDW), pars height (PH), spinal canal depth and width (SCD, SCW), and the sagittal (SA) and transverse (TA) facet angles. 128
Figure A.2.:	Angle measurement gimbal with three angular degrees of freedom and measurement. 129
Figure A.3:	Top view of a human lumbar vertebra and a porcine cervical vertebra (with anterior processes removed). 133
Figure A.4:	Porcine endplate fracture resulting from compressive loading. 137
Figure A.5:	The quadruped porcine must support the cantilevered head with an extensor moment creating approximately 126 N. of compressive load. 140

Figure A.6: Compressive and shear injuries resulting from *in vitro* testing of porcine vertebrae. 138

Figure A.7: Pars interarticularis injury resulting from *in vitro* shear loading of a porcine vertebra. 136

Figure B.1: The spherical seat of the flexion/extension jig used in the repeated *in vitro* testing. Points a and b were the roller bearing which only transmitted normal forces. Fa was the compressive force applied by the Instron test frame. The lower vertebra was mounted to a cup which freely translated on an X-Y table. 146

Figure B.2: Decomposition of the normal forces on the roller bearings into x and y components. 147

Figure B.3: Rotation of the specimen by 20° to demonstrate the invariable relationship between the axial applied compressive force and the force transmitted at point c. 148

Figure B.4: The forces experienced by the motion segment. 149

Reader's Guide to this Thesis

This thesis is a collection of papers (Chapters II-V). The major theme of this thesis was to evaluate low magnitude loading of the spine, and determine if it was a possible mechanism of injury. The introduction includes a brief background of the issues that laid the foundation for this thesis and the general purpose. To facilitate interpretation and implementation of these findings, the introduction also includes a section discussing the limitations and major philosophical issues associated with the work in this thesis. Three of the studies (Chapter II-IV) shared a common methodology. For this reason, an overview of the general methodology has been described at the end of the introduction. The final chapter (Chapter VI) provides an overview and integration of the main findings of each study. The major contribution of each study is also highlighted in the summary. The specific role of each chapter is as follows:

- Chapter I Introduction of the rationale and underlying issues for examining low magnitude prolonged loading of the spine. This chapter also includes a philosophical overview of the major issues associated with this thesis and the pertinent findings. A general in-vivo methodology is also presented which is common to the three in-vivo studies (Chapters II through IV)
- Chapter II Low back loading, muscular activity levels, and lumbar spinal motions during

gait. Three walking cadences were examined as well as the contribution of arm swing.

- Chapter III The analysis of postures and low back loading present during prolonged sitting. This study examined sitting and standing with attention to the time varying modifications present. The magnitude of joint loading, muscular activation levels, and lumbar spine postures were examined for a 2 hour sitting period and two 5 minute standing periods.
- Chapter IV Muscular activation levels, spinal postures, and low back loading present in low back exercises. Typically performed exercises were examined using pain free individuals were examined.
- Chapter V In-vitro load time properties of repeated motions and loads of porcine spinal motion segments. This study examined the interaction of flexion/extension motion, magnitude of compressive load, and angular position versus torque control of specimens on the damage to spinal motion segments, in particular the intervertebral disc, that were cyclically loaded.
- Chapter VI A summary and integration of the major findings from the work presented in this thesis.

Chapter I

Introduction

Most in-vitro spine testing studies aimed at understanding low back pain or injury have examined acute injury mechanisms or the maximum loads which cause spinal fractures. This mode of loading is one very viable mechanism of injury or tissue damage. However, given increasing workplace ergonomic evaluations and increasing awareness of risk of injury from lifting large loads, the exposure to these large loads should occur infrequently. Potvin et al. (1991) calculated a joint force of 4400 N for a 14 kg lift. If this task was performed occasionally, when compared to a conservative estimate of compressive tolerance of approximately 6000 N from in-vitro testing (Genaidy, Waly, Khalil, & Hidalgo. 1993; Jager, Luttmann, & Laurig. 1991) or used by the National Institute Of Safety and Health (NIOSH) there is still a substantial margin of safety. It has been shown that workers or athletes that lift large loads (Cholewicki, McGill, & Norman. 1991) can generate joint loads that surpass even the largest reported in-vitro ultimate strength values (Porter, Adams, & Hutton. 1989; Jager, Luttmann, & Laurig. 1991). However, even these individuals were not injured from a single load exposure. Yet, paradoxically, with increased protection for workers from lifting large loads, there is still a very large percentage (70% (Zdeblick. 1995)) of the population that

reports or experiences back pain at some point in their life. In Canada last reported statistics revealed that there were a total of 10 million back pain absence days a year (Pope, Andersson, & Chaffin. 1991). Examination of cadaveric material has revealed damage to the vertebral trabecular structure. In 22 human cadaver lumbar spines examined (Vernon-Roberts & Pirie. 1973), all had trabecular lesions adjacent to the end-plate. Additionally, damage to the annulus and cartilaginous end-plate was found in 51% of 88 cadaver discs (Tanaka, Nakahara, & Inoue. 1993) from the lumbar 4/5 joint and in 47% of the joints examined from 24 lumbar cadaveric spines (Gunzburg, Parkinson, Moore, et al. 1992). Examining the lumbar spines of 182 cadavers (Farfan, Huberdeau, & Dubow. 1972) revealed that 77% of the lumbosacral joints had annular tears and 77% of the lumbar 3/4 joints had Schmorl's nodes. Clearly there is a large prevalence of injury to the lumbar spine sustained during one's life.

Repeated and prolonged loading have been identified as risk factors for developing low back pain (LBP). Calculated cumulative loading of the lumbar spine in institutional aides (Kumar. 1990) and workers in an automotive assembly plant (Norman, Wells, Neumann, et al. 1998) has been shown to be higher in individuals with LBP. High risk jobs were detected by a model (Marras, Lavender, Leurgans, et al. 1993) that included: trunk velocities; lifting frequency; sagittal angle (flexion); and load moment. The high risk jobs were those that had a high occurrence of LBP reports. Low back pain individuals (cases) were compared to controls (random workers from the same automobile assembly plant) (Punnett, Fine, Keyserling, Herrin, & Chaffin. 1991). Cases were determined to have greater repetition and longer time spent in flexed postures as well as multiple postures. Videman et al. (1990) examined 86 cadavers and linked spine pathologies (end-plate defects, osteophytosis of the vertebral body, facet joint

osteoarthritis, annular ruptures, symmetric disc degeneration) to type of work, level of physical activity, and history of back pain. Driving (repeated loading in a static posture), sedentary work (static postures) and heavy work (repeated heavy lifting) were occupational activities that had increased occurrence of spine pathologies. In addition the individuals that had experienced back pain were also associated with an increased incidence of spine pathology, in essence linking spine trauma to pain. Clearly exposure to static postures and/or repeated loading results in spine pathology which has been linked to LBP.

Currently, repetitive and static postures/loads are identified as risk factors for developing work related musculoskeletal disorders (Hagberg, Silverstein, Wells, et al. 1995). However, there are few values reported to quantify exposure values for repetitive or prolonged loading. Static loading has been approached by primarily looking at muscular fatigue. Jonsson (1978) suggested that static muscle contractions for continuous work should not exceed 2% to 5% of maximum voluntary contraction (MVC). While muscular fatigue is an important mechanism of potential injury, damage to the bone or passive tissues of the spine will result in injuries that are much slower to repair and experience remodeling mechanisms. There has been little work done that attempts to determine a load time integral for either repetitive loading or sustained static loading of the spine.

Ideally, repetitive and static loading of the spine could be analyzed using a mathematical model to assess the potential for injury based on the number of cycles applied, time spent in a static posture, range of motion (at the spinal level) required by a task, and the load on the lumbar spine. The first step in developing such a model requires the examination of the in vivo loads and postures experienced by the low back for both dynamic and static

activities. These parameters can then be examined in vitro to determine their potential for generating spinal injuries. Therefore, the general purpose of this thesis was to assess low level static and dynamic loading on the spine.

In order to achieve this objective, two major areas needed to be examined, resulting in several papers (chapters). First, the loading on the lumbar spine was assessed in vivo for tasks that were considered to consist of low loading and risk of injury of the lumbar spine. Tasks that were considered primarily static and/or dynamic were examined. The tasks examined were: Walking, Standing, Sitting, and Low Back Extensor Exercises. Second, porcine cervical spine motion segments were used as a model of the human lumbar spine for in vitro testing. Highly repetitive tasks were analyzed with low magnitude moments, flexion/extension motions, and compressive forces to determine if these loading scenarios were a potential mechanism of intervertebral disc injury.

MAJOR PHILOSOPHICAL ISSUES RELATED TO THIS BODY OF WORK, SUPPORTING EVIDENCE, AND THEIR PRACTICAL IMPLICATIONS

This thesis was aimed at developing an understanding of the tissue loading that results during repeated and prolonged low-magnitude loads. These low level loads were applied to in-vitro porcine cervical spine specimens to enhance an understanding of their potential injurious effects. This body of work, unified around the theme of low level loading, is linked to several philosophical issues, which both form a rationale and also have implications on direct application of the findings. Several of these issues are discussed here under the heading starting each section.

Too much of any one thing leads to injury.

While this statement may seem infinitely obvious, this notion is rarely observed in practice. Industrial ergonomics has not yet embraced the ideology that not all jobs need to be made less demanding, or that some jobs need much more variety in the patterns of musculoskeletal loading. For example, textbooks still define a "best posture" for sitting. It has been accepted for many years that too great a load placed on a tissue will result in injury. Epidemiological studies (Hilkka, Mattsson, Zitting, Wickstrom, Hanninen, & Waris. 1990; Marras, Lavender, Leurgans, et al. 1993; Norman, Wells, Neumann, et al. 1998; Videman, Nurminen, & Troup. 1990) have supported this notion, identifying peak loading measures (i.e., shear, compression, trunk velocity, extensor moment, heavy work, etc.) as factors that explain the frequency and distribution of reporting of back pain or increased risk of back injury. However, not only peak or single exposures are responsible for back pain and injury. Too many repetitions of force and motion, and/or prolonged postures and loads have also been indicated as potential injury or pain causing mechanisms. There has also been epidemiological investigation of these injury mechanisms. Cumulative loading (i.e., compression, shear, or extensor moment) has been identified as a factor in the reporting of back pain (Kumar. 1990; Norman, Wells, Neumann, et al. 1998). Additionally, cumulative exposure to unchanging work has been linked to reporting of low back pain (Holmes, Hukins, & Freemont. 1993) and intervertebral disc injury (Videman, Nurminen, & Troup. 1990). The experiments designed in this study were intended to sample some of these activities to define some of the lumbar spine postures, muscular activation levels, and resulting spine joint loads. However, it is not as simple as only documenting the effects of a single activity, but rather how these activities are

sequenced. This information could then be used to solve the real world injury problem.

Nonetheless, the data presented here show the differences in motion patterns, muscle activation levels, and spinal loading that occurs during different activities to suggest better sequencing of tasks. What this really means is that the order and type of loading should be considered and the demand on tissues should be varied.

What causes injury too much load or too much bending?

The most recognizable guidelines for reducing risk of injury are based on too much load. Should bending be a consideration? A major contribution of this work was to consistently produce intervertebral disc herniations. Producing these herniations turned out to be a function of repetitive bending rather than a repetitive compressive load which appears to simply be a modulator of injury. Further evidence of this issue comes from the walking data which demonstrated repeated compressive loading of a magnitude that should eventually cause damage. In endurance walking events, participants would easily accumulate the number of cycles (86,400) produced intervertebral disc herniations in the in-vitro study presented here (Chapter 5). However, since the primary intervertebral disc damaging mechanism appears to be bending, and the lumbar spine flexion/extension motions that resulted from walking were not sufficient to reach that threshold level. This explains why some people can accumulate a large number of loading/motion cycles on the spine, such as during endurance walking, and remain uninjured. It would also seem justifiable to begin the establishment of guidelines regulating the number of bending cycles, rest schedules, etc.

Perhaps a precursor or even root cause of low back pain is due to a virus or altered geometry.

It has been suggested that the incidence of some musculoskeletal disorders of the upper extremity are elevated following exposure to a viral infection. Could this also be responsible for low back disorders? In addressing this kind of concern, careful scientific control was exercised in the study. Source animals are screened for disease with only approved specimens being used for testing. A study of the geometrical properties was conducted (Appendix A) which demonstrated the small variations within the controlled animal population used for the in-vitro testing. There was no evidence to contradict that the intervertebral disc damage that resulted from in-vitro mechanical testing (Chapter 5) was a direct result of the variable being manipulated (repetitive flexion/extension motions or magnitude of compressive load). Viral infections have been linked to increasing the probability of developing such diseases as carpal tunnel syndrome or arthritis (Mody & Cassim. 1997; Phillips. 1997; Samii, Cassinotti, de Freudenreich, Gallopin, Le Fort, & Stalder. 1996). However, work related factors were found to account for the majority of the causes attributed to developing carpal tunnel syndrome (Rossignol, Stock, Patry, & Armstrong. 1997). The work performed in this thesis strongly suggests that mechanical loading in isolation can be the sole cause of intervertebral disc herniation. This damage has potential to cause pain based on evidence that the outer annulus is innervated with pain sensing nerve endings (Cavanaugh. 1995). The potential for pain would be dependent on the location of herniation as the lateral margins have less innervation than the dorsal region, as well the fibrocartilaginous end plates, nucleus pulposus, and inner regions of the intervertebral disc have no pain sensing nerve endings (Cavanaugh, Kallakuri, & Özakay.

1995). The specimens tested in this study tended to herniate in a posterolateral location which would be in an area with pain sensing nerve endings, however, not as many as are present in the posterior aspect (Cavanaugh, Kallakuri, & Özaktay. 1995). This could explain the why some individuals suffer no back pain and others suffer low back pain due to intervertebral disc herniation. In summary, the work of this thesis has demonstrated a mechanical cause for disc herniation. However, future research should examine the issues of individual variability and moderating factors such as viral infections on the developing of a low back injury.

What type of loading causes spinal injury versus what is helpful? Searching for the healthy optimum.

Increased levels of motion have been shown to be beneficial in providing nutrition to the structures of the intervertebral disc (Holm & Nachemson. 1983). In contrast, the research presented here has demonstrated that too many motion cycles resulted in intervertebral disc herniation. Intervertebral disc degeneration has been associated with decreased nutrition (Buckwalter. 1995). Too little motion resulting from sedentary work has been shown to result in intervertebral disc injury (Videman, Nurminen, & Troup. 1990). While workers that performed heavy work were also at increased risk of developing a spinal injury (Videman, Nurminen, & Troup. 1990). Workers that were involved in vary types of work, mixed work, had the lowest risk of developing a spine injury (Videman, Nurminen, & Troup. 1990). This presents the idea that too little motion or load or too much can both present a risk of spinal injury. In contrast, Hadler (1997) claims that there has been no reduction in the incidence of back injury over the past 25 years, even after increased research and resources have been

dedicated to the area over that time frame, and suggests that the focus should be turned from biomechanical causes of injury to developing more "comfortable" workplaces. However, the in-vitro component of this thesis (Chapter 5) has clearly shown that too many flexion/extension bending cycles will lead to injury. This potential for injury was compounded when the magnitude of compression was increased. This collective work provides information on the loads present in common components of work and everyday living which can be used to provide a mix of loading and motion profiles. The presence of a "U" shaped risk of injury curve, too much or too little resulting in increased risk of injury, has been demonstrated by this work. There are two types of evidence to explain the risk of developing low back pain and/or injury: epidemiological and those that define biological pathways (etiologial). The epidemiological evidence has been presented above (Too much of any one thing leads to injury). This work demonstrated that mechanical loading (repetitive flexion/extension motions) is a viable biological pathway for developing intervertebral disc herniations.

A Methodological Concern: Position (angular rotation) control versus torque control.

Purposeful creation of intervertebral disc herniation has, up until now, been rarely achieved and only then, through contrived methods. This work defines a specific scenario to consistently replicate intervertebral disc herniations using motions and loads that are representative of daily loading. The use of positional versus load control has been hotly debated for years (Goel, Wilder, Pope, & Edwards. 1995). The question at the heart of this methodological issue is which method more closely replicates in-vivo loading. The use of position control in the in-vitro study increased the probability of producing an intervertebral

disc herniation and resulted in more severe disc herniations (nuclear extrusion). It has been shown that spine flexion increased through the progression of a repeated lifting task (Potvin & Norman. 1992). Increased spinal flexion is thought to be a response to fatigue. As a worker becomes fatigued, they will tend to stop using a squat lifting posture, which has higher metabolic cost, and start using a stoop posture. This would expose the spine to increased force and moment magnitudes as well as increased angular rotations. However, when more experienced lifters were examined trunk flexion angles were found to decrease over a five hour lifting session and hip flexion angles increased (Marras & Granata. 1997). This would result in decreased spine rotations, forces, and extensor moments. This would be in agreement with the finding of this work, that specimens loaded under torque control became more stiffer. The torque required to bend to the same position would be increased so one potential mechanism for compensating would be increasing hip flexion. Both torque control and angular position control loading exposed the in-vitro specimen to a constant magnitude of the controlled variable for repeated testing. In-vivo the moments on the spine and angular rotations would covary. Specimens tested under torque control demonstrated decreased angular rotations as testing progressed (increased angular stiffness). Conversely, specimens loaded using positional control required increased torques to achieve the same angular rotation as testing progressed (increased angular stiffness). Torque control proved to be less damaging and would be more representative of the results found by Marras and Granata (1997) and would better represent any protective mechanism that could be present in the body due to increased joint rotational stiffness. The increased torques exerted on a specimen when tested in angular positional control would represent the data found by Potvin and Norman (1992) and would be more

representative of any other fatigue mechanism that resulted in increased moments or angular rotations. Regardless of the control method used, the same changes (i.e.. increases in rotational stiffness) were found for all test groups.

The in-vitro testing incorporated an animal model. What are the limitations and benefits of this model for human applications?

Why use a porcine cervical spine in lieu of a human lumbar spine? Human cadaveric material has provided a wealth of information in the area of spine injury. However, there are many questions in spine research for which human specimens are not suitable. Young, healthy, human spines are extremely rare as typically donors are elderly and sick or were obtained from younger donors who were either sick or sustained substantial violent trauma. This is an important issue as failure patterns in the spine are a function of biological age, for example older degenerated discs will be less susceptible to herniation (Adams & Hutton, 1982) rendering them unsuitable to investigate herniation mechanics. The unavailability of young, healthy, matched human specimens is a reality. Porcine cervical spines present a healthy homogeneous sample of specimens, specifically providing scientific control over genetic make-up, age, weight, physical activity levels and diet. While controlled experiments are only possible using an animal model, the obvious liability is that of relevance for application to human mechanics and orthopaedics; a complete comparison between the geometrical, anatomical, and functional aspects of the porcine cervical spine and human lumbar spine are included in Appendix A. The average bending moment (156 N*m) and flexion angle (20°) (Osvalder, Neumann, Lovsund, & Nordwall, 1990) at failure of human motion segments were

far stiffer than the porcine motion segments used in this study (61 N*m and 39° for one specimen). However, the majority of human specimens tested have been from old, degenerated, stiffer cadavers. Perhaps older pig cervical spines would behave in the same manner. While porcines are quadrupeds, supporting the weight of the head and additional loads imposed by muscular activity required to leverage the head result in substantial compressive loads on the porcine cervical spine. This load bearing appears to be quite analogous to the human lumbar spine. In summary, both geometrically and functionally one can argue support for the porcine cervical spine. Additionally, the use of an animal model provides the advantage of a controlled cohort to study.

Is the number of in-vitro load cycles representative of the real world?

Normal walking cadence is approximately 100 steps/minute. If it is assumed that a person walks for one hour each day it would take about two weeks to accumulate the 86,400 cycles employed in this study. Punnett et al. (1991) reported dynamic movements as high as 18.5 per minute. At this rate it would only take about 10 working days to reach 86,400 cycles. A more conservative estimate of workplace flexion/extension tasks would be between 3 and 6 motions per minute (Brinckmann, Biggemann, & Hilweg. 1988) which would require a period 2 to 3 weeks to accumulate 86,400 cycles. One major limitation of all in-vitro testing is that it uses material that is no longer living, adapting tissue. The intervertebral disc is an avascular structure that relies on nutrient transport through the vertebral end plate or annulus. Micro fractures to bone have been shown to take approximately two weeks to heal (Brinckmann, Biggemann, & Hilweg. 1988). Proteoglycan turnover takes about 500 days (Urban, Holm, &

Maroudas. 1978) and collagen production even longer (Adams & Hutton. 1982). Therefore, any repair mechanisms to the disk could be outpaced by any of the examples of in-vivo loading presented above. However, rest, other activities, and redistribution of stresses in the intervertebral disc are important mediating factors that could prevent or delay injury. Therefore, it could take years for a herniation to occur, but once an injury has initiated the injury is cumulative in nature until the culminating event of disc herniation. The major strength of this study was the clear definition of a mechanism of intervertebral disc herniation. It is now clear that further work is needed to define the effects of adaption and rest on further tissue degradation. A link will need to be established to specific exposures in the workplace and everyday activities. A more precise documentation of the number of cycles to initiation of intervertebral disc injury and herniation will need to be determined in-vitro. The definition of a safe number of loading cycles is difficult to obtain due to factors such as biological variability. While in-vitro testing is not the ideal situation, the work here provides a first step toward defining a value to limit exposure to repetitive tasks.

Is the rigid link segment model typically used to examine human walking suitable for examining 3-dimensional resultant spine moments and forces?

Rigid link segment modeling has been used for years in gait for analyses from the ground up to the level of the hip joint. The trunk has typically been considered as one segment. It would appear from the work in the gait part of this thesis (Chapter 2) that the answer to this question is "no". Heel strike, which has been shown to contain components up to 50-60 Hz simply doesn't propagate to the lumbar region as is artificially done with rigid link segment

models. While it was not the focus of this thesis to fully address this question, it certainly appears that some reevaluation of the suitability of the rigid link segment assumption is required.

OVERVIEW OF GENERAL IN-VIVO METHODS

Methods used throughout the chapters that follow (II-IV) have been summarized in detail here for the interested reader.

Electromyography

Seven pairs of disposable Medi-Trace surface electromyogram (EMG) electrodes (Ag-AgCl) (Graphic Controls Canada Ltd, 215 Herbert St, Gananoque, Ontario, Canada, K7G 2Y7) were applied to the skin: rectus abdominis, 3 cm lateral to the umbilicus; external oblique, approximately 15 cm lateral to the umbilicus; internal oblique below the external oblique electrodes just superior to the inguinal ligament; latissimus dorsi, lateral to T9 over the muscle belly; thoracic erector spinae, 5 cm lateral to T9 spinous process; lumbar erector spinae, 3 cm lateral to L3 spinous process; and multifidus, 3 cm lateral to L5 spinous process (MacIntosh & Bogduk. 1987). For the gait study (Chapter II) electrodes were applied to the right side of the body, for the sitting/standing (Chapter III) and extensor exercise (Chapter IV) studies electrodes were applied bilaterally (right and left side for a total of 14 pairs).

Prior to data collection all participants performed maximal isometric contractions for all monitored muscle groups to enable EMG normalization. Procedures for obtaining maximum

myoelectric activity for normalization have been previously explained in McGill (1991). The three tasks were used to elicit maximum EMG activity from the seven recorded sights. The abdominal muscle groups were recruited with a modified bent-knee sit-up, the trunk extensors were activated by cantilevering the trunk over the end of a bench, and the latissimus dorsi was recruited with a simulation of a lat pull down exercise. All three maximal effort tasks were performed against an equal resistance (isometric) supplied by the experimenter.

The raw EMG signal was prefiltered to produce a band width of 20 to 500 Hz and amplified with a differential amplifier (common-mode rejection ratio > 90 dB at 60 Hz and input impedance >10 M ohms above 1 Hz) to produce peak to peak amplitudes of approximately 2 v. The amplified signal was A/D converted at 1024 Hz (small differences from these values are reported in the gait study, Chapter II, as different equipment was used).

Digital processing of the raw EMG signals included full wave rectification followed by a Butterworth low pass filter (2.5 Hz cut-off frequency) which resulted in a linear enveloped signal. The filtered signals were then normalized to the maximum muscle activity that was elicited during the isometric contractions.

Lumbar Spine Kinematics

Lumbar curvature was measured for all three in-vivo studies (Chapters II-IV). The curvature was defined as the motion of the top of the lumbar spine (joint of the 12th thoracic and 1st lumbar vertebrae) and the sacrum. This provided the entire motion that was present in the lumbar spine.

For the gait study (Chapter II) six IREDS defining the pelvis and trunk segments were

sampled at 60 Hz using a six camera optoelectronic system (OPTOTRAK, Northern Digital Inc., Waterloo, ON, Canada) and used to calculate the relative motion between the lumbar spine and the pelvis. A rigid plate with three markers was attached to the posterior aspect of the sacrum with a second similar plate attached at the T12/L1 spinal level. The rotational matrix (trunk with respect to pelvis) was decomposed using an Euler XYZ decomposition method to yield three-dimensional relative lumbar spine motion.

The sitting/standing (Chapter III) and extensor exercise (Chapter IV) studies monitored lumbar curvature with a 3SPACE ISOTRAK (POLHEMUS, P.O. Box 560, Colchester, Vermont, 05446). The signal was A/D converted using customized software at 20.5 Hz. The ISOTRAK source, which produces an electromagnetic field, was mounted on the sacrum using a custom built harness and the sensor, which detects the rotational motion (three directional cosines) with respect to the source, was mounted over the trunk midline at the T12/L1 spinal level.

Lumbar curvature was normalized to normal relaxed upright standing (ie zero position) for all three of the in-vivo studies. The three-dimensional lumbar curvature was then calculated with respect to this normal upright standing or zero position.

Modeling Techniques

Rigid link segment modeling of the body was used to calculate reaction forces and moments about a joint in the low back (L4/L5, previously described in McGill and Norman (1985)). Joint displacements were recorded on video camera at 30 Hz to reconstruct the joints and body segments. This modeling technique produced the reaction forces and corresponding

moments about the axes of the low back (flexion-extension, axial twist).

Following the link segment analysis, 3-dimensional joint moments and forces acting on the lumbar spine were calculated using an anatomically detailed, EMG driven spine model (Cholewicki & McGill. 1996; McGill. 1992; McGill & Norman. 1986). The method of satisfying equilibrium constraints at each lumbar level developed by Cholewicki and McGill (1996) was not used here, although the increased anatomical detail was incorporated in the model. This model predicts individual tissue loads in both passive tissues (i.e. ligaments and intervertebral disc) and 104 muscle fascicles as well as 3-dimensional low back joint forces.

The EMG driven model was originally designed to partition the joint reaction moments, from rigid link segment modeling, based on biological signals (EMG and lumbar spine kinematics) measured from each participant. The two measures of joint moment (produced by the tissue surrounding the spine) and the moments calculated by rigid link segment modeling can be adjusted by a gain factor which, essentially modifies the muscle stress (N/cm^2) for each individual. However, two complicating factors required a modification of this technique. The moments that were calculated in the gait study (Chapter II) using the three-dimensional rigid link model did not provide good agreement with previously reported data or the muscular activation patterns recorded for each subject. The moments calculated at the L4/L5 joint did not correspond to the muscle activation patterns which would be required to generate them since the lumbar spine was not sufficiently flexed to recruit a strong passive contribution. Some potential causes for this error are discussed in the discussion of the gait paper and have been presented elsewhere (Callaghan, Patla, & McGill. 1996). The second factor was that when muscular activation levels were of low magnitudes the model tended to behave poorly (i.e.,

increased muscle stress values beyond physiologic limits). This discrepancy was overcome by using a calibration posture that allowed a relation between EMG activity and a known reaction moment to be established and thereby tailor the model to each individual. This method effectively customized the level of maximum muscle stress for each individual.

The model functions in the following manner. Passive tissue forces were estimated by calibrating the lumbar spine range of motion (lumbar spine kinematics) and fitting the spinal curvature with known templates of passive tissues stress-strain relationships. EMG activation levels were used to guide the partitioning of forces generated by active tissues. Specifically, the muscle forces were determined based on: activation (normalized EMG amplitude), instantaneous length and velocity (lumbar spine kinematics)(force velocity updated by Sutarno and McGill (1995)), and physiologic cross sectional area. Based on their anatomic lines of action the contributions to the three joint moments were determined. Lumbar joint forces were calculated by taking the rigid link segment joint reaction forces and adding the joint forces created by muscular activation and passive tissue forces. The joint reaction forces calculated at the L4/L5 joint using the 3-dimensional model in the gait study provided strong agreement with the values reported in the literature (Cappozzo. 1983).

This method of using biological signals to solve the indeterminacy of multiple load bearing tissues facilitates the assessment of the many individual ways that we choose to support loads. In other words, using the EMG and lumbar spine kinematic signals the model was sensitive to the subtle differences that occurred in each subject. Although the major asset of this biologically based approach is that muscle co-contraction is fully accounted for together with being sensitive to the differences in the way that individuals perform a movement,

estimations of muscle force based, in part, on EMG signals are problematic as the force per muscle cross sectional area must be assumed together with other variables that are known to modulate muscle force production. Furthermore, accurate anatomical detail is essential to satisfy the moment requirements about all three joint axes and about several joints simultaneously.

A major drawback of the EMG based approach is the inaccessibility of the deeper torso muscles (i.e., psoas, quadrants lumborum, three layers of the abdominal wall). In an attempt to address this drawback, recent work by McGill, Juker, and Kropf (1996) used indwelling intramuscular electrodes with simultaneous surface electrode sites to evaluate the possibility, and validity, of using surface activity profiles as surrogates to activate deeper muscles, over a wide variety of tasks and exercises (e.g. sit-ups, curl-ups, leg raises, push-ups, some spine extensor tasks, lateral bending, and twisting tasks). Prediction of the activity of these deeper muscles is possible from well chosen surface electrodes within the criterion of 15% of MVC (RMS difference) (McGill, Juker, & Kropf. 1996).

Chapter II

**Low Back Three-Dimensional Joint Forces, Kinematics, and Kinetics
During Walking**

Jack P. Callaghan, Aftab E. Patla, and Stuart M. McGill

Clinical Biomechanics (In Press) 1998

ABSTRACT

Objective: The purpose of this study was to examine the three-dimensional low back loads, spinal motions, and trunk muscular activity during gait. Specific objectives involved assessment of the effects of walking speed, and arm swing on spinal loads, lumbar spine motion, and muscular activation.

Design: An in-vivo modeling experiment using five male participants. Thirty walking trials were performed by each participant yielding five repeats of each condition (3 walking cadences X 2 arm swing conditions).

Background: Walking is often prescribed as a rehabilitation task for individuals with low back

injuries. However, there are few studies which have examined the joint loading, spinal motions, and muscular activity present when walking. Additionally, the majority of studies examining spine loading during gait have used an inverse dynamics model approach, commencing at the cranial aspect of the body, which would tend to underestimate the impulsive phases of gait (i.e. heel strikes and toe-offs).

Methods: Low back joint forces and moments were determined using an anatomically complex three-dimensional model (detailing 54 muscles and the passive structures acting at the low back) during three walking cadences and with free arm swing or restricted arm swing. In order to assess the influence of the transient factors such as heel contact on the joint forces a bottom up (from the feet to the lumbar spine) a rigid link segment analysis approach was used as one input to the three-dimensional anatomic model. Lumbar spine motion and trunk muscle activation levels were also recorded to assist in partitioning forces amongst the active and passive tissues of the low back.

Results: Net joint anterior-posterior shear loading was the only variable significantly affected by walking cadence (fast vs. slow $p < 0.0003$). No variable was significantly affected by the arm swing condition. Trends demonstrated an increase in all variables with increased walking cadence. Similarly, most variables, with the exception of axial twist and lateral bend lumbar spine motion and lateral joint shear, demonstrated increasing trends caused by the restriction of normal arm swing.

Conclusions: Tissue loading during walking appears to be below levels caused by many specific rehabilitation tasks, suggesting that walking is a wise choice for general back exercise and rehabilitation programs. Slow walking with restricted arm swing produced more constant

lumbar spine loading and motion patterns, which could be detrimental for certain injuries and tissues. Fast walking produced a more cyclic loading pattern.

Relevance: This work provides a detailed analysis of low back joint loading, lumbar motion, and muscular activation during walking. The magnitude of joint motions, muscular activation, and joint loading provide further insight into the tissue demands during gait and demonstrate that slow walking produced more constant lumbar spine loading and motion patterns activity that may present difficulty for some low back injured. While, faster walking appears to be a cyclic activity that is only mildly demanding in terms of tissue loading, rendering it a low risk of injury for most individuals.

INTRODUCTION

Thousands of low level loading cycles are experienced by the spine in an average day. During normal gait, activation of the spinal musculature, and accelerations of the trunk result in cyclic spine loads. The magnitude of these loads, in conjunction with spinal motion and muscular activity, present a portrait of what is thought to be a non-injurious activity. Clinically, walking (aerobic exercise) has been presented as potentially beneficial to conditioning and pain relieving (Nutter. 1988) of some forms of low back pain. Additionally McQuade et al. (1988) found that chronic low back pain individuals that were more aerobically fit had fewer limitations and a higher activity level. Yet paradoxically, individuals who are pain free the majority of the time can complain of low back pain after prolonged bouts of slow walking while others report obtaining relief from faster walking. In other words walking appears to help

some individuals, yet hurt others, and even the style of walking appears to have some modulating affect. This motivated investigation into the loads and motion of the lumbar spine and trunk muscular activity during gait.

The literature documenting investigations of three-dimensional low back loading during gait, to date, consists of linked segment analyses commencing at the head and working down through the linkage to the torso (top down model). Further, the models used to estimate joint loading incorporated very simple, or non-existent, anatomical representation of supporting tissues around the joints. The two-dimensional studies have examined the low back moments from either a sagittal view (Winter. 1991) or from a frontal view (MacKinnon & Winter. 1993). While two-dimensional planar analyses simplify motion and facilitate calculations, body segment rotations and translations out of the plane of progression are not quantified, resulting in an inherent problem in the calculation and interpretation of moments and provide only one of the three moment components acting at the joint examined. Cappozzo (1983; 1984) calculated 3D moments at the low back from a top down model using inertial and kinematic variables as inputs. Calculating the low back moments from the top down would tend to underestimate any transient factors, such as the impact occurring at heel strike. In addition all these studies examined joint reaction loads, ignoring the muscular contribution to joint loads. A 3D analyses from the floor upwards was undertaken by Khoo et al. (1995), however, only the 2D (sagittal plane) forces and moments were analysed and joint loading was calculated with a single muscle equivalent model. Cappozzo (1984) used a four muscle model, top down kinematic approach to determine compressive loads. It appears, to date, the details of low back loading are insufficient to provide clinical insight into the links between walking as a

modulator of low back health.

The function of arm swing during walking is not well understood. Elftman (1939) looked at the contribution of the arms using an angular momentum approach which suggested that arm swing served to regulate body rotations. Specifically it has been argued that arm movements reduce rotations about the vertical axis of the whole body (axial twist) and accommodate a change in directions more smoothly. The author continued with a work/energy analysis and determined that the arms are actively controlled (rather than simply resulting from pendulum motion in response to accelerations/decelerations of the trunk in the step cycle). However, the advantage (i.e. reduced muscle activation or lumbar spine motion) of incorporating arm swing during gait is still a matter of considerable debate.

The global objective of this study was to examine the three-dimensional low back loads, spinal motions, and trunk muscular activity during gait. Given the clinical questions posed earlier, specific objectives involved assessment of the effects of walking speed, and arm movement on spinal loads, lumbar spine motion, and muscular activation. These objectives demanded more rigor to understand tissue loading necessitating the use of an anatomically complex (detailing 54 muscles acting at the low back) fully three- dimensional model (McGill. 1992; McGill & Norman. 1986) which incorporated normalized EMG and low back kinematics to calculate L4/L5 joint forces. In this way, the model was sensitive to individual differences, between people and between strides, in the way that the various body segments move, muscles are activated, and joints are loaded.

METHODS

Participants

Given the extensive data reduction required for the anatomically complex, fully three-dimensional dynamic model, and for the comprehensive number of trials only five male participants were recruited from a university student population (Table 2.1). All participants were healthy and had no history of low back pain for a minimum period of one year.

Table 2.1: Anthropometric measurements and normal walking cadence of the 5 participants.

Participant	Height (m)	Mass (kg)	Age (yr)	Normal Cadence (steps/min)
1	1.75	80.5	26	108
2	1.67	81.8	27	100
3	1.75	74	22	100
4	1.80	84	22	108
5	1.83	70	28	100
Mean	1.76	78.1	25	103.2
SD	0.61	5.8	2.8	4.38

Instrumentation

Seven pairs of disposable Medi-Trace surface electromyogram (EMG) electrodes (Ag-AgCl) were applied to the skin on the right side of the body: rectus abdominis, 3 cm lateral to the umbilicus; external oblique, approximately 15 cm lateral to the umbilicus; internal oblique below the external oblique electrodes just superior to the inguinal ligament; latissimus dorsi, lateral to T9 over the muscle belly; thoracic erector spinae, 5 cm lateral to T9 spinous process;

lumbar erector spinae, 3 cm lateral to L3 spinous process; and multifidus, 3 cm lateral to L5 spinous process. Prior to data collection all participants performed maximal isometric contractions for all monitored muscle groups for EMG normalization. Procedures for obtaining maximum myoelectric activity for normalization has been previously explained in McGill (1991). The EMG signals were transmitted to an A/D system from an isolated portable amplifier (mass 1.3 kg) worn on the participants back at approximately the T5 level. The raw EMG signal was prefiltered to produce a band width of 10 to 500 Hz and amplified with a differential amplifier (common-mode rejection ratio > 90 db and input impedance >10 M ohms above 1 Hz) to produce peak to peak amplitudes of approximately 2 v. The amplified signal was A/D converted at 1200 samples/s.

Fifteen infrared emitting diodes (IREDS) were attached to the participants in order to define a five segment rigid link model: right foot, right leg, right thigh, pelvis, and trunk. Three markers were attached to each segment and were used for segment tracking. An upright standing calibration posture based on the methods of Jian et al. (1993) was used to develop the transformation matrix between the marker based axes and the segment's principle axes. Additional points were digitized to define the principle axes (using a 6 IRED probe, OPTOTRAK, Northern Digital Inc., Waterloo, ON, Canada) and enable the determination of the invariable relationship between the tracking markers and the segments principle axes. Segment lengths and perimeters were measured and moments of inertia were calculated based on the regression equations of Yeadon and Morlock (1989). The marker displacement data were recorded with a six camera optoelectronic system (OPTOTRAK, Northern Digital Inc., Waterloo, ON, Canada) at a sample rate of 60 Hz. Prior to collection the three-dimensional

space in which the participants walked was calibrated and the RMS error between calculated and actual distances was less than 0.5 mm.

The six IREDS defining the pelvis and trunk segments were used to calculate the relative motion between the lumbar spine and the pelvis. A rigid plate with three markers was attached to the posterior aspect of the sacrum with a second similar plate attached at the T12/L1 spinal level. The three-dimensional lumbar curvature was calculated with respect to normal upright standing (i.e. zero position). The rotational matrix (trunk with respect to pelvis) was decomposed using an Euler XYZ decomposition method to yield three-dimensional relative lumbar spine motion. Prior to calculation of the kinematic variables the marker displacement data were digitally filtered with a fourth order zero lag butterworth low pass filter at 6 Hz (Winter. 1990).

Ground reaction forces (three orthogonal moments and forces) were measured with a strain gauge force plate (Model OR6-5, Advanced Mechanical Technology Inc., Watertown, MA., USA) and sampled with an IBM PC at 1200 Hz. No filtering was performed on the force plate data, however to synchronize the force data with the kinematic data (@ 60 Hz) every twentieth point was matched with the marker displacement data.

Data Collection

The collection protocol consisted of six different walking conditions with five repetitions of each condition for a total of thirty trials per participant. The conditions were comprised of three walking speeds: fast, normal, and slow coupled with either free arm swing or no arm swing (arms crossed over the abdominal region). Walking speeds were individually assessed by measuring the participant's normal cadence by taking the average cadence of 6

unpaced trials over a 30 metre walkway (steps/min). Fast and slow speeds were defined as a relative increase or decrease of 20 steps/min respectively, which represents a significant alteration from normal cadence. Walking cadence was paced with a metronome and all participants wore similar comfortable footwear. The point of initiation of gait was set so that the right heel contact was recorded with the force plate following two complete strides. A calibration posture (Neumann, Norman, & Wells. 1995) (trunk flexed to 60° from the vertical with a lordotic spine, holding a 10 kg mass in the hands) was recorded to provide an EMG to moment relationship for each participant.

Data Processing

Two different modeling approaches were used: the first three-dimensional linked segment model was used to calculate the three reaction moments and forces at the low back while the second anatomically detailed model partitioned these moments amongst the supporting tissues from which the dynamic spine loads were ultimately calculated. The first model used the ground reaction forces and kinematic variables as input to a three-dimensional inverse dynamic model (KINGAIT3, Mishac Kinetics, Waterloo, ON, Canada). The model started with the most distal joint (right ankle) and terminated at the right hip joint. In order to calculate the joint reaction forces and moments at L4/L5 the pelvic rigid model required both right and left hip moments and forces. The left hip joint variables were generated based on an assumption of symmetric gait in the sagittal plane and corrected for anatomical sense (i.e. - $My_{\text{Right Thigh}} \text{ (external rotation)} = +My_{\text{Left Thigh}} \text{ (external rotation)}$). The left hip joint forces and moments were shifted in time based on right foot event occurrence. Since only the right side EMG was collected the left side EMG was also generated with the same shifting method. This

shifting of EMG patterns demonstrated good agreement with the bilateral patterns reported for extensor activity in the literature (Cappozzo. 1984; Cromwell, Schultz, Beck, & Warwick. 1989; Thorstensson, Carlson, Zomlefer, & Nilsson. 1982). With a complete data set for the rigid pelvic model the three-dimensional L4/L5 joint reaction moments and forces were calculated.

Following the link segment analysis, joint moments and forces acting on the lumbar spine were calculated using a three-dimensional, anatomically detailed, EMG driven spine model (McGill. 1992; McGill & Norman. 1986) (the second model). The EMG driven model was originally designed to partition the joint reaction moments, from rigid link segment modeling, based on biological signals measured from each participant. The moments that were calculated in this study using the three-dimensional rigid link model did not provide good agreement with previously reported data or muscular activation patterns. Briefly, the moments calculated at the L4/L5 joint did not correspond to the muscle activation patterns which would be required to generate them. Some potential causes for this error are discussed in the limitations and have been presented elsewhere (Callaghan, Patla, & McGill. 1996). However, the joint reaction forces calculated at L4/L5 corresponded with values that were present in the published literature (Cappozzo. 1983). This discrepancy was overcome by using a calibration posture that allowed a relation between EMG activity and a known reaction moment to tailor the model to each individual. Passive tissue forces were estimated by calibrating the spine range of motion and fitting the spinal curvature with known templates of passive tissues stress-strain relationships while EMG activation levels were used to guide the partitioning of forces generated by active tissues. Specifically, the muscle forces were determined based on:

activation (normalized EMG amplitude), instantaneous length and velocity, and physiologic cross sectional area. Based on their anatomic lines of action the contributions to the three joint moments were determined. Lumbar joint forces were calculated by taking the rigid link segment joint reaction forces and adding the joint forces created by muscular activation and passive tissue forces.

Following data processing, all the dependent variables were three point (the two right heel contacts and the right toe off) ensembled averaged within condition and participants. The time varying parameters were normalized to one full stride from right heel contact to the subsequent right heel contact with the third constraint being right toe off. Forces were normalized to percent body weight and moments were normalized to percent body weight times height. The dependent variables, both peak values and peak to peak (p-p) ranges, were compared using 2 x 3 repeated measures ANOVA, ARM PLACEMENT X WALKING CADENCE, with a TUKEY post hoc analysis of significant findings.

RESULTS

The overall trends indicate that all forces, moments, relative lumbar motion, and muscle activation levels were increased with increased walking cadence. Similarly the restriction of arm swing resulted in an increase for most variables. The most notable exceptions being the axial twist and lateral bend ranges of motion of the lumbar spine were decreased with restricted arm swing. The only variable that was significantly affected by either of the independent variables was the net anterior posterior shear at the L4/L5 joint. An increase in walking cadence from slow to fast resulted in a significant increase ($P < 0.0003$) in both peak A/P shear

and p-p A/P shear values. Whether the arms were allowed to swing free or were constrained (held folded anterior to the torso) produced no significant differences in any of the dependent variables. There were no interaction effects between the arm condition and walking speed for any of the dependent variables.

Forces and Moments

As expected the joint force "y" component remained entirely compressive throughout the stride period (Figure 2.1a). The joint forces exhibited two peaks between 5-15% and 55-65% of the stride period. These peaks occur at approximately the time of toe off. The two minimum points were approximately at 30-40% and 80-90% of the stride period. The normalized minimum and maximum p-p ranges for the EMG driven model were 46% to 204% and 24% to 69% of body weight for the rigid link segment model. The joint loading calculated by the EMG driven model resulted in large increases in the maximum compressive forces experienced by the low back when compared with the joint reaction forces calculated using inverse dynamics (Tables 2.2 and 2.3 respectively). Including the muscular component resulted in more than a three-fold increase in joint load. The maximum reaction force from the rigid link segment model for one participant was 101% and the EMG driven model calculated a maximum joint load of 345% body weight.

The joint force "x" component (anterior/posterior shear) was distributed symmetrically about the zero force axis (Figure 2.1b). Heel contacts resulted in a posterior shear of the trunk on the pelvis, which was followed by a rapid reversal to peak anterior shear corresponding to toe off. The peak joint loads were 26% and -27% (maximum and minimum) for the rigid link segment model and 24% and -27% body weight for the EMG driven model.

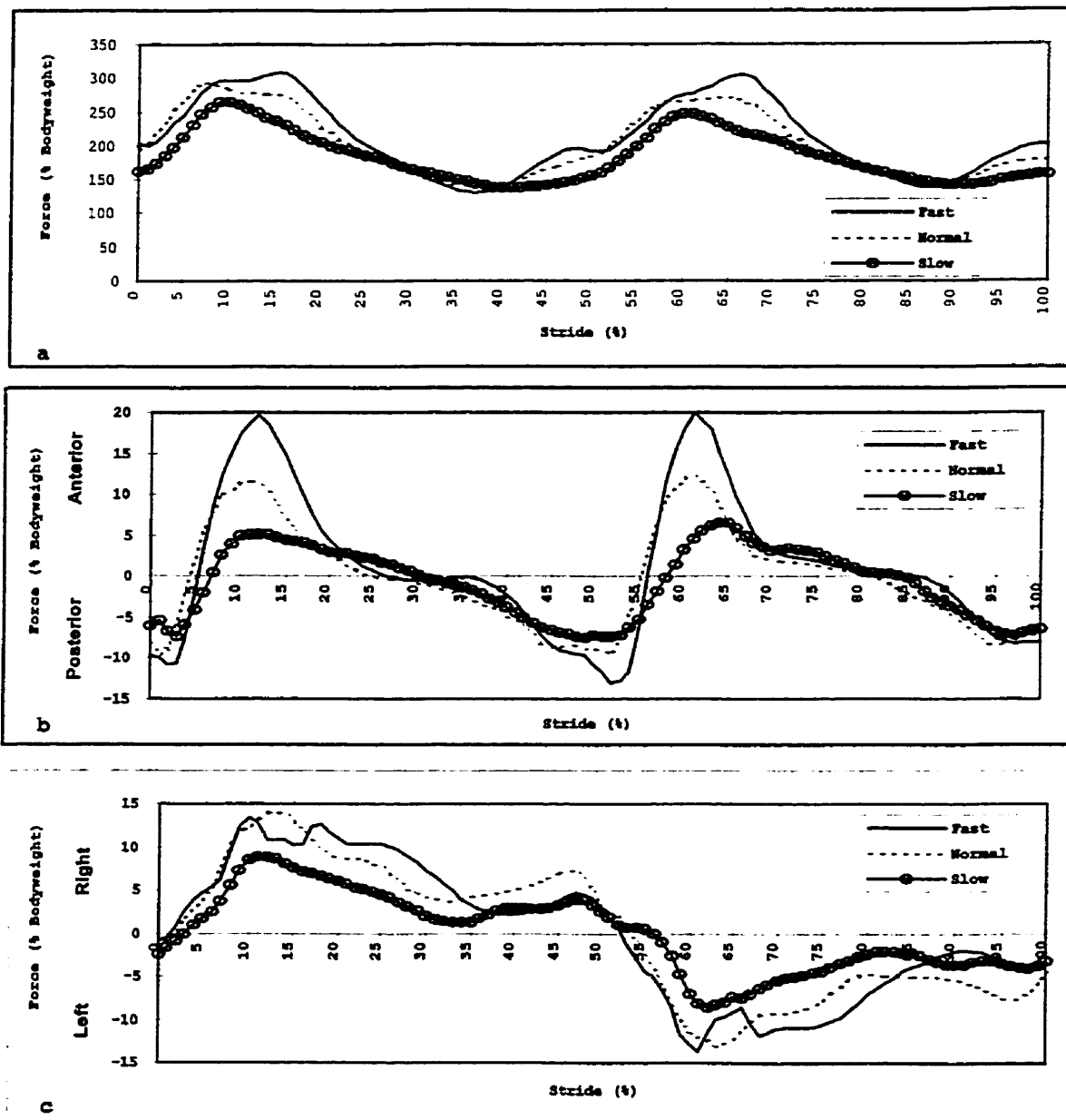


Figure 2.1: Joint forces at L4/L5 (normalized to percent body weight) for one participant for three walking cadences with normal arm swing. The curves are normalized for one stride (RHC to RHC) with toe off occurring at 61% (fast), 63% (normal), and 65% (slow) of stride. **1a** Joint compression force at L4/L5. **1b** Net Anterior posterior joint shear force with positive indicating forward shear of the trunk with respect to the pelvis. **1c** Net lateral joint shear force with a positive value indicating right shear of the trunk with respect to the pelvis.

Table 2.2: Minimum and maximum joint forces (L4/5), calculated using an EMG driven model, for five participants at three walking speeds and two arm conditions. Forces are normalized to percent body weight ((Joint Force/body weight)*100)

Participant	Compression (Fy)				Anterior/Posterior Shear (Fx)				Lateral Shear (Fz)			
	Arms		No Arms		Arms		No Arms		Arms		No Arms	
	min	max	min	max	min	max	min	max	min	max	min	max
Fast Cadence												
1	112	193	116	199	-12	13	-11	16	-11	10	-10	10
2	131	309	142	345	-13	20	-17	14	-14	14	-17	17
3	134	273	145	259	-14	11	-16	9	-8	7	-8	7
4	92	202	94	199	-27	13	-26	19	-31	27	-13	11
5	95	247	102	276	-18	24	-21	20	-14	15	-16	15
Mean	113	245	120	256	-16	16	-18	15	-8	10	-11	14
SD	20	49	23	61	6	5	5	4	4	6	4	5
Normal Cadence												
1	113	179	126	188	-7	11	-10	13	-9	9	-7	7
2	140	294	145	319	-10	12	-15	12	-13	14	-10	11
3	147	223	150	256	-13	8	-16	8	-6	6	-8	7
4	104	185	98	180	-17	14	-16	16	-14	13	-8	6
5	98	208	105	222	-16	15	-19	15	-12	11	-12	12
Mean	120	218	125	233	-12	12	-15	13	-7	8	-9	10
SD	22	46	23	57	4	3	3	3	2	3	4	4
Slow Cadence												
1	124	170	123	169	-4	8	-4	8	-7	9	-6	6
2	138	265	155	278	-7	7	-11	5	-8	9	-6	6
3	133	227	151	245	-11	8	-12	7	-6	6	-6	8
4	103	150	104	162	-13	14	-13	12	-10	10	-7	7
5	119	191	113	194	-14	10	-17	9	-8	9	-10	10
Mean	124	201	129	210	-10	9	-11	8	-6	7	-6	7
SD	13	46	23	50	4	3	4	3	1	2	2	3

Table 2.3: Joint reaction force, normalized to percent body weight ((Joint Force/body weight)*100), minimums and maximums calculated using an inverse rigid link model.

Participant	Compression (Fy)				Anterior/Posterior Shear (Fx)				Lateral Shear (Fz)			
	Arms		No Arms		Arms		No Arms		Arms		No Arms	
	min	max	min	max	min	max	min	max	min	max	min	max
Fast Cadence												
1	26	74	19	81	-13	13	-13	16	-8	8	-9	9
2	23	90	27	94	-11	21	-12	18	-8	8	-10	9
3	40	101	40	95	-13	12	-12	14	-7	7	-8	8
4	26	78	25	87	-26	17	-25	20	-23	21	-21	21
5	27	95	24	93	-20	27	-21	27	-9	9	-12	10
Mean	28	88	27	90	-17	18	-17	19	-11	11	-12	11
SD	7	11	8	6	6	6	6	5	7	6	5	5
Normal Cadence												
1	35	80	33	73	-8	11	-13	11	-5	6	-6	6
2	40	88	38	99	-8	15	-10	15	-8	8	-8	7
3	49	95	46	89	-14	10	-14	12	-8	8	-9	8
4	37	72	38	74	-18	17	-16	20	-13	14	-14	13
5	39	80	40	80	-17	19	-19	20	-10	10	-10	9
Mean	40	83	39	83	-13	14	-14	16	-9	9	-9	9
SD	5	9	5	11	5	4	3	4	3	3	3	3
Slow Cadence												
1	43	78	42	71	-6	7	-5	8	-5	5	-5	4
2	44	78	46	82	-6	9	-7	9	-6	6	-6	6
3	48	89	49	85	-11	9	-11	9	-7	7	-7	7
4	41	65	42	78	-14	16	-14	16	-13	14	-9	10
5	49	78	48	73	-14	13	-15	14	-7	6	-7	6
Mean	45	78	45	78	-10	11	-10	11	-8	8	-7	7
SD	3	9	3	6	4	4	4	4	3	4	1	2

The joint lateral shear (z component) again was evenly distributed around the zero force axis (Figure 2.1c). During single support the shear component was directed towards the support leg (i.e. right shear of trunk on pelvis during right leg single support). P-p normalized minimum and maximum ranges for the EMG driven model and the rigid link segment were 12% to 58% and 9% to 44% respectively.

The shape of the moment about the medial-lateral axis (M_z - Flexion/Extension) was consistent for all participants. The bimodal shape exhibited two maximums, which occurred approximately at toe off (Figure 2.2a). The two minimum values started just prior to heel strike. At heel contact there was a flexor peak moment present followed by an extensor peak around toe off. The normalized p-p range for the EMG driven model was 0.62% to 2.87%. The peak moments that occurred in the stride period were -1.64% (minimum) and 1.76% (maximum) body weight times height (Table 2.4).

The lateral bend moment (M_x) produced a consistent pattern across participants, which oscillated about the moment zero axis. Corresponding to heel contact there was a lateral bend moment to the side of contact (i.e. at right heel contact a right lateral bend moment was present). Prior to toe off and swing phase there was a lateral bend moment to the swing leg side returning to the opposite side following the consequent heel strike (Figure 2.2b). The resultant range of normalized p-p values for the EMG model was 0.31% to 4.44%. The peak minimum and maximum moments were -1.41% and 2.59% body weight times height respectively.

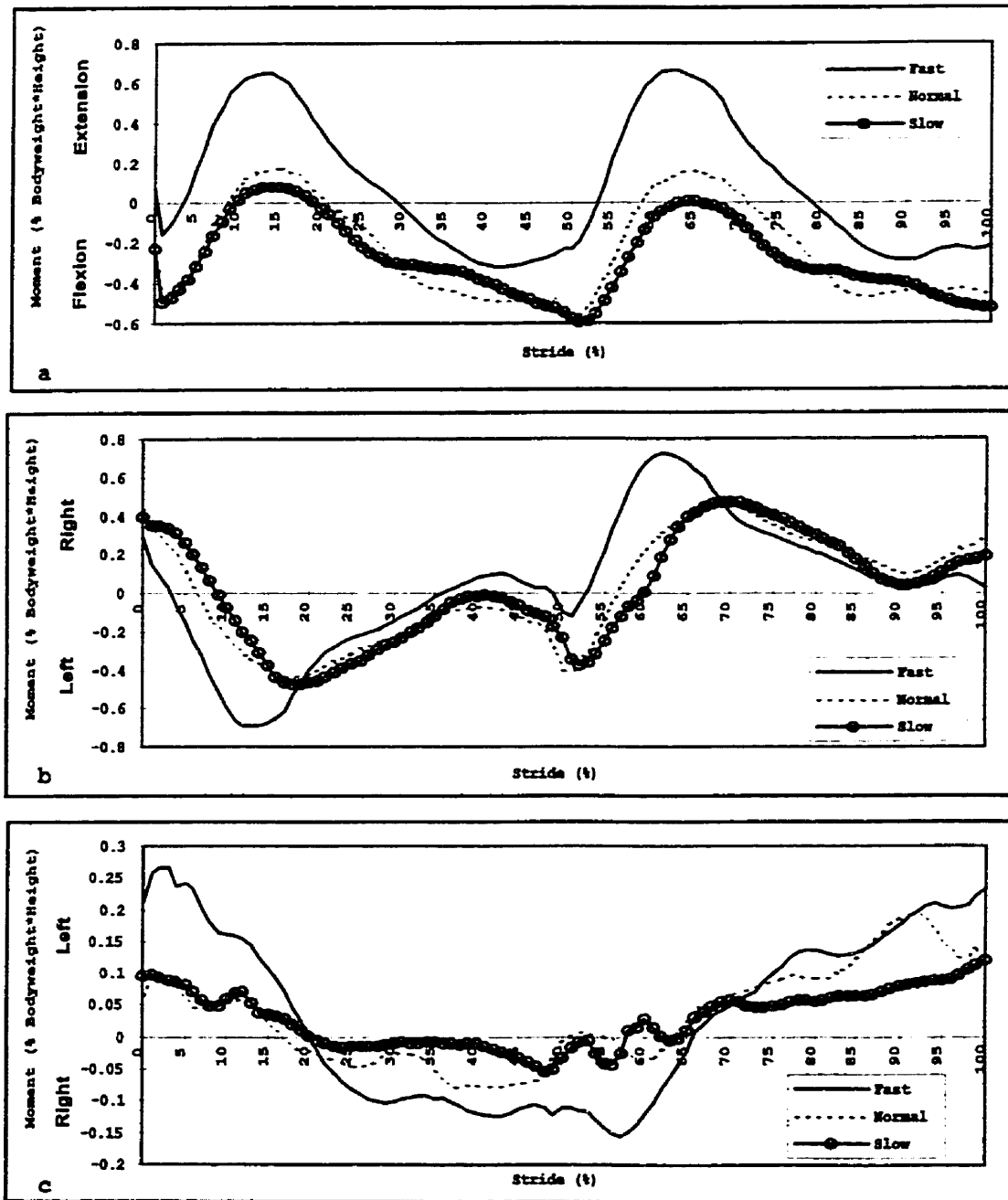


Figure 2.2: Joint moments at L4/L5 (normalized to percent body weight * height) calculated using an EMG driven model for one participant for three walking cadences with normal arm swing. The curves are normalized for one stride (RHC to RHC) with toe off occurring at 62% (fast), 64% (normal), and 65% (slow) of stride. **1a** Joint flexion extension moment. **1b** Lateral bend moment. **1c** Axial twist moment.

Table 2.4: Joint moments at L4/5 (minimum and maximum) for all five participants and six conditions (3 walking speeds by 2 arm conditions). The moments are normalized to percent of the product of body weight and height (Joint Moment / (body weight * height)) * 100.

Participant	Flexion/Extension (Mz)				Lateral Bend (Mx)				Axial Twist (My)			
	Arms		No Arms		Arms		No Arms		Arms		No Arms	
	min	max	min	max	min	max	min	max	min	max	min	max
Fast Cadence												
1	-1.08	-0.19	-1.12	0.09	-0.42	0.43	-0.53	0.54	-0.41	0.03	-0.43	0.07
2	-0.50	1.37	-0.25	1.76	-0.41	0.40	-0.69	0.86	-0.07	0.10	-0.11	0.17
3	-0.32	0.67	-0.67	0.14	-0.69	0.72	-0.79	0.94	-0.15	0.27	-0.01	0.22
4	-1.42	-0.01	-1.01	0.68	-0.73	0.92	-0.96	1.09	-0.38	0.66	-0.04	0.56
5	-1.45	0.79	-1.64	1.22	-1.42	2.13	-1.85	2.59	-0.74	0.09	-0.75	0.26
Mean	-0.96	0.52	-0.94	0.78	-0.73	0.92	-0.96	1.20	-0.35	0.23	-0.27	0.26
SD	0.52	0.63	0.52	0.72	0.41	0.71	0.52	0.80	0.26	0.26	0.31	0.18
Normal Cadence												
1	-1.03	-0.07	-1.60	-0.14	-0.31	0.17	-0.42	0.25	-0.33	0.06	-0.45	0.05
2	-0.38	1.26	-0.11	1.59	-0.24	0.27	-0.46	0.64	-0.07	0.11	-0.10	0.11
3	-0.58	0.17	-0.76	0.45	-0.43	0.46	-0.74	0.90	-0.08	0.19	-0.06	0.15
4	-1.25	0.29	-0.96	0.96	-0.67	1.00	-0.70	0.95	-0.19	0.47	-0.05	0.25
5	-1.64	0.76	-1.36	1.15	-1.17	1.79	-1.66	2.10	-0.63	0.41	-0.61	0.11
Mean	-0.98	0.48	-0.96	0.80	-0.56	0.74	-0.80	0.97	-0.26	0.25	-0.26	0.13
SD	0.51	0.53	0.58	0.67	0.38	0.67	0.50	0.69	0.23	0.18	0.26	0.07
Slow Cadence												
1	-0.90	-0.28	-1.17	-0.17	-0.31	0.22	-0.23	0.08	-0.31	0.02	-0.38	0.01
2	-0.28	1.03	-0.12	1.10	-0.27	0.23	-0.30	0.27	-0.05	0.11	-0.07	0.11
3	-0.59	0.08	-0.73	0.08	-0.47	0.47	-0.50	0.52	-0.05	0.12	-0.04	0.20
4	-1.22	0.20	-1.08	0.26	-0.55	0.81	-0.64	0.86	-0.14	0.26	-0.08	0.28
5	-1.59	0.90	-1.34	1.24	-1.05	1.30	-1.17	1.42	-0.34	0.12	-0.42	0.08
Mean	-0.91	0.39	-0.89	0.50	-0.53	0.61	-0.57	0.63	-0.18	0.13	-0.20	0.14
SD	0.51	0.56	0.48	0.63	0.31	0.46	0.38	0.53	0.14	0.09	0.19	0.10

Axial twist moments (M_y) were small across all participants, p-p normalized range 0.15% to 1.04% body weight * height. Maximum twist moments occurred at approximately toe off (Figure 2.2c). From toe off to the following heel contact there was a twist moment to the contralateral side. The moment profiles were consistent within participants and exhibited similar patterns between participants. Maximum and minimum peak moments were -0.74% and 0.66% of body weight * height respectively.

Lumbar Kinematics

The lumbar spine motion with respect to the pelvis demonstrated consistent patterns within and between participants, however quite often different participants presented biases in one of the two potential directions about the zero position.

The motion of the lumbar spine about the z axis (flexion/extension) possessed several dominant phases. Following heel contact a flexion phase was present until the relative spine motion reached maximum flexion just following toe off (Figure 2.3a). The spine then either remained in a relatively constant posture, as shown in Figure 2.3a, or had a bimodal pattern with an additional extension phase during single stance. The relative lumbar spine motion then entered an extension phase prior to the next heel contact, reaching peak extension around heel contact. The p-p range of spinal motion was between 2.72° to 10.25° . The maximum and minimum lumbar spine positions were -7.58° (flexion) and 11.12° (extension) respectively (Table 2.5). Four of the five participants had profiles that oscillated around the calibration posture. One participant (#5) demonstrated a clear shifting to an extended posture.

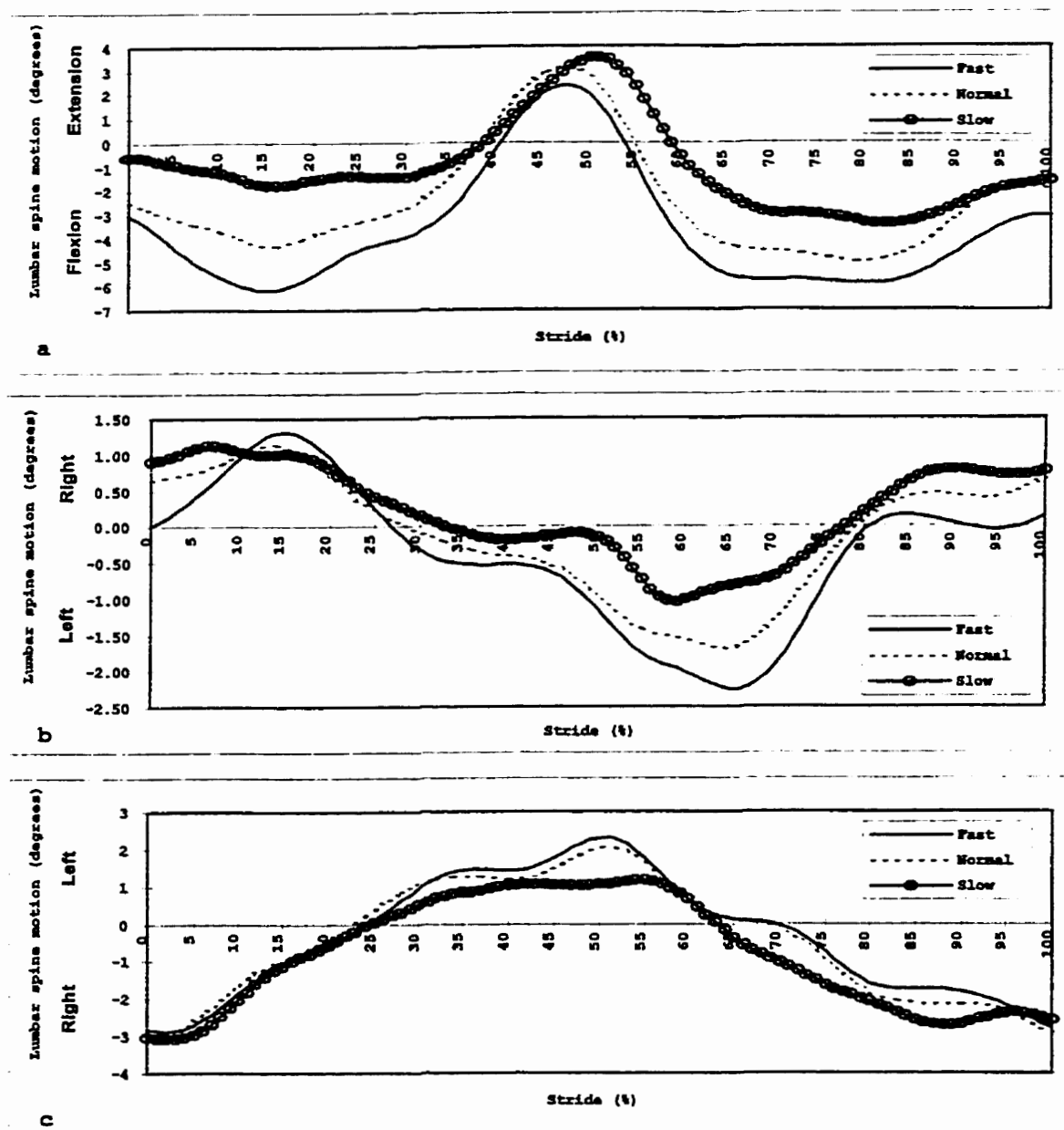


Figure 2.3: Relative lumbar spine motion with respect to the pelvis. The ensembled data for one participant for three walking cadences with normal arm swing are shown. The curves are normalized for one stride (RHC to RHC) with toe off occurring at 61% (fast), 63% (normal), and 65% (slow) of stride. **1a** Lumbar spine flexion extension, positive indicates an extension of the trunk with respect to the pelvis. **1b** Lateral bend of the trunk with respect to the pelvis. A positive value indicates right lateral bend of the trunk with respect to the pelvis. **1c** Positive axial twist movement was defined as left twisting of the trunk with respect to the pelvis.

Table 2.5: Minimum and maximums of lumbar spine motion (degrees) for the three walking speeds and two arm conditions. The measures are expressed relative to a normal upright standing posture.

Participant	Flexion/Extension				Lateral Bend				Axial Twist			
	Arms		No Arms		Arms		No Arms		Arms		No Arms	
	min	max	min	max	min	max	min	max	min	max	min	max
Fast Cadence												
1	-4.29	-0.63	-3.73	-0.08	-1.93	4.66	-2.12	4.97	0.02	7.19	0.95	5.51
2	-6.16	2.37	-3.43	5.90	-2.25	1.31	-1.50	1.57	-2.88	2.30	-2.85	2.72
3	-7.58	-4.01	-2.27	2.47	-5.25	3.23	-4.09	2.65	-5.09	1.97	-5.56	0.97
4	4.49	11.12	0.39	7.47	-6.44	0.71	-7.73	0.70	-10.45	4.24	-10.01	1.32
5	-7.20	3.06	-1.16	7.96	-10.69	5.32	-5.97	4.53	-1.97	7.85	-1.91	3.77
Mean	-4.15	2.38	-2.04	4.75	-5.31	3.05	-4.28	2.89	-4.07	4.71	-3.88	2.86
SD	4.99	5.63	1.70	3.45	3.57	2.02	2.61	1.84	4.01	2.72	4.14	1.86
Normal Cadence												
1	-4.25	0.09	-3.99	0.99	-1.82	4.50	-2.14	4.58	-0.20	6.43	0.80	5.69
2	-4.95	3.16	-3.71	4.69	-1.69	1.14	-1.58	0.68	-3.11	2.06	-2.25	1.61
3	-5.22	0.43	-2.03	3.62	-4.33	4.09	-4.77	2.59	-4.61	2.29	-4.06	2.08
4	2.64	8.62	-1.16	2.97	-6.69	0.43	-5.99	0.54	-10.20	4.10	-6.25	1.63
5	-4.94	3.32	-2.34	4.98	-9.95	5.40	-2.72	3.01	-4.61	6.16	-1.60	3.99
Mean	-3.34	3.12	-2.64	3.45	-4.90	3.11	-3.44	2.28	-4.55	4.21	-2.67	3.00
SD	3.36	3.42	1.18	1.60	3.49	2.19	1.87	1.69	3.64	2.07	2.65	1.80
Slow Cadence												
1	-4.64	0.23	-2.93	2.33	-0.82	4.06	-0.64	4.22	0.75	5.80	1.44	5.76
2	-3.38	3.57	-1.71	5.28	-1.04	1.12	-0.37	0.75	-3.06	1.16	-2.48	1.03
3	-4.22	2.13	-0.57	4.83	-3.42	2.62	-4.14	3.24	-3.60	1.61	-4.41	0.63
4	5.97	8.68	7.06	10.79	-6.51	0.19	-5.98	0.06	-6.59	3.86	-7.40	2.46
5	-3.57	3.14	0.87	7.99	-2.68	2.60	-3.83	2.67	-1.94	4.19	-0.51	3.01
Mean	-1.97	3.55	0.54	6.24	-2.89	2.12	-2.99	2.19	-2.89	3.32	-2.67	2.58
SD	4.47	3.15	3.90	3.24	2.30	1.50	2.42	1.74	2.67	1.92	3.43	2.03

The phases of lateral flexion (x axis) displayed two main characteristics (Figure 2.3b). At heel contact there was a lateral flexion to the contralateral side (i.e. at right heel contact, left lateral flexion of the spine). The spine laterally flexed following heel contact to the maximum value at toe off, to the side opposite of the upcoming toe off (i.e. left lateral flexion at right toe off). From toe off until heel contact the spine returned toward the zero position with a small lateral flexion remaining to the contralateral side of heel contact. The p-p range of motion varied from 1.12° to 7.13° with maximum excursions of 10.7° left and 5.4° right. All participants exhibited the same pattern, however two participants had small biases to the right side.

The spine motion had peaks occurring around heel contact events (Figure 2.3c). The relative lumbar spine motion showed a twist to the side of heel (i.e. right axial twist at right heel contact) contact followed by a fairly constant rotation to the opposite side reaching the peak value coinciding with the consequent heel strike. Two of the participants had small biases of left axial twist that the curves oscillated about as opposed to oscillating around zero as in the remaining participants. The maximum postures recorded were 10.45° right twist and 7.85° left twist. The p-p range of motions lay between 3.51° to 14.69° .

Trunk EMG

Both the rectus abdominis and external oblique had low levels of activation with no discernible pattern for the majority of participants (Figure 2.4). In the cases where higher levels were recorded and a pattern visible, peak activation occurred around ipsilateral heel contact. Internal oblique exhibited a common unimodal activation pattern for all participants, peak activation coincided with ipsilateral heel contact. The two upper posterior trunk channels

(latissimus dorsi and thoracic erector spinae) both had bimodal patterns with one peak larger than the second. The larger of the two peaks occurred with ipsilateral toe off, the second smaller peak was approximately at contralateral toe off. The lower erector spinae and multifidus also had bimodal activation patterns, however the two peaks were much more equal than the two superior channels. In contrast to the upper channels the lower two erector groups had the larger activation about contralateral toe off with the smaller of the two peaks around ipsilateral toe off.

Walking Cadence Effects

While there were no significant differences found, all six EMG model calculated variables (3 forces and 3 moments) and the three rigid link segment calculated forces had trends of increased p-p ranges with increased walking cadences (Tables 2.2 and 2.3). The trends in the lumbar kinematics demonstrated increased p-p range of motion with increased walking cadences (Table 2.5). Relative lumbar spine posture became more flexed with increased walking cadence. While there were no significant differences found, there was a trend to less flexion-extension range of motion present at slower walking speeds. There was less lateral bend relative motion at slower walking cadences (Table 2.5). Axial twist demonstrated reduced range of motion at slower cadences (Table 2.5). Increasing speed was associated with increased activation for all seven EMG channels (Table 2.6).

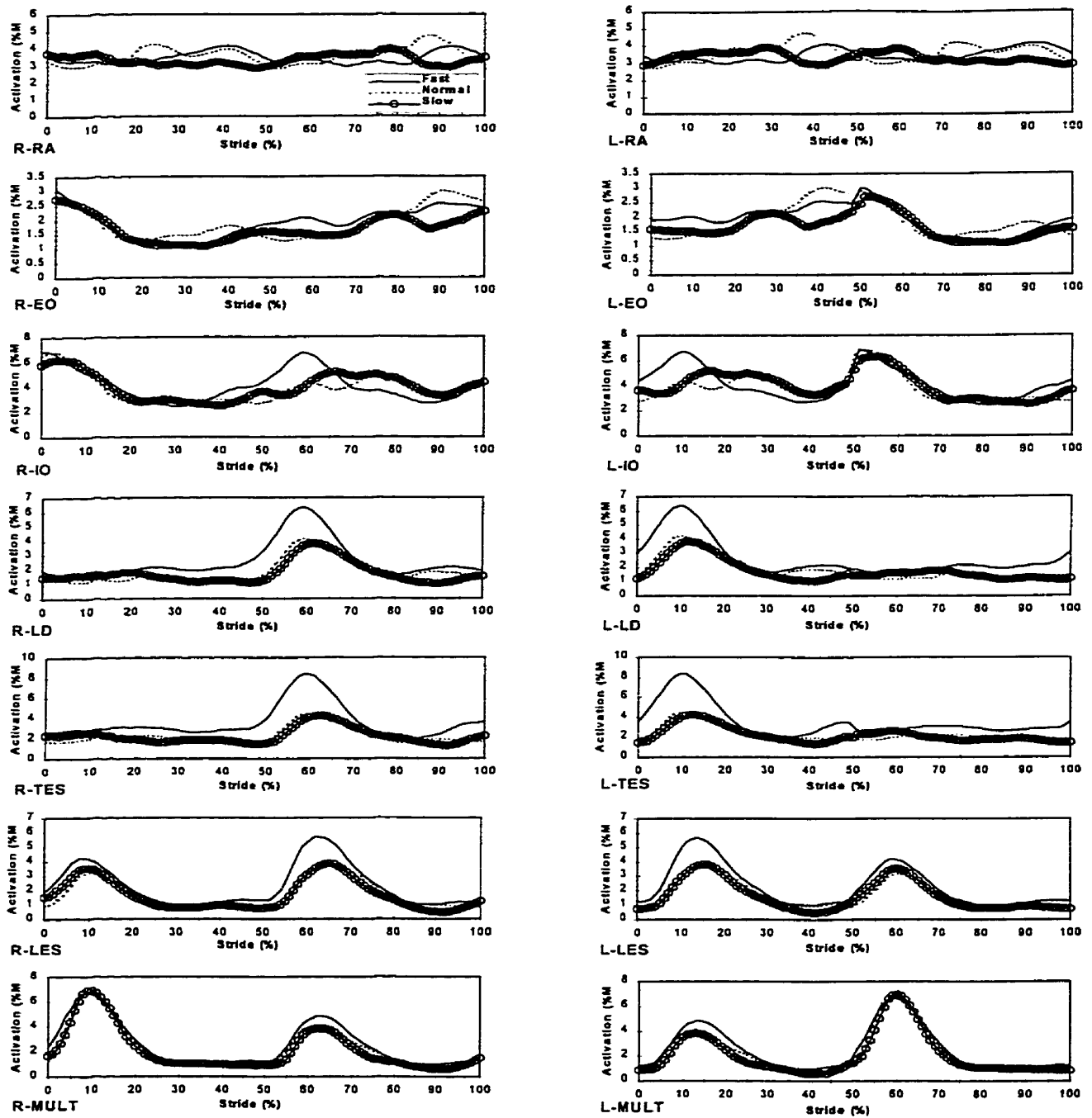


Figure 2.4: The fourteen EMG channels used for the gait analysis. Ensembled data for one participant for three walking cadences with normal arm swing are shown. The right (R-) data was the collected signals with the left (L-) channels being calculated based on symmetrical gait. The curves are normalized for one stride (RHC to RHC) with toe off occurring at 61% (fast), 63% (normal), and 65% (slow) of stride. The seven channels recorded were: rectus abdominis (RA), external oblique (EO), internal oblique (IO), latissimus dorsi (LD), thoracic erector spinae (TES), lumbar erector spinae (LES), and multifidus (MULT).

Table 2.6: Peak activation levels for each of the seven surface EMG sites. The activation has been normalized to maximum voluntary contraction (%MVC).

Participant	Rectus Abdominis		External Oblique		Internal Oblique		Latissimus Dorsi		Thoracic E.S.		Lumbar E.S.		Multifidus	
	Arms	No Arms	Arms	No Arms	Arms	No Arms	Arms	No Arms	Arms	No Arms	Arms	No Arms	Arms	No Arms
Fast Cadence														
1	12	9	7	20	9	9	2	4	5	6	5	6	18	18
2	4	4	2	3	7	11	5	6	13	14	8	10	10	11
3	4	4	3	3	7	12	6	4	8	6	6	5	7	7
4	6	5	5	7	16	13	6	8	3	5	12	15	12	14
5	8	7	12	13	35	41	10	4	11	15	11	18	12	16
Mean	7	6	6	9	15	17	6	5	8	9	8	11	12	13
SD	3	2	4	7	12	14	3	2	4	5	3	6	4	4
Normal Cadence														
1	9	10	6	22	6	7	1	3	5	6	6	5	16	17
2	4	4	2	2	6	6	4	6	12	15	7	8	8	9
3	5	4	3	3	7	11	4	8	5	9	4	5	7	7
4	7	4	6	6	11	12	4	9	4	5	14	17	11	12
5	8	6	8	10	24	28	4	3	8	10	10	14	11	15
Mean	7	5	5	8	10	13	3	6	7	9	8	10	11	12
SD	2	2	2	8	8	9	1	3	3	4	4	5	3	4
Slow Cadence														
1	9	7	5	14	6	6	1	2	3	4	4	5	12	13
2	4	3	2	2	5	4	3	4	12	14	6	7	9	8
3	4	5	3	3	6	8	4	6	4	8	4	4	7	8
4	6	5	5	5	10	10	2	5	2	3	11	11	9	11
5	8	7	8	8	21	20	4	3	8	10	10	14	11	13
Mean	6	6	5	6	10	10	3	4	6	8	7	8	10	11
SD	2	2	2	5	7	6	1	2	4	4	3	4	2	3

Arm Swing Effects

Restricting arm swing during gait increased the amplitude of most variables with the exception of both lateral shear forces (EMG model and rigid link model) and the EMG driven model axial twist moment. Additionally, both the axial twist and lateral bend relative lumbar spine motions p-p ranges were decreased by restricted arm swing. Flexion extension range of motion (p-p) was not altered by lack of arm swing during gait. There was less lateral bend range of motion when arm swing was restricted (Table 2.5). Axial twist demonstrated trends of less rotation when the arms were restricted from free swinging (Table 2.5). The restriction of arm movement increased the activation level of all six of the seven EMG channels (Table 2.6) with the exception of rectus abdominis.

DISCUSSION

In addressing the original objectives, it appears that the lumbar spine experiences low to moderate level loads, depending on walking speed. Additionally increased walking speed increases the lumbar spine range of motion and activation levels of the musculature surrounding the trunk. The restriction of arm swing, a normal testing condition in gait labs and often present in elderly or slow walkers, resulted in increased compressive joint loading and muscular activation levels with decreased lumbar spine motions. At slower speeds walking involves small lumbar spine motion and a more constant joint loading. The addition of muscle forces included in the modeling of the lumbar spine resulted in large increases in compressive loads. This research provides a very detailed approach to gain insight into the magnitude of low

back joint loading during a variety of walking conditions. In addition, while there have been separate studies of lumbar kinematics (Rowe & White. 1996), trunk EMG activation (Cappozzo. 1984; Cromwell, Schultz, Beck, & Warwick. 1989; Keller, Spengler, & Hansson. 1987; Thorstensson, Carlson, Zomlefer, & Nilsson. 1982) and low back loads (Cappozzo. 1983; Cappozzo. 1984; Khoo, Goh, & Bose. 1995) during gait. this study encompasses a comprehensive analysis of the low back during gait.

While this study incorporated a "feet up" analysis of gait, the moments calculated through rigid link segment modeling did not agree with the muscular activation patterns in this study or reported moment profiles (Cappozzo. 1983). However, the forces calculated with this method provided good agreement with previously published literature (Cappozzo. 1983). Potential sources for the error in moment calculation include the assumption of symmetric gait to generate left hip joint moments, modeling of the body (particularly the foot and pelvis) as rigid links, and the inherent assumptions of rigid link segment modeling (point mass at constant location, constant inertia, etc.). The study was limited to five participants due to the intensive data collection and analysis demands. While this limited the power for statistical analyses, the results were quite consistent across participants giving good confidence in the trends found. The results found in this study were calculated based on walking on a flat smooth surface and are not necessarily relevant to all walking scenarios. Walking cadences were altered to generate different conditions (normal, fast, and slow); no attempt was made to control the walking speed or stride length of the participants.

Rigid link segment forces were within the same range as the values reported by Cappozzo (1983). Surprisingly, the peak compressive loads calculated in this study from the

feet upwards using rigid link segment modeling with heel strike transients did not produce maximum joint reaction forces larger than those calculated by Cappozzo (1983) using a kinematic hands down approach. However, both shear components (anterior posterior and medial lateral) exhibited higher peak joint reaction forces when calculated from the floor upward through the rigid link segment structure compared to those reported in the literature (Cappozzo, 1983). Since the peaks coincide with heel contact and toe off the increase in these components can be directly attributed to the impulsive phases of the gait stride.

The shapes of the lumbar kinematics were very consistent with previously reported research (Rowe & White, 1996; Whittle & Levine, 1995). Motion of the pelvis or the opposite motion of the trunk would result in the same relative measure. Smidt et al. (1995) examined the motion of the pelvis during 90% of the maximum straddle position. While the position assumed for the measure of pelvic rotation (Smidt, McQuade, Wei, & Barakatt, 1995) was probably more extreme than the straddle position present at heel contact/toe off, the rotations reported indicate that a large component of the relative lumbar spine motion is as a result of pelvic motion during gait. In contrast Thorstensson et al. (1984) examined the motion of the trunk during human locomotion. The motion of the trunk, at least at the straddle position, seems to offset the rotation of the pelvis maintaining a smaller net range of motion for the lumbar spine. Flexion extension of the trunk was found to be the most variable measure in lumbar kinematics. The data of both Rowe et al. (1996) and Whittle et al. (1995) also demonstrated this large variability between participants. Typically a forward lean when compared to upright standing has been reported for gait (Rowe & White, 1996; Whittle & Levine, 1995). Flexion extension was found to oscillate around upright standing posture for

this study. This discrepancy could be explained by the large spread of postures among the 10 participants examined by Rowe et al. (1996). A second potential explanation of the reduced forward lean could have been attributed to the backpack worn during data collection (mass 1.3 kg). This additional mass could have caused the participants to adopt a forward lean posture as the normal upright standing calibration position thereby obscuring the normal forward lean associated with gait. There have been few studies reporting the magnitudes of lumbar spine range of motion during gait. Rowe et al. (1996) found group averages of 2.3° (flexion/extension), 4.0° (lateral bend) and 6.6° (axial rotation). The only other study reporting lumbar spine motion ranges was by Whittle et al. (1995) with group average ranges of 4.2° (flexion/extension) and 2.9° (lateral bend). The mean ranges of motion for this study are 6.21° (flexion/extension), 6.67° (lateral bend), 7.07° (axial twist) across participants, cadences and arm conditions. While the axial twist provides good agreement with previous research (Rowe & White. 1996) both the lateral bend and flexion extension appear much larger. However, when the differences between the two previous studies (Rowe & White. 1996; Whittle & Levine. 1995) are examined the results of this study lay within the same range of difference. Even with the larger values reported here the maximum p-p ranges are still a very small percentage of the lumbar spine's range of motion (McGregor, McCarthy, & Hughes. 1995). The p-p maximum of axial twist was 14.69°, which corresponds to 26% of the lumbar spine's total range. Both flexion extension (maximum = 10.25°) and lateral bend (maximum = 7.13°) also represent small proportions, 11% and 10% respectively, of the total range of motion of the lumbar spine.

The relatively small motions of the lumbar spine about the neutral position (upright standing) indicate that there will be relatively small contributions of passive structures to the resultant joint moment. The passive structures were calculated to contribute less than 2 N*m of the flexion/extension moment, less than 0.1 N*m of the axial twist moment, and less than 0.005 N*m of the lateral bend moment (mean peak passive moment during the stride). The joint reaction moment should therefore be equivalent to the moment calculated through an EMG modeling approach. This theory is examined in more detail in another publication (Callaghan, Patla, & McGill. 1996). The joint reaction moments calculated using a top down kinematic approach by Cappozzo (1983) provided excellent agreement in moment profiles and exhibited p-p ranges and peak values similar to those calculated in this study using the EMG driven model. The peak moments recorded correspond to 7.2% (flexion extension), 20.6% (lateral bend), 10.7% (axial twist) of the peak isometric moments recorded for a trunk angle of zero degrees (Kumar, Dufresne, & Van Schoor. 1995a; Kumar, Dufresne, & Van Schoor. 1995b).

Calculation of joint forces using a single muscle equivalent model (Khoo, Goh, & Bose. 1995) resulted in a mean peak compressive forces of 171% body weight (range 145% to 207%) during stance phase. Two more detailed models of the trunk musculature (Cappozzo. 1984; Cromwell, Schultz, Beck, & Warwick. 1989) have been used to quantify the joint compressive forces during gait. Cappozzo (1984) implemented a four component single muscle equivalent model to calculate joint compressive forces. Peak loads were 100% to 250% body weight depending on walking speed. Cromwell et al. (1989) utilized an EMG driven model to calculate peak compressive forces of 120% body weight. However, it appears the determination

of joint force was based on equivalent moments in calibration tasks. Therefore during gait the forces calculated would be representative of the muscular contribution and not joint forces since no joint reaction forces were added during the gait analysis. This omission would surely underestimate the total compression force, which is supported by the fact that the values calculated through inverse dynamics result in peaks of 100% body weight. The peak compressive forces calculated using the EMG driven model in this study were between 92% and 345% body weight. While, both these models (Cappozzo. 1984; Khoo, Goh, & Bose. 1995) provide excellent approximations of joint compressive forces, they are limited since no cocontraction was permitted and they are solely dependent on the moments calculated, regardless of muscular activation patterns.

There has been only one study to examine net anterior posterior joint shear force during gait. Khoo et al. (1995) with their single muscle equivalent model reported a mean joint shear value of 22% body weight (range 6% to 63%). Since the model only had muscle forces acting parallel to the spine no component of muscle force (either additive or restorative) were considered. The mean value corresponds to peak values reported from linked segment modeling (Cappozzo. 1983) and the peak values from rigid link segment modeling and EMG modeling employed in this study. There were small reductions in anterior posterior shear calculated from the EMG driven model when compared to the rigid link segment values due to muscle activation. The net joint lateral shear component has not been examined by any other researchers to our knowledge. The inclusion of muscle forces (EMG model) increased the lateral shear forces when compared with the rigid link segment analysis. The anterior posterior shear values calculated using the EMG model represent approximately 15% of the in vitro

anterior failure load (Krypton, Berleman, Visarius, Begeman, Nolte, & Prasad. 1995). There have been no studies examining the lateral shear strength of the lumbar spine.

The restriction of arm swing reduced the lumbar spine range of motion, primarily in the axial twist and lateral bend directions particularly at the normal and faster walking cadences. This would appear to contradict the finding that arm swing reduced axial rotation presented by Elftman (1939). However, the regulation of axial rotation suggested by Elftman (1939) was for whole body. Additionally, he did not fully test this hypothesis by examining various walking styles with and without arm motion. The lack of differences at slow walking could be attributed to the reduced amplitude of arm swing present when walking slowly. While arm swinging does not appear to be of benefit in reducing the range of motion that the lumbar spine experiences during gait, the free swinging of the arms demonstrated reduced peak muscle activation in all muscles recorded with the exception of rectus abdominis. Clearly one benefit of arm swing during gait is reduction of trunk musculature activation levels. This could support the theory of Elftman (1939) that the arms help control the rotations, since when they were restricted from swinging there was an increased muscle activation required.

There was no clear pattern to abdominal muscle recruitment although it was consistently at a low level of activation ($\approx 5\%$ MVC), except for internal oblique which exhibited higher activation in some participants ($\approx 10\%$ MVC). The spinal musculature demonstrated a clear unimodal or bimodal activation pattern dependent on spinal level. The range of peak activation was 10-15 %MVC with clear rest periods between the peaks occurring at toe off. The patterns recorded for the abdominal channel correspond to the description by Cromwell et al. (1989). The erector spinae muscle groups exhibited similar

patterns to those reported in the literature (Cappozzo. 1984; Cromwell, Schultz, Beck, & Warwick. 1989; Thorstensson, Carlson, Zomlefer, & Nilsson. 1982).

Tissue loading during walking appears to be below levels caused by many specific rehabilitation tasks (Axler & McGill. 1995; Callaghan, Gunning, & McGill. 1998), suggesting that walking is a wise choice for general back exercise and rehabilitation programs. For example if the average body mass and normal walking with free arm swing are used for comparison the peak compressive joint loading would be 1670 N. Even the simplest specific back exercise (Callaghan, Gunning, & McGill. 1998) (single leg extension from a kneeling position) surpasses this magnitude of loading. Furthermore, the mild muscle activation levels provide aerobic conditioning which has been suggested to increase muscular endurance (Nutter. 1988). This is an important conditioning concern since a lack of isometric endurance has been shown to be an indicator of potential for developing low back pain (Luoto, Heliövaara, Hurri, & Alaranta. 1995). The risk of developing low back pain was the highest for the individuals in the lowest third of endurance capability. This would strengthen the argument for using walking as an initial aerobic conditioning exercise for several reasons. The first being the low levels of loading, spine motions, and muscular activation should present low risk of injury. Second, the aerobic benefits realised will be more substantial for injured or untrained individuals with reduced benefits as the level of fitness of the participant increases. Holm and Nachemson (1983) demonstrated that motion increased the nutrition to the intervertebral disc indicating that slower walking (a more constant loading on the spine with reduced motion) would not be as beneficial as faster walking with a normal arm swinging motion.

Chapter III

**Low Back Joint Loading and Kinematics During
Standing and Unsupported Sitting**

Jack P. Callaghan and Stuart M. McGill

Submitted to Ergonomics

September, 1998

ABSTRACT

The aim of this study was to examine lumbar spine kinematics, joint loads, and trunk muscle activation patterns during a prolonged (2 hours) period of sitting. An additional question, spurred by controversy in the literature, was whether the low back joint loads were higher in standing or sitting given that many types of jobs require prolonged sitting, standing, or both. Joint loads were predicted with a highly detailed anatomical biomechanical model that incorporated 104 muscles, passive ligaments, and disc which utilized biological signals of spine posture and muscle EMG from each trial of each subject. Sitting resulted in significantly

higher low back compressive loads than those experienced by the lumbar spine during standing ($P < 0.001$). Subjects were equally divided into adopting one of two sitting strategies: a single "static"; or a "dynamic" multiple posture approach. Standing provided a distinctly different spine posture compared with sitting when averaged across all 8 subjects. A rest period was present for all muscles monitored in both sitting and standing tasks. The upper and lower erector spinae muscle groups were more active during sitting. There were no clear muscle activation level differences in the individuals who adopted different sitting strategies. While, standing appears to be a good rest from sitting with respect to lumbar spine posture there would be little rest/change for muscular activation or joint loading. An alternative rest activity such as fast walking provides a cyclic activity for joint loads, muscular activation, and spine postures (Callaghan, Patla, & McGill. 1998) that are uncharacteristic of sedentary workplace tasks such as prolonged sitting or standing.

INTRODUCTION

With increasing computer and desk work associated with most jobs; sitting has become an integral part of most working environments. Prolonged sitting has been linked to causing back pain (Chaffin & Andersson. 1990; Wilder, Pope, & Frymoyer. 1988) which has been attributed to the required changing of the curvature of the lumbar spine (Wilder & Pope. 1996). Sitting has also been linked to spinal tissue damage, with workers spending half their workday seated having three times the likelihood of developing disc herniations (Goel & Weinstein.

1990). Loading that leads to specific damage must be understood in order to develop justifiable injury prevention strategies.

There have been few studies that have examined spine postures assumed when seated in various positions (Keegan. 1953). Seated postures resulted in an increased flexion of the spine, in some postures approaching the same spinal flexion as a fully stooped position. When in-vivo analysis of the relative range of flexion from upright standing to full flexion (Adams & Hutton. 1982; Pearcy, Portek, & Shepherd. 1984) is compared with lumbar spine motion during sitting, it appears that some motion segments could be strained close to the maximum of their in-vivo limit. However, the seated postures examined were recorded for contrived positions assumed for the measurement of spine posture.

Loading on the lumbar spine when seated has been reported to increase when compared to upright standing (Nachemson. 1966). However, these loads measured by in-vivo intradiscal pressure (IDP) have been questioned (Adams & Hutton. 1981). In contrast the in-vivo spine has been shown to increase in stature when seated after a period of standing (Althoff, Brinckmann, Frobin, Sandover, & Burton. 1992), leading to the conclusion that spinal loads are actually lower while seated. An examination of the muscle activation patterns does not provide any clarification in the difference in joint loading between seated and upright postures. The comparison of muscle recruitment between standing and sitting has revealed little difference (Althoff, Brinckmann, Frobin, Sandover, & Burton. 1992; Chaffin & Andersson. 1990).

The primary purpose of this work was to determine low back loading and postural responses to a prolonged sitting posture. Secondary purposes were to assess the difference in joint loading between upright standing and a seated position and determine if spine postures are

altered significantly to allow for unloading of the disc and or load migration to any other tissues at risk. Additionally the range of motion of the lumbar spine was assessed prior to and following seating to examine if prolonged sitting increases the laxity of the spine. An additional goal of this research was the examination of whether the physical demands of standing differ significantly from those of sitting to provide a basis for resting the passive and active tissues in the seated worker.

METHODS

Participants:

Eight male volunteers were recruited from a university student population (age mean 22.4 yr., S.D. 2.4, height mean 174.7 cm, S.D. 9.0, mass mean 74.4 kg, S.D. 7.0). All subjects were healthy and had not experienced any low-back pain for a minimum of one year. Informed consent was obtained from all subjects for the protocol which had been reviewed and received prior approval from the Human Research Ethics Committee of the University of Waterloo's Office of Human Research and Animal Care.

Instrumentation:

Fourteen pairs of disposable Medi-Trace surface electromyogram (EMG) electrodes (Ag-AgCl) were applied to the skin bilaterally: rectus abdominis, 3 cm lateral to the umbilicus; external oblique, approximately 15 cm lateral to the umbilicus; internal oblique below the external oblique electrodes just superior to the inguinal ligament; latissimus dorsi, lateral to T9

over the muscle belly; thoracic erector spinae, 5 cm lateral to T9 spinous process; lumbar erector spinae, 3 cm lateral to L3 spinous process; and multifidus, 3 cm lateral to L5 spinous process (MacIntosh, Valencia, Bogduk, & Munro, 1986). Prior to data collection all subjects performed maximal isometric contractions for all monitored muscle groups to enable EMG normalization. Procedures for obtaining maximum myoelectric activity for normalization have been previously explained in McGill (1991). The raw EMG signal was prefiltered to produce a band width of 20 to 500 Hz and amplified with a differential amplifier (common-mode rejection ratio > 90 dB at 60 Hz and input impedance >10 M ohms above 1 Hz) to produce peak to peak amplitudes of approximately 2 v. The amplified signal was A/D converted at 1024 Hz.

Lumbar curvature was monitored with a 3SPACE ISOTRAK (POLHEMUS, P.O. Box 560, Colchester, Vermont, 05446) and A/D converted using customized software at 20.5 Hz. The ISOTRAK source, which produces an electromagnetic field, was mounted on the sacrum using a custom built harness and the sensor, which detects the rotational motion (three directional cosines) with respect to the source, was mounted over the trunk midline at the T12/L1 spinal level. Lumbar curvature was normalized to normal relaxed upright standing (ie zero position).

Synchronization of the ISOTRAK and EMG signals was accomplished in the following way. The computer controlling the ISOTRAK, at the beginning of the trial, sent a pulse through the A/D converter of a second computer which initiated collection of the EMG signals. Later, selected samples from the A/D converted data (at 1024 Hz) were matched with the appropriate lumbar kinematics frame (at 20.5 Hz).

Data Collection/Reduction:

Collection protocol consisted of three different tasks to determine the level of muscle activation and spinal loading present: sitting for 2 hours, 2 trials of standing for 3 minutes each and 4 lumbar spine range of motion (ROM) tests (Figure 3.1). The chair used by each subject was the seat pan of a normal stenographic type chair with the back support removed. A calibration posture (trunk flexed to 60° from the vertical with a lordotic spine, holding a 10 kg mass in the hands) was recorded (Neumann, Norman, & Wells. 1995) to provide an EMG to moment relationship.

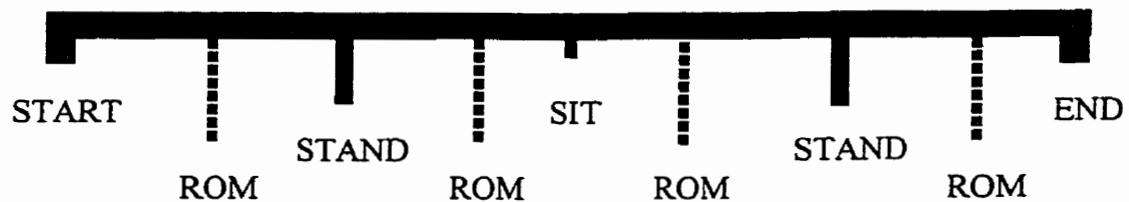


Figure 3.1: The time line of the testing protocol for the 8 subjects. The sitting period was for 2 hours with the standing prior to and following sitting having a duration of 3 minutes. The lumbar spine range of motion tests (ROM) were completed before and after every major task.

Both the EMG and the lumbar spine kinematics were sampled for 3 minutes out of every 15 minute period of sitting (total data collection of 30 minutes out of the 2 hour period) and for the full duration of the standing trials. The time varying demands on the lumbar spine and trunk musculature experienced by the subjects during sitting and standing was the focus of this study, therefore, the Amplitude Probability Distribution Functions (APDF) of the 14 muscles recorded and flexion/extension spine postures were examined. Digital processing of the raw EMG signals included full wave rectification followed by a Butterworth low pass filter

(2.5 Hz cut-off frequency) to produce a linear envelope. The filtered signals were then normalized to the maximum muscle activation that was elicited during the isometric contractions and synchronized to the ISOTRAK signal. Lumbar spine flexion was normalized to the first ROM test that was performed by the subject at the beginning of the test period. The normalized EMG and lumbar spine kinematics levels were then binned in 1% (zero activation was a bin from zero to 0.5%, 1% activation was a bin from 0.5% to 1.5%, etc.) increments to generate an APDF for each individual in sitting and standing as well as an average APDF across all 8 subjects for each of the fourteen EMG channels and flexion/extension of the lumbar spine.

The 3-dimensional moments and L4/L5 joint forces were calculated using an anatomically complex, detailing 104 muscles, dynamic EMG driven low back model (Cholewicki & McGill. 1996; McGill. 1992; McGill & Norman. 1986). The model utilizes calibrated and normalized EMG and low back kinematics to account for passive tissue components. Briefly, first the passive tissue forces are predicted by assuming stress-strain or load-deformation relationships for the individual passive tissues. These passive forces are calibrated for the differences in flexibility of each subject by normalizing the stress-strain curves to the passive range of motion of the subject, detected by electromagnetic instrumentation which monitors the relative lumbar angles in 3D. Then the remaining moment is partitioned amongst the many laminae of muscle based on their myoelectric profile, their physiological cross sectional area, and modulated with known relationships for instantaneous muscle length and either shortening or lengthening velocity (Sutarno & McGill. 1995). This method of using biological signals to solve the indeterminacy of multiple load bearing tissues

facilitates the assessment of the many individual ways that we choose to support loads. In other words, using the EMG and spine posture signals the model was sensitive to the subtle differences that occurred in each trial of every subject. Furthermore, the model was tailored to each individual using the calibration posture which allowed a relationship between EMG activity and a known reaction moment to be established.

One way (dependent variable = task (i.e. sit1 vs stand1), $\alpha = 0.05$) repeated measure analyses of variance (ANOVA) were performed on all levels of activation of the APDFs of the 14 EMG channels, lumbar compression in sit vs stand, and lumbar spine ROM. Post hoc multiple comparisons (TUKEY) were used to examine tasks when a significant difference was found.

RESULTS

Sitting resulted in significantly higher low back compressive loads than those experienced by the lumbar spine during standing ($P < 0.001$). There were two clear patterns of sitting strategies adopted by the individuals in this study; not all subjects sat the same way. Either a single "static" posture was adopted for the duration of sitting or a more "dynamic" multiple postures approach was taken (Figures 3.2 and 3.3). Standing provided a distinctly different spine posture compared with sitting (Figure 3.4). All the muscles monitored exhibited a rest period in both sitting and standing tasks. The peak flexion of the lumbar spine during the four ROM trials demonstrated a non-significant trend towards increased spine flexion

following the two standing tasks and decreased lumbar spine flexion following sitting (Table 3.1).

Table 3.1: Mean and one standard deviation of peak lumbar spine flexion range of motion tests (n =8) expressed as a percent of the initial test (test 1).

Test 1	Test 2	Test 3	Test 4
100	101.4	100.3	103.0
(0)	(2.9)	(4.8)	(6.3)

The mean joint forces at L4/L5 calculated using the EMG driven model demonstrated higher compressive forces in the postures assumed when sitting compared with standing (Figures 3.5 and 3.6). This increase in joint compression was due to increased force levels in the extensor musculature, as a result of slight increases in levels of activation, and increased passive force contribution (in both the ligaments and muscles) due to a more flexed lumbar spine in sitting (Table 3. 2). There was a non-significant increase of approximately 100 N in the joint compressive forces calculated for the standing trial following sitting for two hours compared to the standing trial prior to sitting. Anterior-posterior joint shear forces were higher during sitting than standing (135 N and -13 N respectively, Note: a positive shear value indicates an anterior shearing of the trunk on the pelvis). However, both values are substantially below peak *in-vitro* anterior-posterior shear tolerance values (McGill, Norman, Yingling, Wells, & Neumann. 1998). The medial lateral joint shear values in both sitting and standing were insignificant (approximately 30 N).

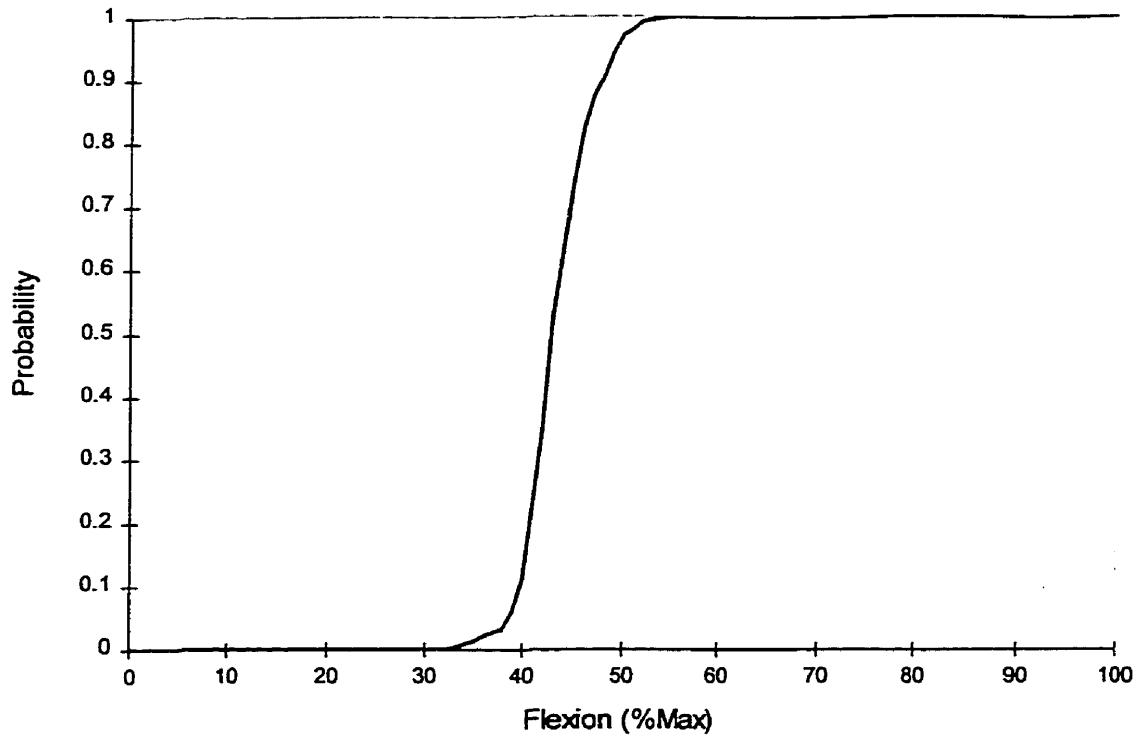


Figure 3.2: An APDF of a static lumbar spine posture adopted by one subject for the duration of a 2 hour period of sitting.

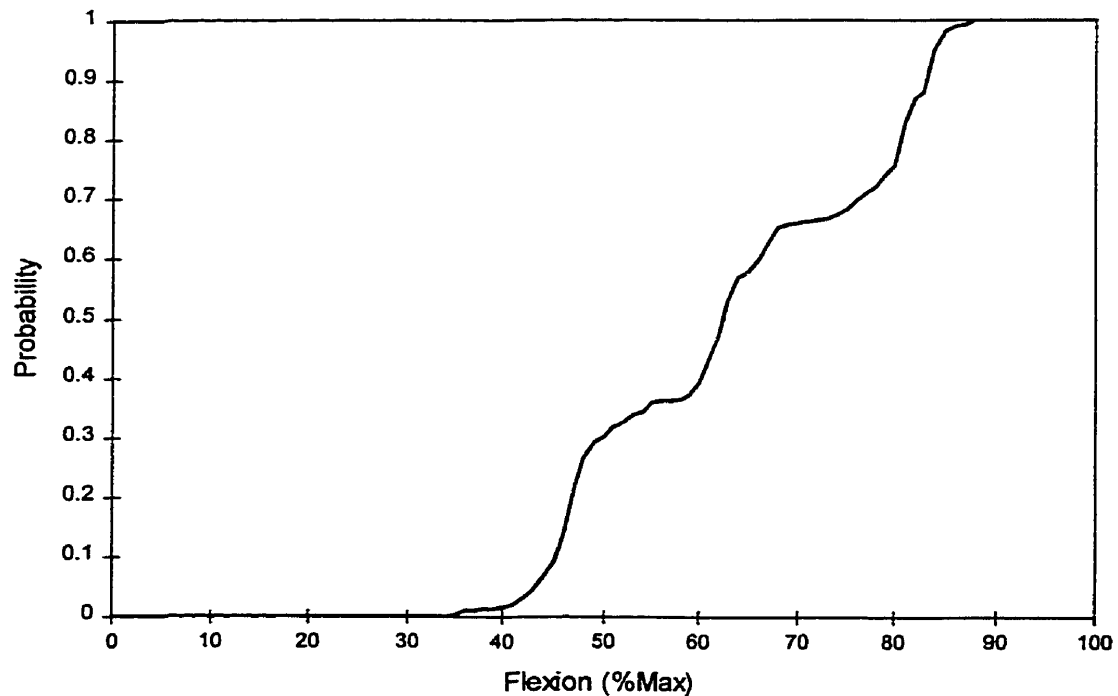


Figure 3.3: An APDF of one subject who adopted "dynamic" lumbar spine postures that varied over a wide range for the 2 hour period of sitting. There are 3 clear postures in which the individual equally divided the sitting period.

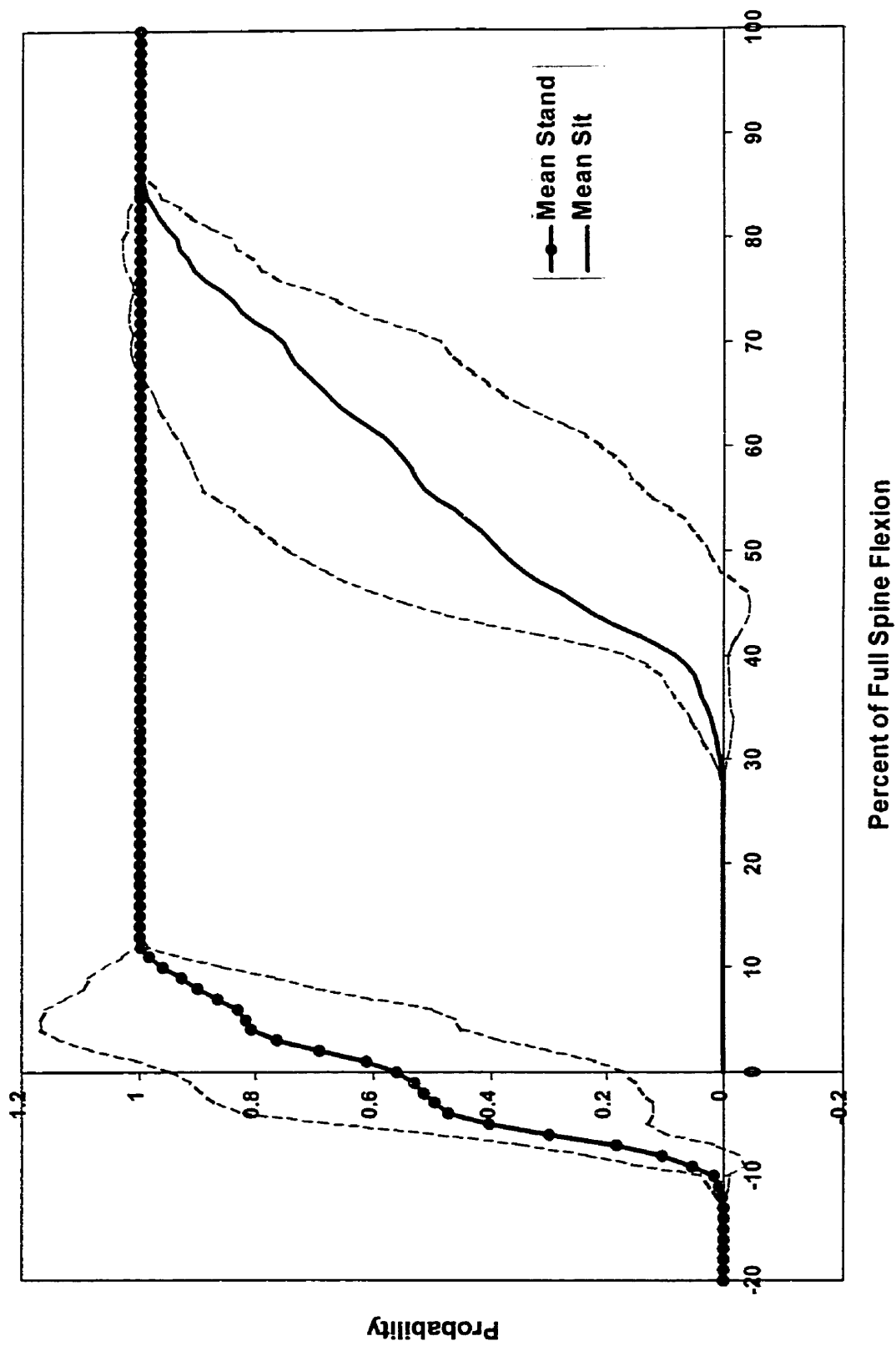


Figure 3.4: Mean and $\pm 1SD$ ($n = 8$) of the postures assumed during the sitting and standing tasks.

The upper and lower erector spinae muscle groups exhibited a shifting of the average APDF curves to the right during sitting. A shift in the APDF curve to the right indicates more time spent at higher activation levels. These shifts were statistically significant at the 1% MVC level for all 4 channels (minimum level of significance $P < 0.05$). The upper erector spinae was also significantly shifted to the right at the 2% MVC level bilaterally (Right: $P < 0.01$; Left $P < 0.05$) and at the 3% MVC level ($P < 0.05$) for the left upper erector spinae across subjects (Figure 3.7). The right latissimus dorsi demonstrated a significant shift ($P < 0.001$) to the right in sitting across subjects, however there was no corresponding change on the left side. There were no changes in any of the abdominal muscle or multifidus activation levels when the sitting APDF was compared to the standing APDF. Individuals who adopted different sitting strategies did not demonstrate any clear differences in the corresponding muscle activation level APDFs. All muscle groups recorded (averaged across the 8 subjects) demonstrated a probability greater than zero of a zero percent activation level on the APDF graphs, indicating that the muscles were all able shut off during both sitting and standing.

Individual subjects presented sitting strategies varying from those adopting a single "static" position (Figure 3.2) which utilized less than a window of 10% of the total flexion ROM of the lumbar spine, to those that had multiple or continuously changing "dynamic" postures (Figure 3.3) which utilized up to a window of 50% of the total lumbar spine flexion ROM. Standing presented a much narrower range of lumbar spine motion than sitting when averaged across all 8 subjects (Figure 3.4). Sitting resulted in lumbar spine postures that varied

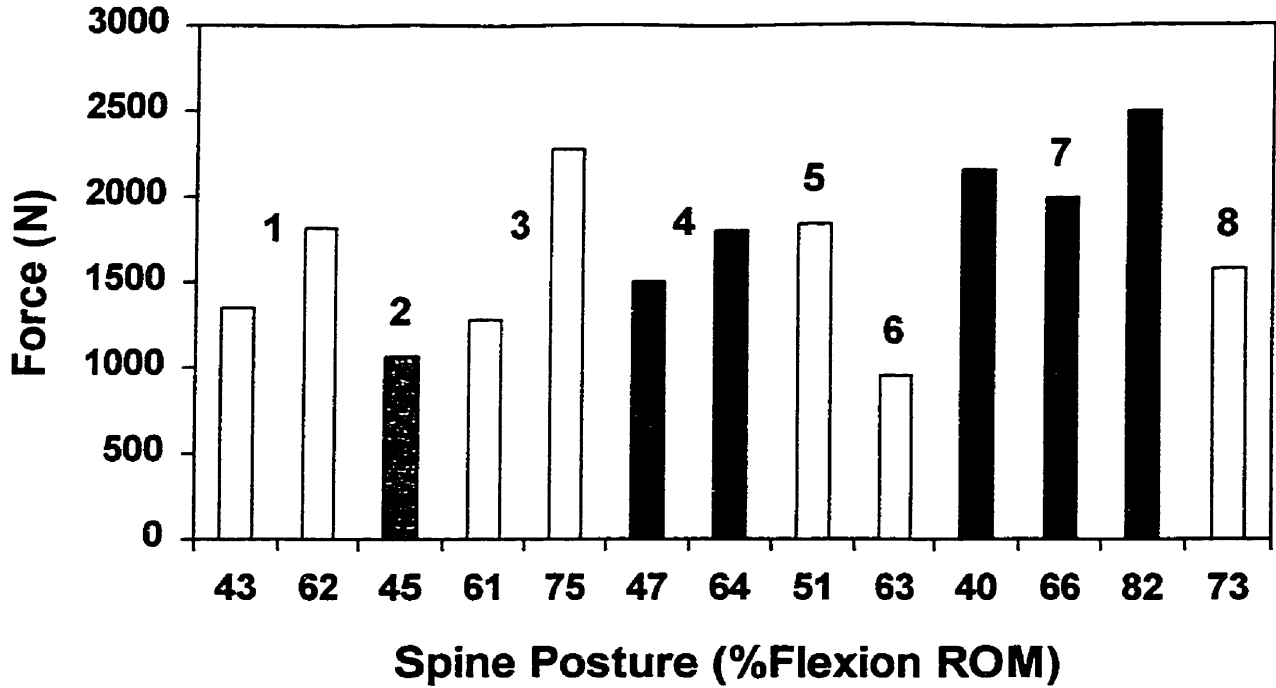


Figure 3.5: The L4/L5 joint compression forces calculated using a three-dimensional EMG driven model for the primary postures adopted while sitting. A representative posture/s for each subject (numbered 1 through 8) was selected based on the APDF of their lumbar spine kinematics.

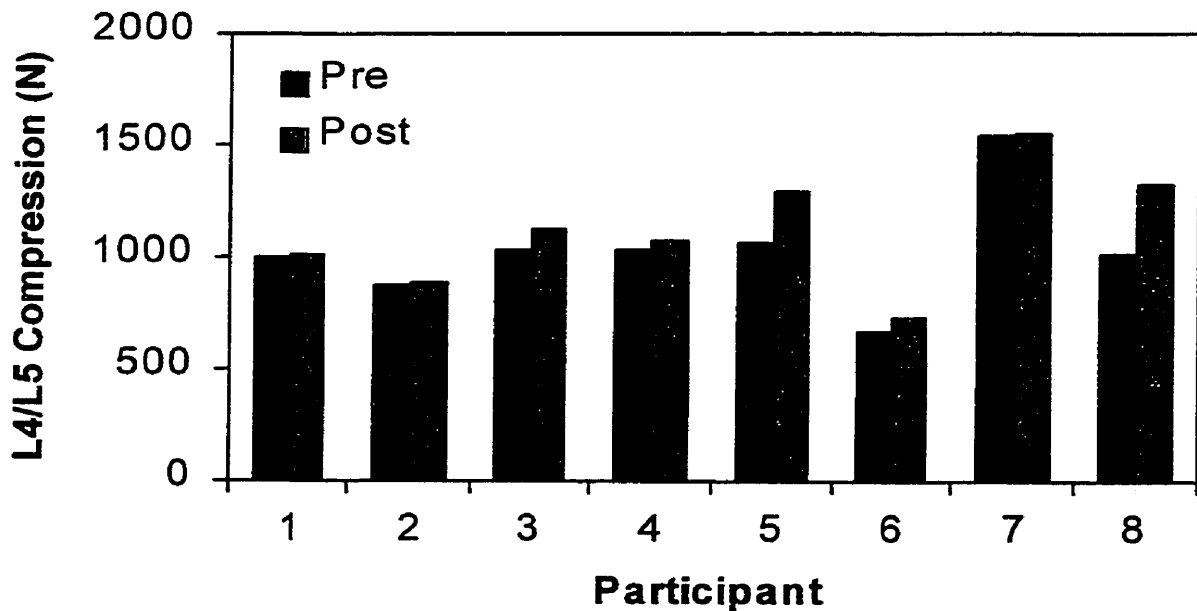


Figure 3.6: Low back joint compression forces (L4/L5) calculated during 3 minutes of standing before and after sitting for 2 hours.

Table 3.2: Muscle and ligament forces from the EMG driven model for subject 1 in standing trial 1 and sitting posture 2 (62% of lumbar spine flexion) and each fascicles active and passive contribution to joint compression and shear.

Muscle	Force (N)		Compression (N)		A/P Shear (N)	
	Stand	Sit	Stand	Sit	Stand	Sit
R RECT AB	17	9	17	8	2	2
L RECT AB	22	19	21	18	2	6
R EX OB 1	4	5	4	5	2	1
L EX OB 1	12	8	11	8	4	4
R EX OB 2	8	3	6	2	4	2
L EX OB 2	17	7	13	4	7	5
R IN OB 1	28	13	25	8	-15	-10
L IN OB 1	27	16	24	14	-13	-8
R IN OB 2	60	25	46	9	-11	-13
L IN OB 2	53	58	41	27	-6	-28
R TRAN AB	5	23	0	1	-3	-17
L TRAN AB	10	21	1	1	-5	-16
R PL 1	12	52	11	51	1	14
L PL 1	11	67	11	65	1	17
R PL 2	13	61	13	60	1	16
L PL 2	12	78	12	76	1	20
R PL 3	16	70	14	66	-6	-12
L PL 3	15	88	13	84	-5	-12
R PL 4	19	79	15	72	-11	-23
L PL 4	17	102	14	94	-10	-26
R ILIOLUM	19	56	19	55	-2	11
L ILIOLUM	25	66	24	65	-2	13
R LONG TH	25	72	25	71	-2	14
L LONG TH	30	85	30	84	-3	17
R QUAD LM	15	52	13	52	6	2
L QUAD LM	13	68	12	68	5	9
R LATDORS	14	26	11	23	2	-2
L LATDORS	8	23	7	22	1	2
R MULT 1	8	31	7	29	0	5
L MULT 1	7	39	6	36	0	7
R MULT 2	8	31	7	30	2	8
L MULT 2	6	39	6	38	2	10
R PSOAS 1	25	11	24	10	4	2
L PSOAS 1	17	30	16	29	3	5
R PSOAS 2	25	11	24	10	4	2
L PSOAS 2	17	30	16	29	3	5
R PSOAS 3	25	11	24	10	4	2
L PSOAS 3	17	30	16	29	3	5
R PSOAS 4	25	11	24	10	4	2
L PSOAS 4	17	30	16	29	3	5
Ligaments						
ANT L	1	0	1	0	0	0
POST L	0	11	0	11	0	2
LIGFLAV	3	8	3	8	0	1
R IN TR	0	1	0	1	0	0
L IN TR	0	2	0	2	0	0
R ARCTIC	0	1	0	1	0	0
L ARCTIC	0	3	0	2	0	2
R ART 2	0	0	0	0	0	0
L ART 2	0	3	0	2	0	0
IN SPN1	0	2	0	2	0	1
IN SPN2	0	16	0	10	0	14
IN SPN3	0	14	0	8	0	12
SUP SPN	0	7	0	7	0	1
R LDF	0	2	0	2	0	0
L LDF	0	6	0	5	0	0
Upper Body Weight (N)			350	350		
Sum			993	1813	-23	79

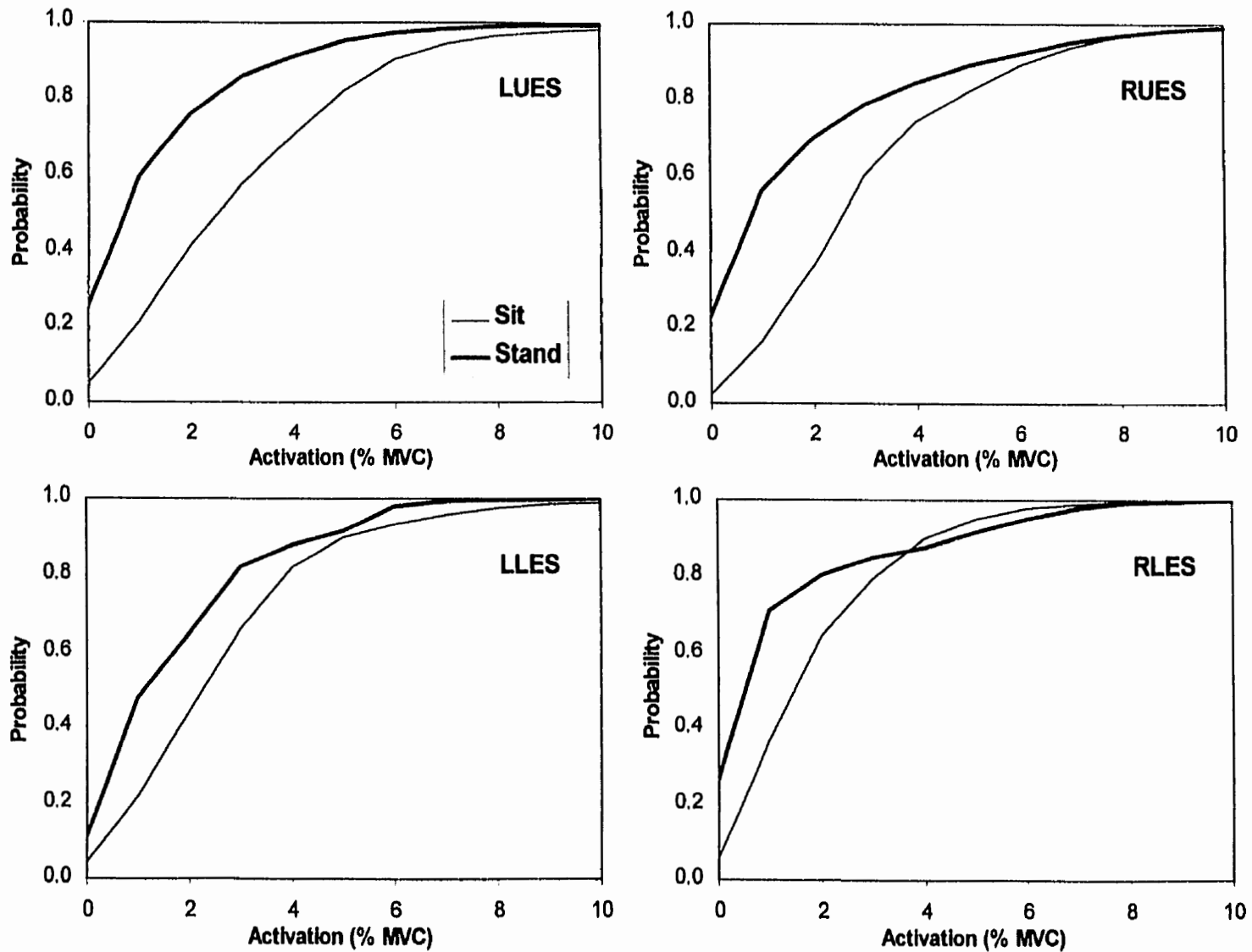


Figure 3.7: Average muscle activation APDFs across 8 subjects for the 2 hour sitting period and the 2 standing periods. (RUES: Right Upper Erector Spinae; RLES: Right Lower Erector Spinae; LUES: Left Upper Erector Spinae; LLES: Left Lower Erector Spinae).

between approximately 30% and 80% of the lumbar spine ROM with 0% referring to the posture assumed during normal upright standing and 100% representing full forward flexion. Whereas standing resulted in a much narrower range of lumbar spine motion, varying approximately 10% of the ROM around the normal upright standing posture of the lumbar spine. The average APDF of standing posture demonstrated a shift to postures that were completely outside the postures assumed during sitting.

DISCUSSION

While spine loading during prolonged sitting and standing tasks was quite low, each task presents sufficiently different lumbar spine postures to constitute a rest break for workers who are able to alternate sitting with standing. However, due to the prolonged loading caused by the exposure to these tasks there appears to be potential for injury through fatigue mechanisms. The human body requires movement to both nourish structures, in this case the nucleus pulposus and the intervertebral disc (Holm & Nachemson. 1983), and provide periodic rest of muscles to prevent fatigue (Jonsson. 1978; Veiersted, Westgaard, & Andersen. 1990) and occasional migration of loads on various passive tissues from posture change. In sitting, individuals that adopted multiple postures and cycled between them across a wider band of lumbar spinal motion also created motion that appeared to prevent static loads on the spine. However, while passive tissues might be relieved in these individuals, there was little difference in the magnitude of the joint compressive forces present in the multiple positions

adopted. Standing resulted in a very different lumbar spine posture than that adopted during sitting which could provide relief/rest for the passive and active structures of the low back.

The compressive forces on the low back were increased when a sitting posture was assumed. The difference between the standing and sitting joint loading was due to the increased flexed posture of the lumbar spine assumed when seated and slight increases in extensor EMG levels. Low levels of EMG were recorded for all channels in both sitting and standing activities. There was a trend of decreased flexion ROM after sitting (*non-significant) which would appear to support the finding that the lumbar spine increases height while exposed to sitting (Althoff, Brinckmann, Frobin, Sandover, & Burton. 1992) (increased disc height = reduced joint laxity). However, one potential confounder to this line of thought could be the finding that motion increased nutrition to the intervertebral disc (Holm & Nachemson. 1983) and sitting presents a far less static loading on the spine than standing for some individuals. During sustained flexion tests the nucleus has been shown to migrate posteriorly and result in increased stress concentrations in the posterior aspect on the intervertebral disc (Adams & Hutton. 1985; Adams, McNally, Chinn, & Dolan. 1994). This shifting of the nucleus could also be another factor that could alter the flexion ROM test following sitting.

There have been few studies that have examined spine postures assumed when seated in various positions. Keegan (1953) used lateral x-rays on four normal adults (2 male, 2 female) to assess the postural changes that occurred in the lumbar spine when various seated or flexed postures were assumed. Half of the subjects in this study adopted a single "static" posture which remained relatively constant throughout the two hours of sitting. However, by examining an extended period of seated work, it was also discovered that 50% of the

individuals studied preferred to alter their lumbar spine posture frequently. A consideration for chair design/use driven by the examination of individual sitting postures suggests that varying sitting posture allows the spine to move, rather than constraining individuals to an "ideal" position.

An examination of the muscle activation patterns reported in the literature does not provide any clarification in the difference in joint loading between seated and upright postures. The comparison of muscle recruitment between standing and sitting has revealed little difference in activation profiles (Althoff, Brinckmann, Frobin, Sandover, & Burton. 1992; Chaffin & Andersson. 1990). These findings were supported by the current study for the abdominal musculature, the latissimus dorsi, and the multifidus. However, both the upper and lower erector spinae exhibited a decreased amount of time spent at lower levels of contraction during sitting. While these levels were still within the proposed levels to avoid static overload of the musculature (Nakata, Hagner, & Jonsson. 1992) and demonstrated periods of rest when averaged across the 8 subjects, this could be a potential source of the back pain reported by many individuals when exposed to prolonged periods of sitting.

While electromyographic analysis of the trunk musculature has shown that both lumbar supports and seat back inclination angle reduce activation (Andersson, Murphy, Örtengren, & Nachemson. 1979; Chaffin & Andersson. 1990; Knutsson, Kindh, & Telhag. 1966), the current study only examined sitting with no back support. This was primarily due to instrumentation requirements but also provided insight into the unconstrained lumbar spine kinematics that are present during sitting. Additionally, when people work at a desk they often lean forward and do not rest against the back support of a chair. Sitting periods of 2 hours were examined. While

some individuals often sit for periods exceeding this duration, 2 hours was thought to represent the longest typical uninterrupted period of exposure for most office employees before receiving a lunch or coffee break.

CONCLUSIONS

The forces experienced by the lumbar spine during these activities fall well below any single exposure tissue tolerance value. However, prolonged static loads could present a cumulative injury mechanism. Standing appears to be a good rest from sitting with respect to lumbar spine posture. Therefore, the two activities (sitting and standing) used alternatively as a rest could form a basis for injury prevention when designing work. However, there would be little rest/change for muscular activation or joint loading. Combining an activity such as walking (fast) would provide a cyclic activity for joint loads, muscular activation, and spine postures (Callaghan, Patla, & McGill. 1998). This would suggest that walking would be a beneficial rest activity in combination with sitting, or standing.

Chapter IV

**The Relationship Between Lumbar Spine Load and Muscular Activity
During Extensor Exercise**

Jack P. Callaghan, Jennifer L. Gunning, and Stuart M. McGill

Physical Therapy Volume 78(1), 8-18, 1998

ABSTRACT

Background and Purpose. There have been no previous studies that quantitatively assessed the spine loading present during trunk extensor exercises. The purpose was to investigate the lumbar spine joint loading and trunk musculature activation levels while performing typical trunk extensor strengthening exercises.

Subjects. Thirteen male participants (mean age=21.0 years, S.D.=1.0, range=19-23; mean height=176.0 cm, S.D.=6.2, range=165-188; mean mass=77.0 kg, S.D.=7.0, range=63-89).

Methods. The participants performed four different back exercises. Myoelectric activities were recorded from 14 trunk muscles. The postures that corresponded to the maximum external

moment were identified and quantified using rigid body modeling combined with an EMG driven model to determine joint loading at the L4/L5 joint. Exercises were then evaluated based on the lumbar spine loading and peak muscle activation levels. A reference task of lifting 10 kg from mid thigh was included for comparison.

Results. The exercises involving active trunk extension produced the highest joint forces and muscle activity levels. Exercises involving leg extension with the spine held isometrically demonstrated asymmetrical activity of the trunk muscles thereby reducing loads on the spine.

Conclusion and Discussion. The back extensor exercises examined provided a wide range of joint loading and muscle activity levels. Single leg extension tasks appear to constitute a low risk exercise for initial extensor strengthening, given the low spine load and mild extensor muscle challenge. When combined with a contralateral arm extensions the challenge and demand of the exercise was increased. The compressive loading and extensor muscle activity levels were highest for the trunk extension exercises.

INTRODUCTION

Low back extensor exercises are prescribed for a variety of reasons, but mainly for rehabilitation of the injured low back, prevention of injury, and as a component of fitness training programs to enhance performance levels. The objective of exercise is often to place stress on both damaged and other healthy supporting tissues to foster tissue repair and strengthening while avoiding excessive loading that can exacerbate an existing structural weakness. From our experience, many traditional extensor exercises generate high spine loads

as a result of externally applied compressive and shear forces (either from free weights or resistance machines). Although knowledge of tissue forces is important to avoid further injury, little work has been performed to quantify these forces during trunk exercises. The overall objective of our research was to examine the load on the low back together with muscle activity levels during typical back extensor exercises.

The reported effectiveness of various training and rehabilitation programs for the low back is quite variable, with some authors claiming great success but other authors reporting no, or even negative results (Battie, Bigos, Fisher, et al. 1990; Koes, Bouter, Beckerman, van der Heijden, & Knipschild. 1991). The cause of this tissue damage has been attributed to excessive spine flexion (Halpern & Bleck. 1979; Nachemson. 1966; Nachemson & Morris. 1964), disadvantageous muscle lengths in some postures (Vincent & Britten. 1980), or inappropriate orientation of internal structures of the torso with respect to the legs (Jette, Sidney, & Cicutti. 1984). The contradictory findings regarding the effectiveness and safety of exercise programs in various reports (Malmivaara, Hakkinen, Aro, et al. 1995) may be due to the prescription of inappropriate exercises. Specifically, a poorly selected exercise could exacerbate an existing injury by excessively loading the damaged structure.

Although some exercises for the low back have been recommended for their capacity to maximize muscle activity (Flint. 1965; Walters & Partridge. 1957), virtually none have been examined by analysing the forces they generate on the spine. Fortunately sophisticated techniques are being developed that facilitate investigation of the loads that lead to injury in a variety of possible injury sites. Knowledge of the tissue loads is necessary to permit the testing

of hypotheses designed to reduce the risk of injury, from a preventative standpoint, and to optimize the loading that results from various rehabilitation programs for the injured.

The purpose of our research was to quantitatively identify exercises that optimized the challenge to extensor muscles, which stabilize and support the low back, while simultaneously placing minimal load on the lumbar spine. We hypothesized that some low back extensor exercises result in higher extensor muscle activity levels but lower lumbar spine loading due to the reduced muscular co-contraction.

METHODS

Participants:

Thirteen male volunteers were recruited from a university student population (mean age=21.0 years, S.D.=1.0, range=19-23; mean height=176.0 cm, S.D.=6.2, range=165-188; mean mass=77.0 kg, S.D.=7.0, range=63-89). None of the subjects had experienced any low-back pain for a minimum of one year. Therefore, whether patients with low back pain would perform the exercises similarly and have similar muscle activity and load levels was not studied. Informed consent was obtained from all participants for the protocol which had been reviewed and received prior approval from the Human Research Ethics Committee of the University of Waterloo's Office of Human Research and Animal Care

Instrumentation:

Fourteen pairs of disposable Medi-Trace surface electromyogram (EMG) electrodes (Ag-AgCl) (Graphic Controls Canada Ltd, 215 Herbert St, Gananoque, Ontario, Canada, K7G

2Y7) were applied to the skin bilaterally: rectus abdominis, 3 cm lateral to the umbilicus; external oblique, approximately 15 cm lateral to the umbilicus; internal oblique below the external oblique electrodes just superior to the inguinal ligament; latissimus dorsi, lateral to T9 over the muscle belly; thoracic erector spinae, 5 cm lateral to T9 spinous process; lumbar erector spinae, 3 cm lateral to L3 spinous process; and multifidus, 3 cm lateral to L5 spinous process (MacIntosh & Bogduk, 1987). Prior to data collection all participants performed maximal isometric contractions for all monitored muscle groups to enable EMG normalization. Procedures for obtaining maximum myoelectric activity for normalization have been previously explained in McGill (1991). Briefly, three tasks were used to elicit maximum EMG activity from the 14 recorded sites. The abdominal muscle groups were recruited with a modified bent-knee sit-up, the trunk extensors were activated by cantilevering the trunk over the end of a bench, and the latissimus dorsi was recruited with a simulation of a lat pull down exercise. All three maximal effort tasks were performed against an equal resistance (isometric) supplied by the experimenter. The raw EMG signal was prefiltered to produce a band width of 20 to 500 Hz and amplified with a differential amplifier (common-mode rejection ratio > 90 dB at 60 Hz and input impedance >10 M ohms above 1 Hz) to produce peak to peak amplitudes of approximately 2 v. The amplified signal was A/D converted at 1024 Hz.

A sagittal view of the participants right side for all trials was recorded on video tape, at a frame rate of 30 Hz, which allowed flexion/extension moments about the L4/L5 joint to be calculated. A transverse plane view was also recorded for two exercises (single leg extensions) to allow the twist moment about L4/L5 to be determined. Lumbar curvature was monitored with a 3SPACE ISOTRAK (POLHEMUS, P.O. Box 560, Colchester, Vermont, 05446) and a/d

converted at 20.5 Hz using customized software developed at the Occupational Biomechanics and Safety Laboratories at the University of Waterloo (Waterloo, Ontario, Canada). The ISOTRAK source, which produces an electromagnetic field, was mounted on the sacrum using a custom built harness and the sensor, which detects the rotational motion (three directional cosines) with respect to the source, was mounted over the trunk midline at the T12/L1 spinal level.

Synchronization of the ISOTRAK, EMG and video signals was accomplished in the following way. The computer controlling the ISOTRAK, at the beginning of the trial, sent a pulse through the A/D converter of a second computer which initiated collection of the EMG signals. The same synch pulse activated a light emitting diode in the field of view of the camera to mark the beginning of the trial. Later, selected samples from the A/D converted data (at 1024 Hz) were matched with the appropriate video frame (at 30 Hz).

Data Collection:

Seven exercises were performed to determine the level of muscle activation and spinal loading. For the first 4 exercises the participants were positioned on their hands and knees. Exercise 1 and 2 consisted of a single leg lift, performed by extending one leg out to the horizontal and returning it to the starting position. In Exercise 1 the right leg was lifted and in Exercise 2 the left leg was lifted (Figure 4.1). Exercises 3 and 4 coupled the exercises in one and two with the contralateral arm raised simultaneously to the horizontal before being returned to the original position. Exercise 3 (Figure 4.2) involved lifting the right leg and left arm. Exercise 4 required lifting the left leg and right arm. For exercises 5 and 6 the participants were in a prone position. In exercise 5 (Figure 4.3) the upper body and legs are raised

simultaneously from the floor to a maximal comfortable elevation, with active spine extension, before being returned to the starting position. The trunk was cantilevered over a bench in exercise 6 (Figure 4.4). A Velcro® (Velcro USA Inc, 406 Brown Ave, Manchester, NH 03108) strap fastened proximal to the ankle was used to secure the lower limbs to the bench. The exercise started with the participants in a fully flexed posture followed by trunk extension until it was parallel with the ground. For all of the above exercises, ten seconds were allotted to perform one trial that consisted of three repetitions of the movement in succession. Participants rested for at least one minute between trials. The seventh exercise was performed to enable a calibration of EMG activity to external moment. Participants stood with feet shoulder width apart and knees slightly bent. Holding a 10 kg weight in front of them, arms hanging straight down, they positioned their trunk at an angle of 60 degrees from the vertical, maintaining a lordotic curvature in the spine. This posture was held for 10 seconds.

Three repetitions of all exercises were performed, for a total of 21 exercises per subject. The order of exercises was randomly assigned. For exercises 1 and 2 sagittal and transverse views were captured on video. Sagittal views were filmed for exercises 3 through 7.

Data Reduction:

The peak loading experienced by the subjects during the back exercises was the focus of this study. We therefore analyzed the postures representing this component of the exercises.

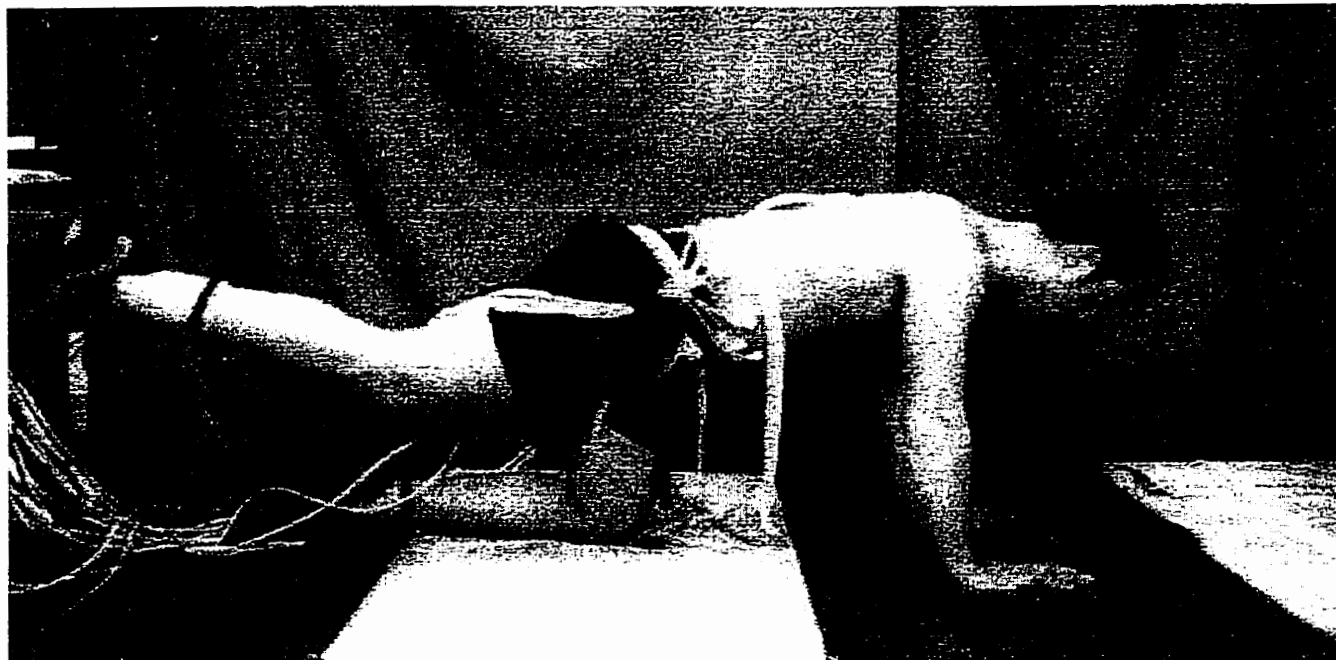


Figure 4.1: Exercise one and two involved extension of the leg to horizontal. The exercise was performed for both legs (Right Leg (RL) and Left Leg (LL)). The posture shown was chosen as representing the most challenging instant.

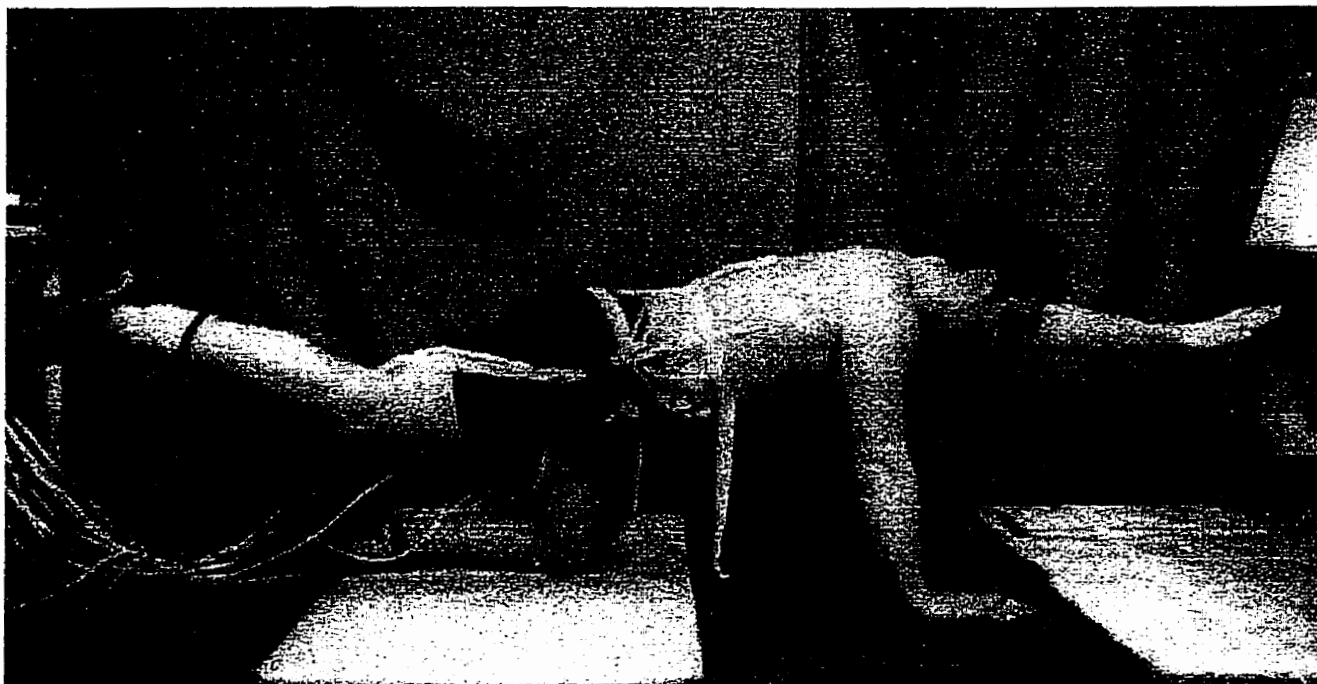


Figure 4.2: Extension of the contralateral arm combined with leg extension constituted exercises three and four. The posture shown was used to represent the instant of peak loading. Both sides of the body were exercised (Right Leg - Left Arm (RL&LA) and Left Leg - Right Arm (LL&RA)).

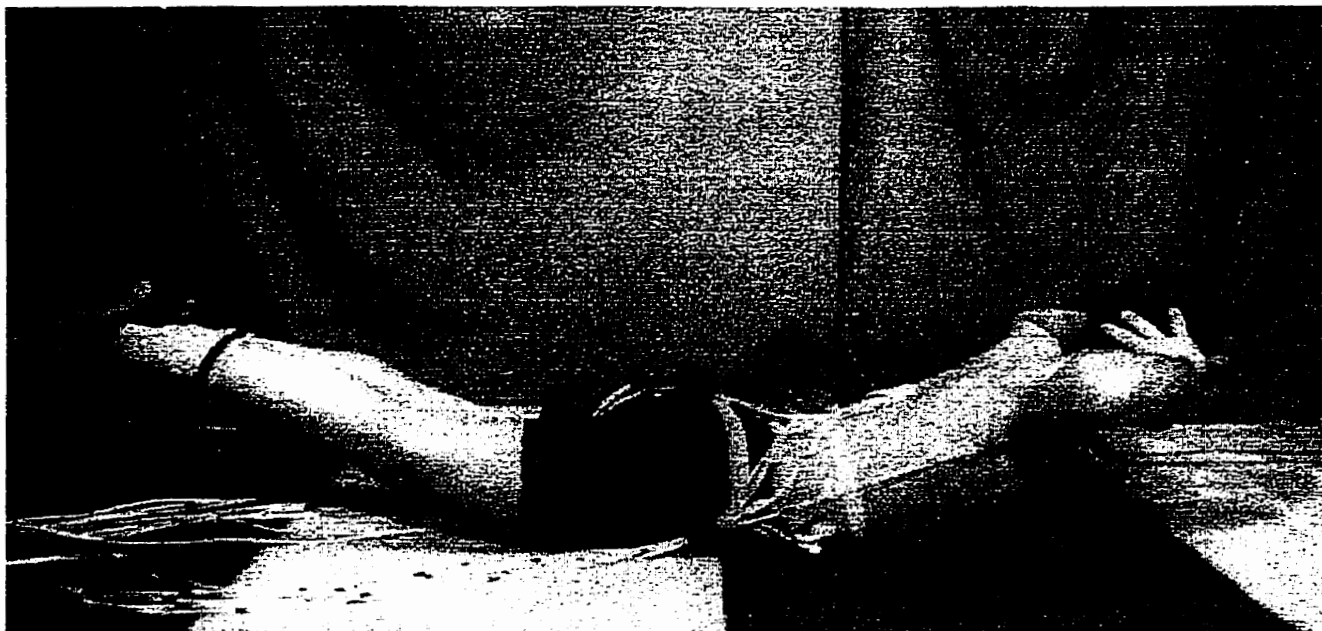


Figure 4.3: Active trunk extension combined with leg extension was the fifth exercise (T&L). The exercise was initiated from a prone posture on the floor, the participants performed active trunk and leg extension (maximum comfortable) and returned to the prone position.

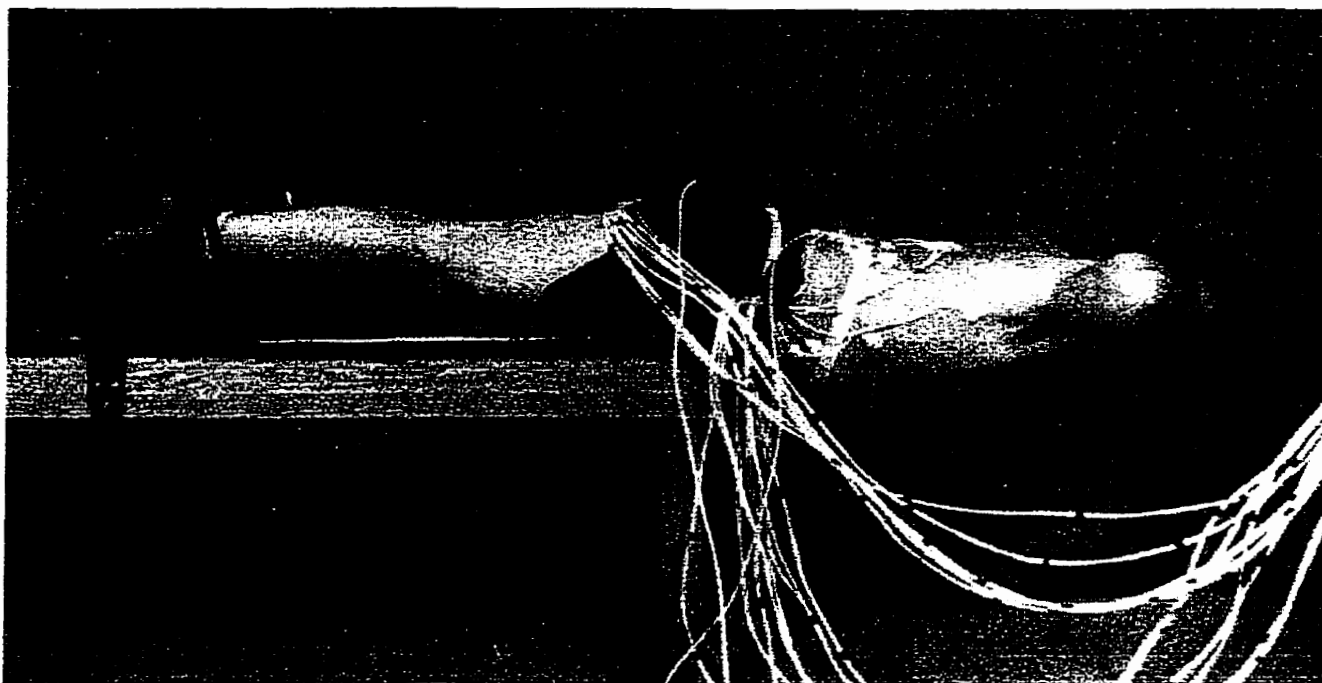


Figure 4.4: Exercise six involved a large range of motion. The start position was a fully flexed posture, followed by active extension until the trunk was horizontal to the ground (T), which corresponded to the peak loading posture (shown here).

The ISOTRAK data, representing lumbar curvature, was used to determine the interval of maximum spinal extension. A window containing the point of maximal extension and one degree before and after it was selected. This interval also represented the greatest extensor moment, as identified by video analysis. The chosen intervals for each repetition of an exercise were averaged to get a single value of spine curvature. Spinal curvature was normalized to the curvature during relaxed upright standing (i.e., 0°). Defining the posture of the lumbar spine during the normal standing position as zero degrees (the reference point between flexion and extension) allows the amount of spine motion to be quantified within each individual and provides a common definition of the zero point for comparison between individuals.

Digital processing of the raw EMG signals included full wave rectification followed by a Butterworth low pass filter (2.5 Hz cut-off frequency) which resulted in a linear enveloped signal. The filtered signals were then normalized to the maximum muscle activity that was elicited during the isometric contractions and synchronized to the ISOTRAK signal. The corresponding EMG windows for each repetition of an exercise were averaged for each of the fourteen EMG channels.

A representative posture of maximum extension was identified using synchronized ISOTRAK data for all exercises. The corresponding video data was digitized using a video capture system. Scaled joint co-ordinates were obtained with the use of customized software and were used to calculate extensor moments about the L4/L5 joint for all exercises as well as twist moments for exercises 1 and 2, using typical two-dimensional rigid link-segment modeling.

A Brief Description of the Laboratory Modeling Approach

Individual tissue loads have been predicted from a laboratory technique and model developed over the past fourteen years by McGill and colleagues (Cholewicki & McGill. 1996; McGill. 1992; McGill & Norman. 1986). The model is composed of two distinct parts. First, a rigid link segment representation of the body was used to calculate reaction forces and moments about a joint in the low back (L4/L5, previously described in McGill and Norman (1985)). Joint displacements were recorded on video camera at 30 Hz to reconstruct the joints and body segments. The first model produces the reaction forces and corresponding moments about the axes of the low back (flexion-extension, axial twist). The second anatomically detailed model enables the partitioning of the reaction moments obtained from the link segment model into the substantial restorative moment components (supporting tissues) using an anatomically detailed 3-dimensional representation of the skeleton, muscles, ligaments, non-linear elastic intervertebral discs, etc. This part of the model was first described in McGill and Norman (1986), with full 3-dimensional methods described in McGill (1992), and the most recent update provided by Cholewicki and McGill (1996), where a total of 90 low back and torso muscles are represented.

First, the passive tissue forces are predicted by assuming stress-strain or load-deformation relationships for the individual passive tissues. These passive forces are individualized for the differences in flexibility of each subject by scaling the stress-strain curves to the passive range of motion of the subject. The active range of motion was detected by electromagnetic instrumentation that monitors the relative lumbar angles three-dimensionally. Once the contributions of the passive tissues have been calculated, the

remaining moment is then partitioned amongst the many laminae of muscle based on their EMG profile, their physiological cross sectional area and modulated with known relationships for instantaneous muscle length and either shortening or lengthening velocity (force velocity updated by Sutarno and McGill (1995)). This method of using biological signals to solve the indeterminacy of multiple load bearing tissues facilitates the assessment of the many ways that we choose to support loads, an objective that we believe is necessary for evaluation of various tasks prescribed in exercise and rehabilitation programs.

Although the major asset of this biologically based approach is that muscle cocontraction is fully accounted for together with being sensitive to the differences in the way that individuals perform a movement, estimations of muscle force based, in part, on EMG signals are problematic as the force per muscle cross sectional area must be assumed together with other variables that are known to modulate muscle force production. Furthermore, accurate anatomical detail is essential to satisfy the moment requirements about all three joint axes and about several joints simultaneously.

A major drawback of the EMG based approach is the inaccessibility of the deeper torso muscles (e.g. psoas, quadratus lumborum, three layers of the abdominal wall). In an attempt to address this drawback, recent work by McGill, Juker, and Kropf (1996) used indwelling intramuscular electrodes with simultaneous surface electrode sites to evaluate the possibility, and validity, of using surface activity profiles as surrogates to activate deeper muscles, over a wide variety of tasks and exercises (e.g. sit-ups, curl-ups, leg raises, push-ups, some spine extensor tasks, lateral bending, and twisting tasks). Prediction of the activity of these deeper

muscles is possible from well chosen surface electrodes within the criterion of 15% of MVC (RMS difference) (McGill, Juker, & Kropf. 1996).

One way (dependent variable = task, $\alpha = 0.05$) repeated-measures analyses of variance (ANOVA) were performed on all 14 EMG channels, lumbar compression, and shear loading results. TUKEY's *post hoc* multiple comparisons were used to examine tasks when a significant difference was found.

RESULTS

Tasks involving active trunk extension against gravity produced the highest demands on the musculoskeletal system. The two trunk extension trials (trunk and leg extension , trunk extension) resulted in the highest extensor muscle activation (Table 4.1) combined with the largest compressive joint forces (Figure 4.5). Overall, the tasks involving the lowest joint load and muscular activity levels were the two single leg extension tasks (right leg extension, left leg extension). Leg extension coupled with contralateral arm extension (right leg and left arm extension, left leg and right arm extension) significantly increased the joint compression forces (1000 N, $P < 0.001$) and upper erector spinae activity levels (30%, $P < 0.0001$) compared with single leg extension. The joint compressive force showed a significant increase with increasing demand of the exercise when single leg extension was compared with combined arm and leg extension (1000 N, $P < 0.001$), and combined arm and leg extension was compared with trunk extension (1200 N, $P < 0.001$). Due to the different loading of the tasks involving leg extension and those requiring trunk extension, (i.e. upper vs. lower body support) the polarity of the

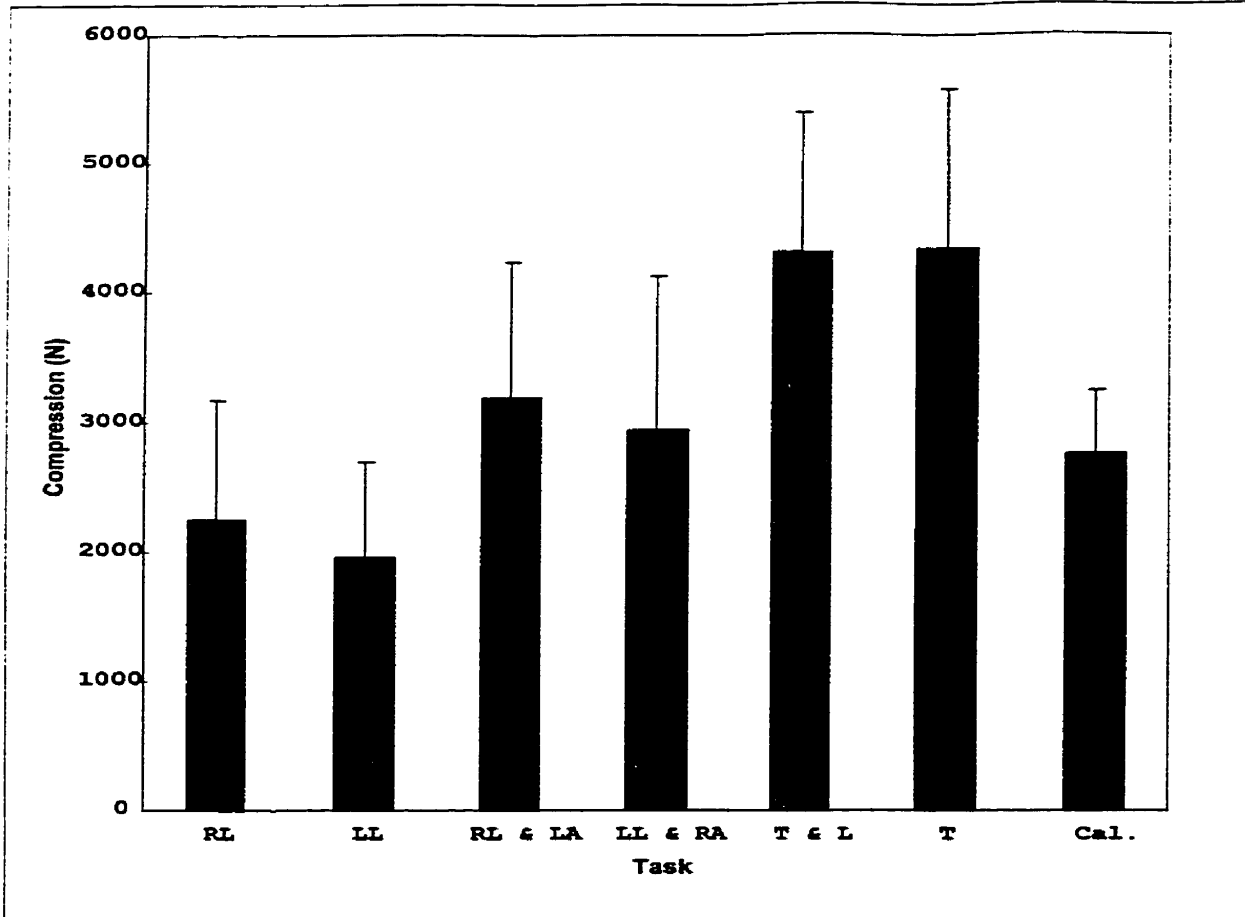


Figure 4.5: EMG model predictions of joint compression, mean and standard deviation for all trials and across all participants.

anteroposterior shear forces were opposite (Figure 4.6). The magnitude of the shear forces for all exercises, however, fall below that occurring in the 10 kg lift and are small compared to recently suggested in-vitro tolerance levels (Krypton, Berleman, Visarius, Begeman, Nolte, & Prasad. 1995; Yingling & McGill. 1998). Similarly, all lateral shear magnitudes were negligible (Figure 4.7), primarily due to the symmetrical nature of the tasks involving active trunk extension (bilateral muscle activation) and offsetting muscle activation in the isometrically held trunk in leg extension. Although there were clear asymmetrical activation patterns for the tasks involving leg extension (i.e. right erector activity with right leg extension)

Table 4.1: Mean activation (SD) levels of the 14 EMG channels for the thirteen participants expressed as a percentage of MVC (100%).

Channel*	Right Leg Extension (RL)	Left Leg Extension (LL)	Right Leg & Left Arm (RL&LA)	Left Leg & Right Arm (LL&RA)	Trunk & Legs (T&L)	Trunk (T)	Calibration Posture
Right RA	3.3 (2.4)	2.7 (1.9)	4.0 (2.0)	3.5 (2.0)	4.7 (2.2)	3.1 (1.8)	1.4 (1.0)
Right EO	8.4 (4.9)	4.9 (1.5)	16.2 (6.0)	5.2 (2.3)	4.3 (2.5)	3.7 (1.7)	1.0 (0.6)
Right IO	12.0 (6.8)	8.2 (2.5)	15.6 (8.2)	12.0 (4.2)	12.1 (10.1)	12.7 (10.8)	1.9 (1.2)
Right LD	8.1 (5.4)	5.8 (3.5)	12.0 (9.6)	12.5 (6.2)	11.2 (4.3)	6.5 (4.0)	5.9 (8.5)
Right TES	5.7 (2.0)	13.7 (7.5)	11.5 (6.6)	46.8 (29.3)	66.1 (18.8)	45.4 (10.6)	21.0 (9.0)
Right LES	19.7 (9.1)	11.7 (4.9)	28.4 (10.2)	19.4 (11.0)	59.2 (11.7)	57.8 (8.5)	21.3 (4.6)
Right Mult	21.9 (6.3)	10.8 (6.0)	31.5 (8.2)	16.1 (12.0)	51.9 (14.7)	47.5 (12.3)	16.4 (5.6)
Left RA	4.3 (3.4)	3.6 (3.6)	4.4 (3.8)	4.2 (3.9)	6.5 (3.4)	3.7 (2.4)	2.2 (2.1)
Left EO	5.4 (2.0)	9.0 (3.8)	6.2 (2.5)	15.9 (6.6)	6.3 (3.2)	5.2 (5.2)	1.8 (1.0)
Left IO	16.0 (8.6)	11.3 (7.0)	22.6 (9.2)	15.2 (6.7)	11.0 (5.9)	12.5 (6.1)	1.6 (1.3)
Left LD	4.5 (4.3)	5.0 (4.5)	10.7 (18.2)	6.2 (4.4)	9.2 (5.1)	5.1 (4.1)	6.1 (8.5)
Left TES	15.0 (7.5)	4.5 (2.0)	42.9 (20.5)	10.5 (5.9)	63.6 (22.7)	41.6 (10.0)	21.2 (9.8)
Left LES	11.3 (6.6)	16.8 (4.5)	19.5 (7.4)	25.5 (7.3)	56.8 (14.5)	57.0 (14.7)	23.3 (8.4)
Left Mult	11.9 (7.0)	22.3 (6.1)	16.6 (7.2)	33.8 (6.7)	57.3 (11.4)	53.3 (12.0)	18.7 (4.3)

* EMG Channel: RA Rectus Abdominis, EO External Oblique, IO Internal Oblique, LD Latissimus Dorsi, TES Thoracic Erector Spinae, LES Lumbar Erector Spinae, Mult Multifidus

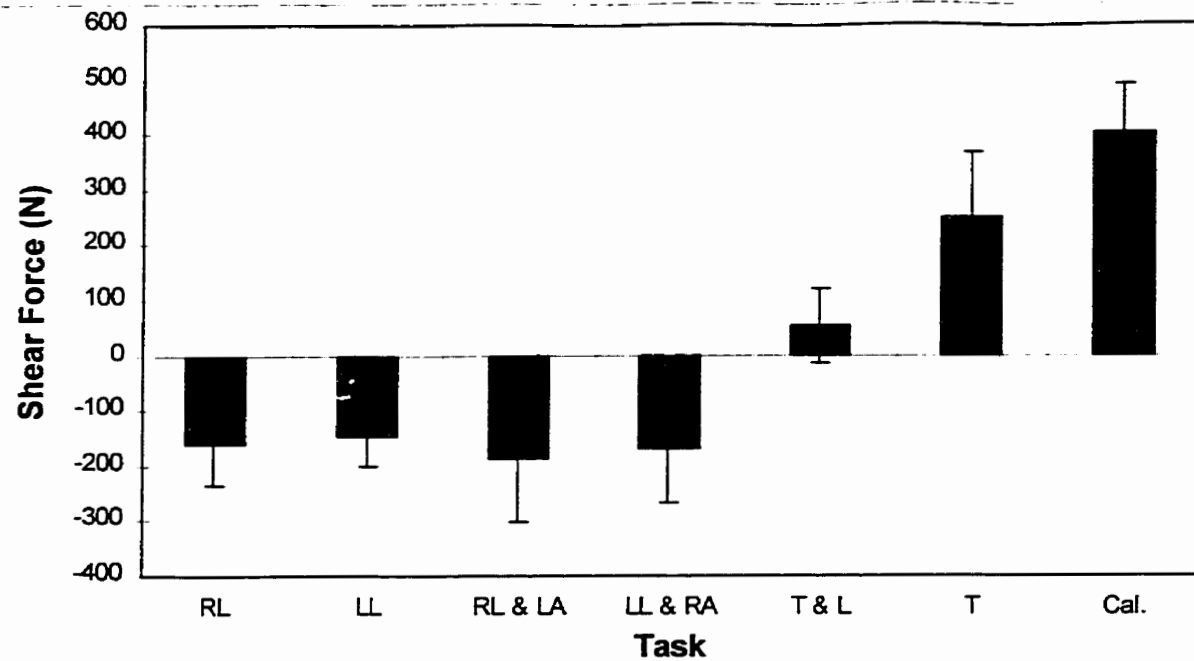


Figure 4.6: Anterior - posterior joint shear forces (mean and standard deviation) calculated by the EMG driven model. A positive shear value indicates a net anterior shear of the trunk with respect to the pelvis.

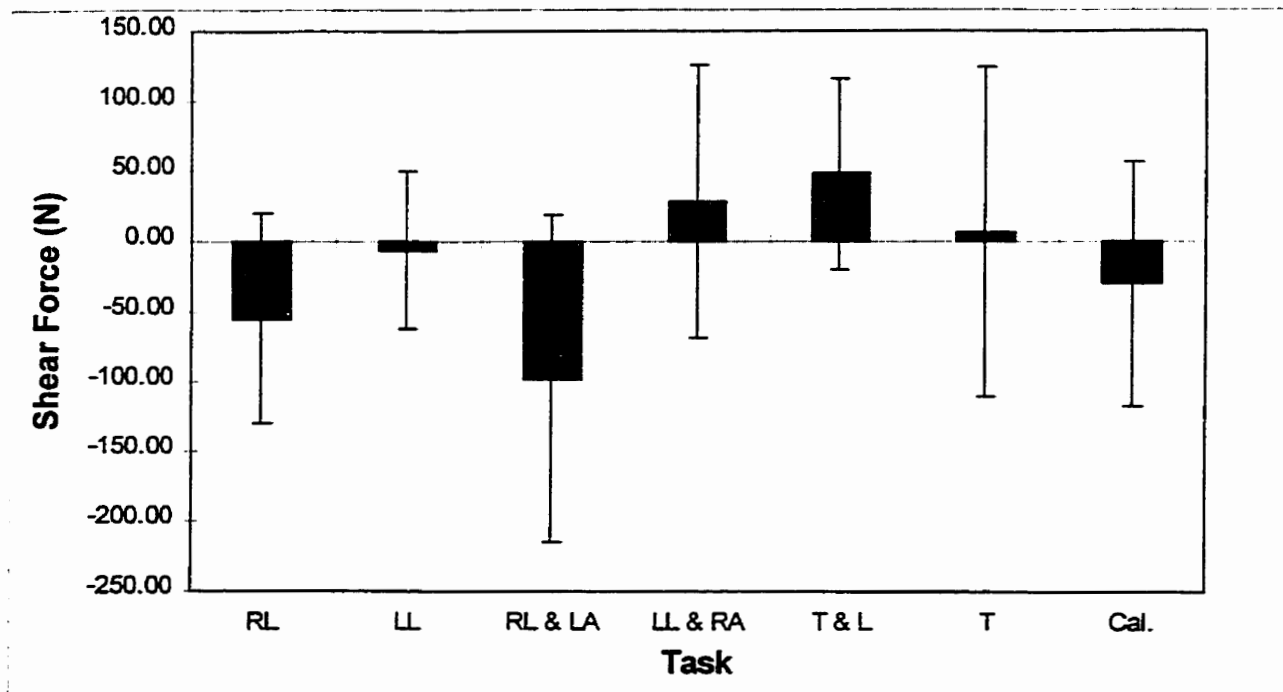


Figure 4.7: Mean and standard deviation of medial - lateral joint shear forces from the EMG driven model. A positive value indicates the trunk is shearing to the participants right with respect to the pelvis.

the contralateral abdominal muscles were activated to maintain a neutral pelvis and spine posture, in effect balancing the internal moments and lateral shear forces. The lumbar curvature

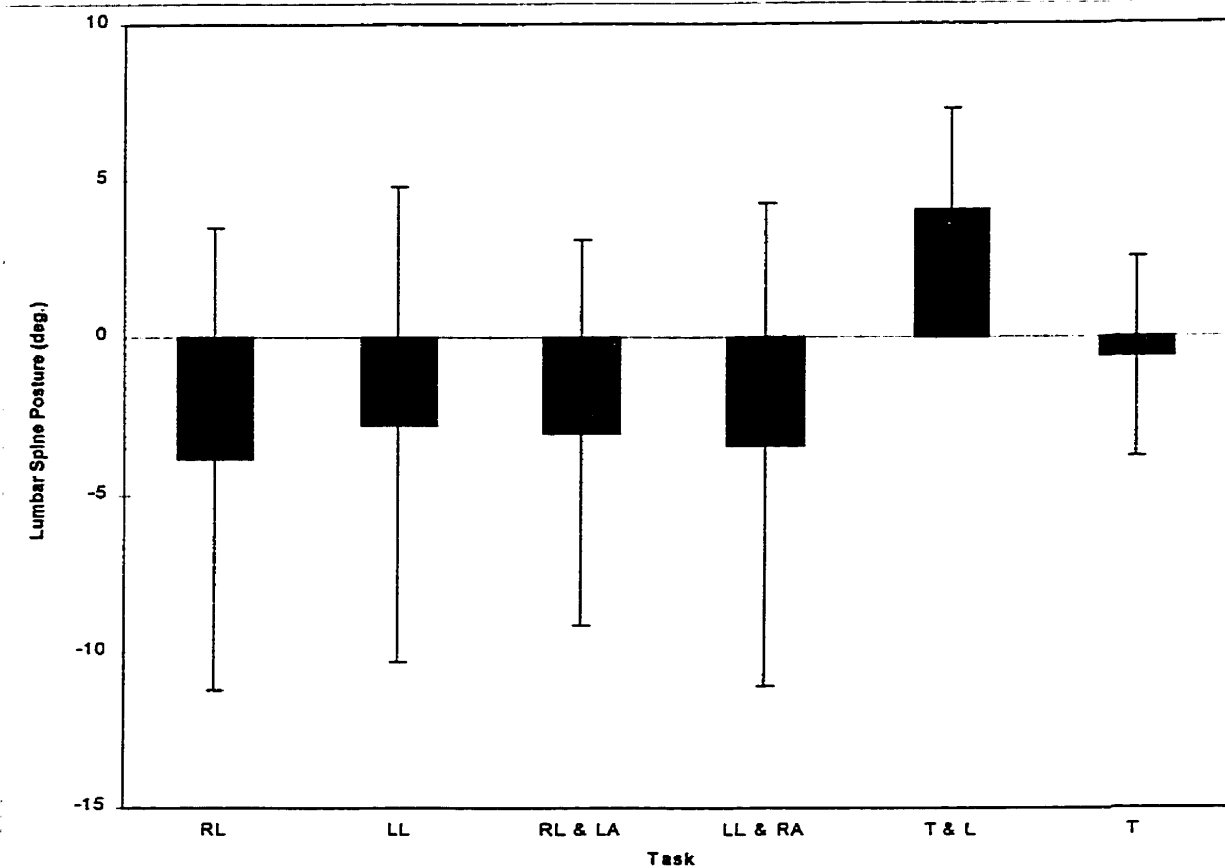


Figure 4.8: Lumbar sagittal plane spine posture (mean and one standard deviation) for all participants in the peak load position. A positive posture indicates trunk (T12 level) extension with respect to the sacrum, a negative represents lumbar spine flexion.

at the instant of peak loading showed consistent low levels of spine flexion across the four tasks involving leg extension (Figure 4.8). The active trunk and leg extension task resulted in an extended spine posture. The trunk extension task peak load posture was chosen when the trunk was parallel to the floor, thereby artificially creating what appears to be a neutral spine posture. Activity of the abdominal muscles was low for all tasks. Both the rectus abdominis

and internal oblique muscles were recruited bilaterally for all tasks. The external oblique demonstrated increased recruitment on the same side as the active leg in all four leg extension tasks. Activity of the latissimus dorsi muscle remained at relatively low levels for all exercises, with the highest levels associated with arm extension. The thoracic erector spinae demonstrated the opposite pattern to the external oblique for the combined arm and leg extension tasks and to a lesser degree in the leg extension tasks. Increased levels of thoracic erector spinae muscle activity were associated with elevation of the ipsilateral arm. The three back extensor groups monitored (thoracic and lumbar erector spinae, and multifidus) followed the same trend as the joint compressive force. The trunk extensor tasks required the highest activation levels with the leg extension being the least demanding.

DISCUSSION

Of the four typical exercises examined only the single leg extension tasks provided both low joint loading and muscular activity suggesting that this would be a wise choice for those beginning the muscle development part of a rehabilitation program. When compared with lifting a 10 kg mass (from approximately mid thigh level), only the single leg extension exercise resulted in less joint compression. The remaining three exercises (trunk extension, trunk and leg extension, leg and arm extension) generated high spinal loading and muscle activity levels. Very little co-contraction was present during any of the exercises. The hypothesis that some exercises would have higher extensor activation with lower joint loading, therefore, was not demonstrated for our subjects without low back pain. Whether this finding

would be true for persons with low back pain is not known. The modeling procedure that was used in our study predicted that exercises, when performed with the low back close to neutral lordosis, reduce disc deformation, ligament loading, and ultimately spine loading.

Hyperlordosis (extension) has been shown to shift loading to the posterior elements, whereas hypolordosis (flexion) has been linked to a lower failure tolerance of the spine (Adams & Hutton. 1982), higher ligament loading (Panjabi, Goel, & Takata. 1982), and a higher risk of disc herniation (Gordon, Yang, Mayer, Mace, Kish, & Radin. 1991). The literature supports the importance of hip flexibility for successful low back rehabilitation. Lumbar flexibility remains questionable for some low back disorders, and in some cases spinal hypermobility has been associated with low back pain (Biering-Sorensen. 1984; Burton, Tillotson, & Troup. 1989). Saal and Saal (1989) noted success with carefully formulated exercises that emphasized muscle co-contraction with the spine in a neutral posture. The data that we report also show that the tasks involving leg extension preserve a more neutral lumbar posture and reduce spine load since only one side of the extensors dominates the contraction.

Only male subjects without low back pain were studied, and they are not representative of the patients who perform these exercises as a treatment for back pain. However, our objective was to quantify muscle activity and lumbar loading. The type of tasks studied presented a challenge from a modeling perspective because the subjects were positioned prone on the floor in some tasks, with contact forces distributed over their torso, making the external moment calculations more difficult. This difficulty was overcome by establishing a fixed relationship of maximum possible stress (in Newtons per square centimeter) for each subject. This relationship was established during the calibration task (exercise 7). Finally, although the

tasks involved movement, measurements were taken only when the extreme positions were obtained, and this generated the largest external moments and levels of muscle activity and spinal loading. The tasks were performed smoothly and at a slow speed, thereby reducing inertial components at the initiation of each repetition.

CONCLUSION

The exercises examined provide a range of joint loading and muscle activity levels. The leg extension tasks could be suitable for the majority of patients who need increased endurance and strength enhancement. The increased demand of combining arm extension with leg extension suggests that this exercise constitutes an increased level of challenge. Although commonly used in rehabilitation protocols, the exercises involving trunk extension while lying prone on the floor require very high muscular activity levels and resulted in substantial joint loads suggesting that their use is unwise.

Chapter V

**Studies on Disc Damage from Highly Repetitive Flexion/Extension Motions
with Compressive Force**

Jack P. Callaghan and Stuart M. McGill

Submitted to SPINE

December, 1998

ABSTRACT

Study Design. This study was designed to examine the biomechanical response and failure mechanics of porcine spine motion segments to highly repetitive low magnitude complex loading.

Objective. The primary objective was to determine whether low magnitude joint forces, repeated motion, and flexion/extension moments consistently produce herniation in a porcine cervical spine motion segment. Secondary objectives were to examine the modulating effects of the magnitude of axial compressive force, and positional versus torque control on tissue injury.

Summary of Background Data. The porcine cervical spine appears to be a reasonable model for evaluating human lumbar injury mechanics. Furthermore, while the majority of studies performed in-vitro have examined uniaxial or fixed position loading, there have been few studies that have examined whether the intervertebral disc can be injured by low magnitude repeated combined loading. This controlled animal model provided the opportunity to study highly repetitive motion and loading.

Methods. Porcine cervical spine motion segments (C3-C4) were used as an in-vitro model. Specimens were mounted in a custom jig which allowed the application of axial compressive loads and a pure flexion/extension moment. The range of motion of each specimen was quantified prior to testing and the test parameters were selected from the initial linear component of the torque vs angular rotation response. Dynamic testing was conducted under either torque or angular positional control to a maximum of 86,400 cycles (24 hours). The resulting torques, angular rotations, axial deformations were collected for the duration of the test.

Results. Low magnitude joint forces, motions, and flexion/extension moments resulted in disc herniations. Increased magnitudes of axial compressive force resulted in more frequent and more severe disc injuries. Specimens tested using angular position control produced more consistent injuries than specimens loaded under torque control. Specimens exhibited a significant increase in angular stiffness ($P < 0.0001$) throughout the duration of the dynamic test.

Conclusions. The results support the conclusion that cumulative compression in concert with repeated flexion extension motions is a viable mechanism for producing intervertebral disc

herniations. Furthermore, the herniation is a progressive/cumulative phenomenon which tracks posteriorly through the annulus until the nth repetition forms the culminating event. This type of disc failure can occur under quite modest forces and torques if sufficient flexion/extension cycles are applied.

INTRODUCTION

The in-vivo spine is exposed to repeated loadings each day through such activities as walking, sitting, or repeated assembly tasks. Exposure to repeated flexion bending tasks has been associated with the reporting of LBP (Chaffin & Andersson. 1990; Norman, Wells, Neumann, et al. 1998; Punnett, Fine, Keyserling, Herrin, & Chaffin. 1991; Wilder, Pope, & Frymoyer. 1988), however, there have been few in-vitro studies that have examined the tissue response to prolonged repeated loading and joint flexion extension. The majority of in-vitro research has examined repeated axial loading in the neutral posture (Brinckmann, Biggemann, & Hilweg. 1988; Hansson, Keller, & Spengler. 1987; Liu, Njus, Buckwalter, & Wakano. 1983; Smeathers. 1984; Smeathers & Joanes. 1988). These studies have examined a range of frequencies (0.01- 10 Hz) and a large range of compressive loads (750 N - 100% of compressive strength). All the studies that have examined repeated axially loading to failure (Brinckmann, Biggemann, & Hilweg. 1988; Liu, Njus, Buckwalter, & Wakano. 1983; Wilder, Pope, & Frymoyer. 1988) resulted in the same compression fractures seen in single cycle destructive in-vitro tests (end-plate or vertebral body failures) despite disc herniation being observed clinically.

A few studies have examined non-neutral loading positions combined with repeated loading (Adams & Hutton. 1983; Adams & Hutton. 1985; Wilder, Pope, & Frymoyer. 1988). Wilder et al. (1988) loaded human and bovine motion segments in a combination of flexion, lateral bend, and axial twist. The bovine specimens were more susceptible to herniation (75%) than the older human tissue (0%) (Wilder, Pope, & Frymoyer. 1988). This result was probably attributable to the different levels of disc degeneration, which has been shown to affect the susceptibility of the intervertebral disc to herniation (Adams & Hutton. 1982). Intervertebral discs that were slightly degenerated (grade 2 (Galante. 1967)) or non degenerated (grade 1) were more likely to herniate than moderately degenerated discs (grade 3) (Adams & Hutton. 1982). Severely degenerated discs (grade 4) did not herniate during in-vitro testing (Adams & Hutton. 1982). Human in-vitro motion segments were positioned in slight lateral bend with flexion to the elastic limit and cyclically loaded with a compressive force (which induced bending moments at the same time as compressive and shear loading) (Adams & Hutton. 1983; Adams & Hutton. 1985). No disc herniations were observed in the initial test condition (Adams & Hutton. 1985). By increasing the joint angle, as creep allowed, then increasing the compressive load once a stable position was achieved, 6 of 29 motion segments failed by nuclear protrusion. However, the lumbar spine in-vivo appears to have a margin of safety in forward bending (Adams & Hutton. 1986) so it would be unlikely that the postures required for failure in this mode would occur in-vivo.

The lumbar spine in-vivo undergoes motions while being exposed to varying loads. There have been few studies that have examined combined load and motion in-vitro testing (Brinckmann & Porter. 1994; Gordon, Yang, Mayer, Mace, Kish, & Radin. 1991; Hardy,

Lissner, Webster, & Gurdjian. 1958). Hardy et al. (1958) used intact human lumbar spines (L1 to sacrum) with the posterior elements removed, which contribute resistance to flexion (Adams, Hutton, & Stott. 1980). There were no disc herniations produced (without gross avulsion) with the maximum number of flexion/extension cycles required to failure reaching as high as 153,400. Four human lumbar motion segments were axial loaded off-center to provide 0° to 5° of flexion or 0° to 4° of extension motions combined with compressive loads of 1000N for a total of 1000 cycles at 0.25 Hz (Brinckmann & Porter. 1994). No failures were detected in any of the specimens tested. The most consistent development of disc herniation with repeated loading conditions was achieved by Gordon et al. (1991). In-vitro human lumbar motion segments were flexed from a neutral posture to 7° of flexion with a small axial twist motion ($< 3^{\circ}$). All 14 of the motion segments examined failed with herniations of the intervertebral disc (either nuclear protrusion or extrusion) with an average of 40,000 loading cycles to failure.

The main purpose of this study was to determine whether low magnitude joint forces, flexion motion, and flexion/extension moments could consistently produce disc herniation in porcine cervical spine motion segments. Secondary purposes were to examine the modulating effects of the magnitude of axial compressive force, and positional versus torque control on disc injury.

MATERIALS AND METHODS

The cervical spines (Appendix A) of 26 porcine (age mean 6 months, weight mean 785 N) specimens (C1-C7) were obtained immediately following death. All specimens were sealed in doubled polythene bags and stored at -20°C. Prior to testing, the frozen specimens were thawed in a refrigerator (+4°C) for 24 hrs (Callaghan & McGill. 1995). Any residual coldness dissipated during dissection prior to testing. The surrounding musculature was then stripped leaving the osteo-ligamentous structures intact.

Specimens were then divided into two segments (two adjacent vertebral bodies and the intervening intervertebral discs) of C3-C4 and C5-C6. Only the C3-C4 motion segments were used for this study. The intervertebral discs of the sectioned ends of the specimens were examined for degeneration and were graded according to the scale proposed by Galante (1967). Only specimens that met the Grade 1 criteria were chosen for use (in this case - all of them). The remains of any soft tissue and discs were dissected from the cranial and caudal end plates. A mixture of barium sulphate (radio-opaque), blue dye (Coomassie Brilliant Blue G₂₅ - mix: 0.25% dye, 2.5% MeOH, 97.25% distilled water), and distilled water were mixed in a ratio of 2:1:2 and approximately 0.7 cc was injected into the intervertebral disc's nucleus. Specimens were then x-rayed prior to mounting to document the distribution of the nucleus in the sagittal and transverse planes. Specimens were fixed in aluminum cups using a non-exothermic dental stone (Denstone®, Miles Inc., South Bend, IN, U.S.A) and 19 gauge steel wires looped bilaterally around the anterior processes and the lamina of both vertebrae. Wood screws were also used to hold the specimen in the cup. The screws pierced the centre of the end plate and

never protruded farther than 1 cm into the vertebral body. The fixation material covered the proximal half of the cranial vertebra and the distal half of the caudal vertebra. The mounted specimens were then placed in the testing fixture (Figure 5.1). The testing jig was designed to allow the centre of rotation to be moved and aligned (vertically and horizontally) with the geometric centre of the intervertebral disc. The torques applied were applied as a pure moment (not generated by a force-moment arm application) in the sagittal plane. The specimens were free to translate in the horizontal plane (x-y table mounted beneath the specimen) and freely rotate about the vertical axis. Additionally, the specimens could deform axially in response to the compressive loads applied. As a result of the jig design, specimens were only exposed to compressive loads (Appendix B). Specimens were wrapped in two layers of a cotton fibre plastic backed material that had been soaked in a physiologic saline solution. An additional third plastic film was wrapped around the specimen to prevent drying from exposure to room air. Testing was conducted at room temperature, which due to radiant machine heat was approximately 32.8 °C (porcine body temperature approximately 39 °C). A preload (260N for 15 minutes) was applied to all specimens to counter any swelling that had occurred postmortem. During the preloading phase, the servo motor was driven to a zero torque and the angular position at the end of the preload was taken as zero position for each specimen. The specimens were then exposed to one of the 3 compressive loads examined in the study (260, 867, or 1472 N) using a servo hydraulic dynamic testing system (model 8511, Instron Canada Inc., Burlington, ON, Canada). The torque versus angular rotation profile of each specimen was determined using 4 repeats of a range of motion test (ROM), flexion and extension, at a rate of 0.5°/s. The point where the torque versus angular position curve deviated from the initial linear

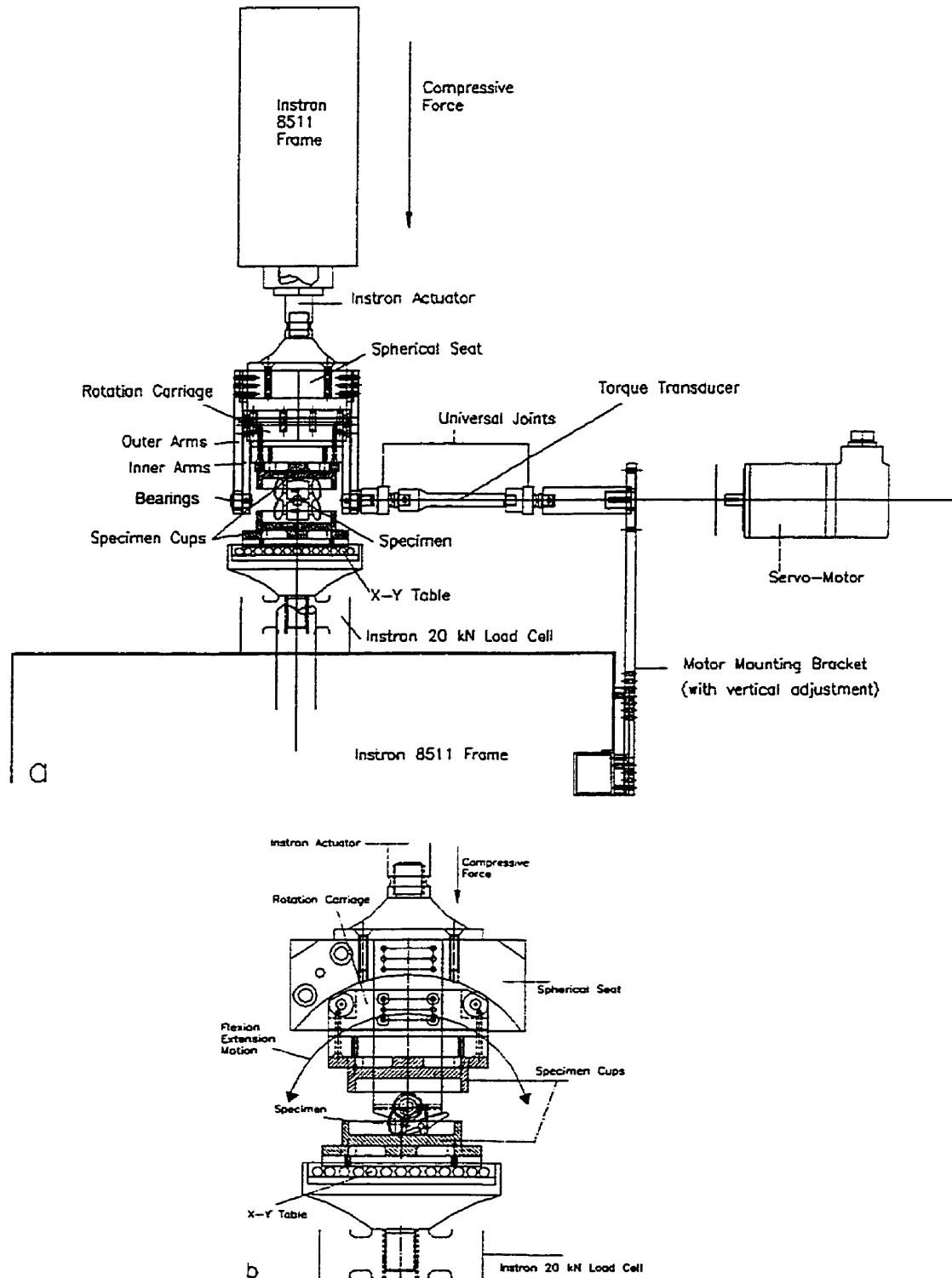


Figure 5.1: Frontal (a) and sagittal (b) views of the test apparatus used to apply coupled axial compressive load and pure flexion moments to produce repeated flexion extension motions. The X-Y table permitted translations as opposed to artificially constraining each end.

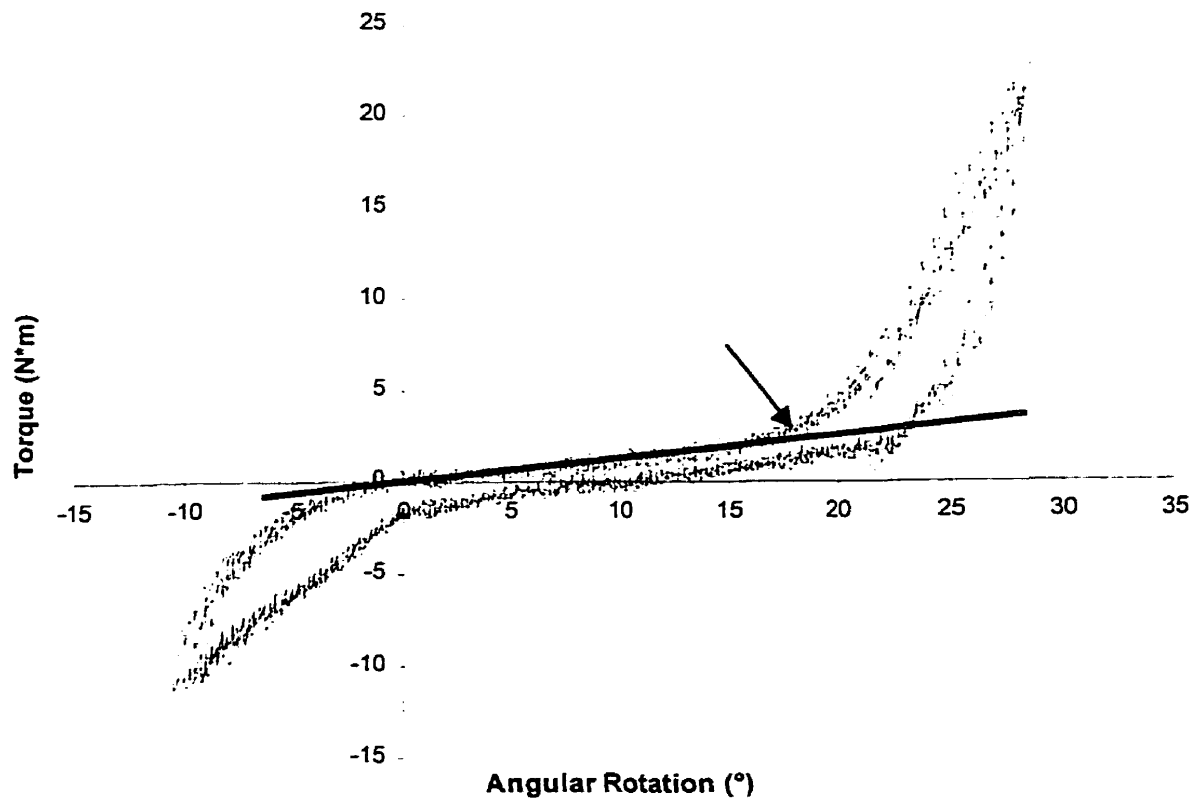


Figure 5.2: Range of motion test for one specimen tested with a compressive load of 260N. The point where the curve deviates from the superimposed line (arrow) indicates either the torque or angular position employed for the repeated dynamic test.

section (Figure 5.2), similar to the neutral zone defined by Panjabi et al. (1989), was chosen as the testing value (either angular position or torque) for the dynamic test. The specimens were then cyclically loaded in either angular positional (rate of $45^\circ/\text{s}$) or torque control (rate was dependent on the sample and axial load, range of $10 \text{ N}\cdot\text{m}/\text{s}$ to $44 \text{ N}\cdot\text{m}/\text{s}$) at a rate of 1 Hz to a maximum of 86,400 cycles using an electrical brushless servomotor (model BNR3018D, Cleveland Machine Controls Inc., Billerica, MA, USA) and a 40:1 planetary gear head (model 34PL0400, Applied Motion Products, Watsonville, CA, USA). The servo motor was controlled using custom software which interfaced with an ISA bus motion controller (model DMC1701,

Galil Motion Control Inc., Mountain View, CA, USA). Torque was measured using a strain gauge torque transducer (model 01190-152, Sensor Developments Inc., Lake Orion, MI, USA) and angular position data was obtained using an incremental optical encoder attached to the motor shaft (model LDA-048-1000, SUMTAK Corporations of America, Piscataway, NJ, USA). The angular position, torque, axial force, and axial deformation were all A/D converted at a rate of 30 Hz for the full duration of each trial.

Following dynamic testing, four repeats of the ROM test were performed. The moments at the maximum angles achieved in the ROM test performed prior to dynamic testing were compared with the moments produced at the same joint angles from the ROM test following the dynamic testing. The specimens were x-rayed (note: several specimens were x-rayed at repeated intervals in an attempt to track disc herniations) following testing to document both sagittal and transverse plane structure. An examination of the ligamentous structure and posterior elements was conducted and any failure or damage recorded. Specimens were then dissected through the plane of the intervertebral disc and examined for any soft tissue damage, indicated by the blue dye injected prior to testing.

To determine the magnitude of angular rotations and joint torques that the C3-C4 porcine cervical joint could withstand one specimen was loaded to failure in flexion using the ROM test protocol at a rate of 0.5 degrees per second. The specimen resisted a flexion moment of 61 N*m, an extension moment of -44 N*m, and had angular rotations of 39° and -24° in flexion and extension respectively. (Note: the specimen was not taken to failure in extension)

The data were reduced by selecting the peak values of the dependent variable (torque in angular positional control and angular position in torque control) in flexion and extension for

each cycle of loading. The response of each specimen to the dynamic loading was examined by comparing the initial values of the dependent variable at the beginning of the test with the final values at the end of the dynamic test. Three beginning versus end values of the dependent variables were examined: peak flexion; peak extension; and range (peak flexion - peak extension). Additionally the average stiffness for the first cycle of loading was compared with the average stiffness during the last cycle. The dynamic axial creep was obtained by taking the axial displacement measured by the INSTRON at the zero position for specimens loaded in positional control for each cycle of loading. Since the specimens loaded in torque control tended to creep into a flexed posture, the joint angle closest to zero position that was present throughout the duration of testing was used to track axial displacement.

Data were analysed using one way analyses of variance (independent variable=axial compressive load, $\alpha=0.05$) for tests that resulted in one measure per specimen (i.e. preload creep). TUKEY's *post hoc* multiple comparisons were used to compare groups when a significant difference was found. Data that involved a repeated measure on a specimen (ie pre vs post dynamic test properties measured during the ROM test) were analysed using a split plot design ($\alpha=0.05$) with a pre-post split within axial compressive load. Any significant finding of the main effects was tested *post hoc* using repeated t-tests.

There were no significant differences in the amount of creep sustained by any of the groups during the 15 minute preload (Table 5.1). Additionally, the maximum flexion and maximum extension angles (Table 5.1), obtained during the ROM testing prior to dynamic testing, were not significantly different between any of the six groups suggesting successful assignment of specimens to produce homogeneous groups.

RESULTS

Herniation occurred with modest levels of compression and flexion/extension moments but with a high number of motion cycles. Increasing magnitudes of compressive load increased the likelihood that a herniation would develop (Table 5.1) in both the angular position control and torque control groups. However, loading of specimens in angular positional motor control resulted in more severe and consistent herniations. All herniations that were created during testing occurred in the posterior or posterior-lateral areas of the annulus. The posterior herniation was clearly indicated in x-rays taken of specimens prior to and following testing (Figures 5.3a and 5.3b). Additionally, upon post testing dissection the blue dye could frequently be seen upon external examination of the posterior annulus following removal of the neural arch (Figure 5.4a). A horizontal transection through the intervertebral disc revealed posterior displacement of the annulus and quite often a nuclear delamination, indicated by the blue dye traveling circumferentially through the annulus (Figure 5.4b). In contrast, specimens that demonstrated no failure had a nucleus that was still gelatinous and contained within the nuclear cavity, even after 24 hours of testing (Figure 5.4c).

Over the duration of the dynamic test, specimens greatly stiffened. This effect was enhanced with higher loads, specifically there was a very clear interaction effect for every comparison with the exception of the change in flexion torques under positional control. The

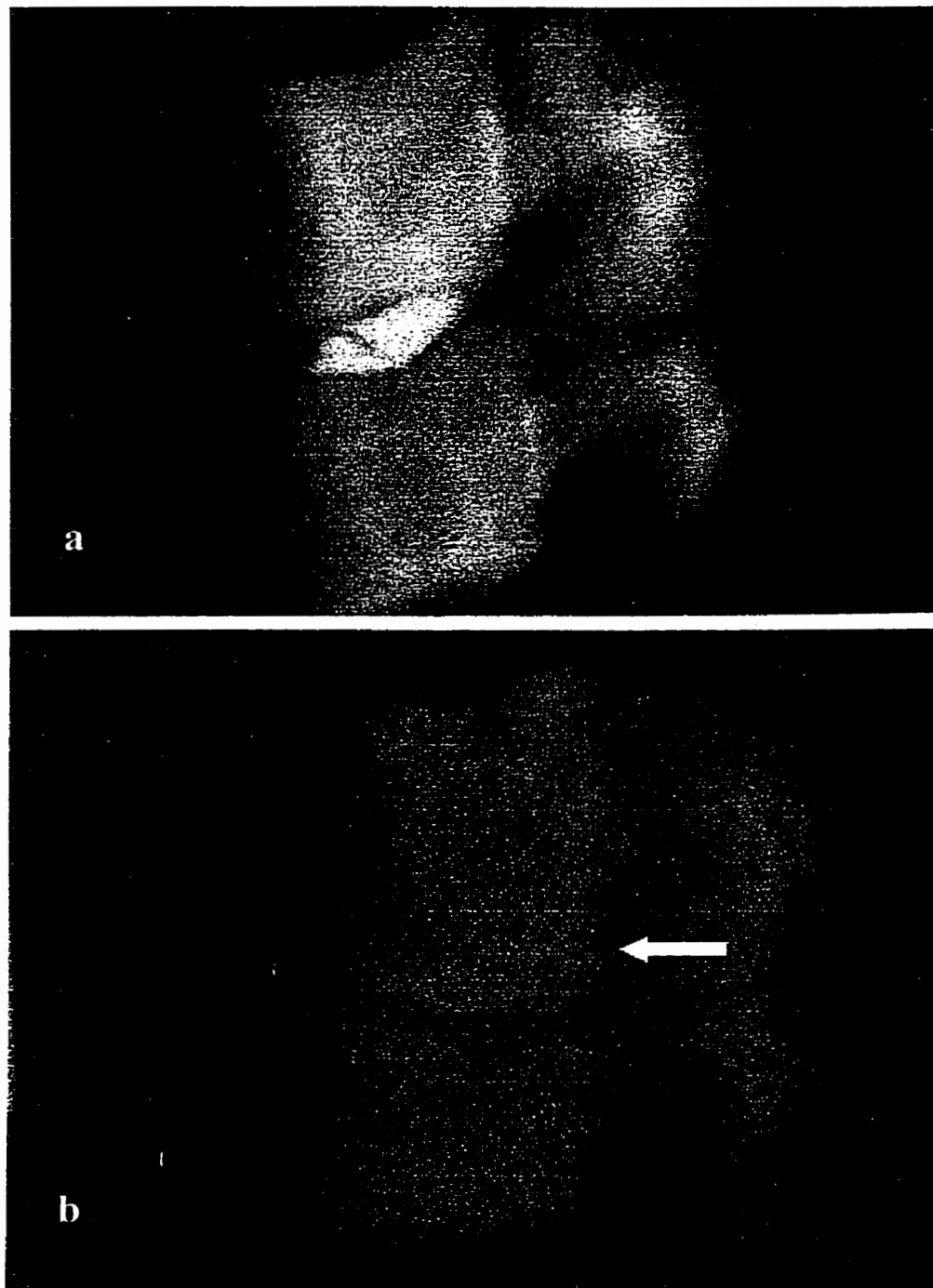


Figure 5.3: An x-ray for one specimen prior to (a) and following (b) repeated testing. The arrow indicates the posterior tracking of the radio-opaque dye indicating a herniation.

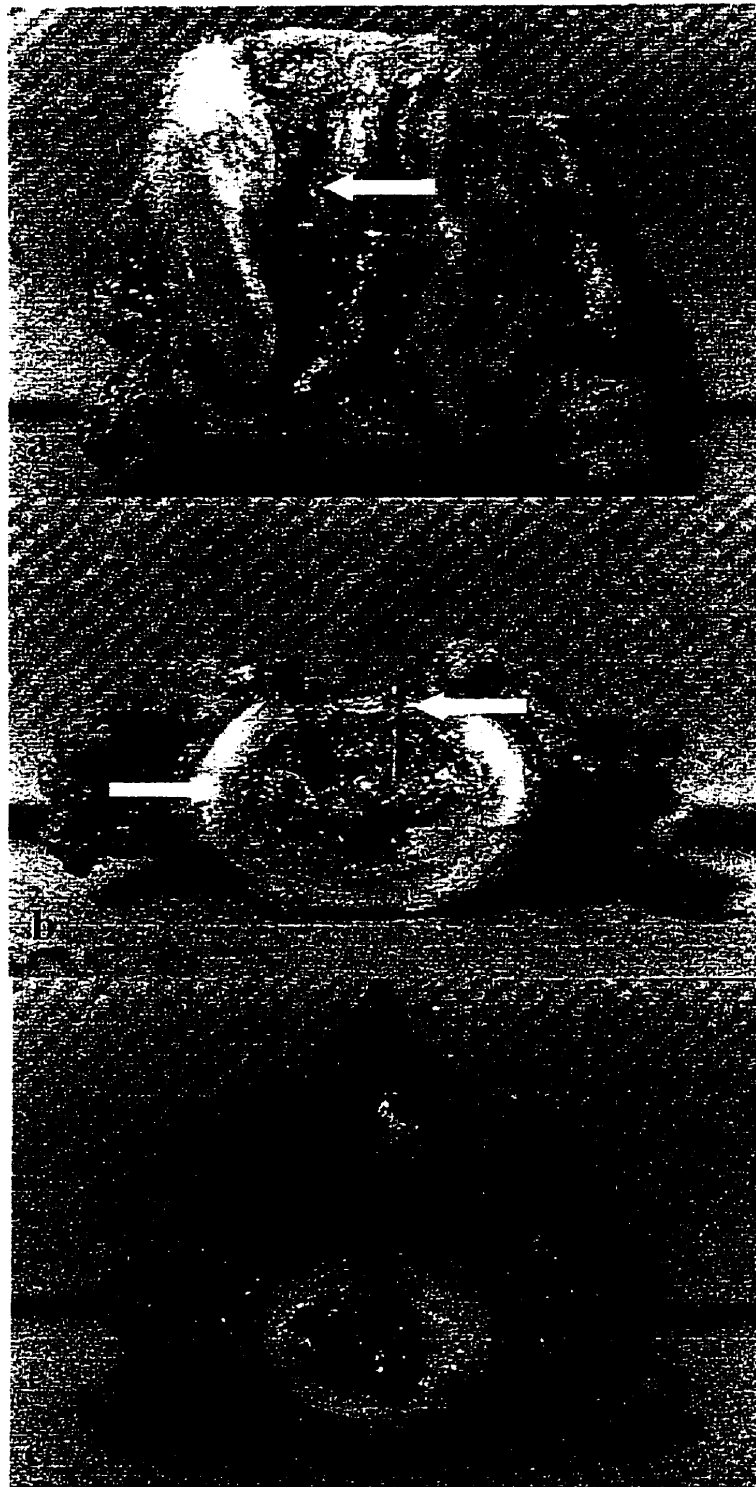


Figure 5.4: a) The posterior extrusion of blue dye was evident when the neural arch was removed. b) A transverse section through the intervertebral disc reveals the posterior herniation as well as delamination of the annulus. c) An intervertebral disc from the 267N group loaded for 86,400 cycles with the nucleus pulposus still intact.

increased compressive load resulted in significant increases in all flexion ($P < 0.0003$), extension ($P < 0.0005$) (Table 5.1), and range ($P < 0.0001$) (Figure 5.5) of moment values in positional control. The 260N vs 867N, 260N vs 1472N, and 867N vs 1472N comparisons were all significantly different for the three parameters examined. Torque control demonstrated less marked changes due to the compressive load effect. The only parameter that was significantly affected was the peak flexion angle (Table 5.1) beginning versus end comparison ($P < 0.0428$), with only the 260N vs 1472N pairing being significantly different ($P < 0.0139$). The extension angles (Table 5.1) and range of angle (Figure 5.5) were not significantly different across compression load magnitude. The only measure not significantly affected by the dynamic testing (beginning versus end effect) was the peak flexion angle of the torque control group (Table 5.1). All other parameters within both the position and torque control groups were significantly changed with a minimum P value of 0.003. Specimens loaded in torque control exhibited a decreased extension angle, total range, and a trend of decreased flexion angle. Inversely, angular position control resulted in increased flexion torques, extension torques, and range of torque over the dynamic test period. Both positional control and torque control exhibited an increased joint angular stiffness ($P < 0.0001$) during dynamic testing (Figure 5.6). The only exception was the 260N condition in the torque control group, which demonstrated a slight increase in flexion angle over time (Table 5.1). Additionally, increased magnitudes of compressive load resulted in significant increases in joint angular stiffness ($P < 0.0001$) (Figure 5.7). Again, there was an enhanced effect with higher loads.

Table 5.1: Specimen Data means (and 1 standard deviation). Rotational measures used the following convention: positive values indicate flexion, negative values indicate extension.

Compressive Load (N)	n	Number of Flexion/Extension Cycles	Preload Creep (mm)	ROM		Injury Classification(Adams & Hutton. 1985)			Axial Creep (mm)	Dynamic Test			
				Peak Flex Angle (°)	Peak Ext Angle (°)	No Damage	Track Initiation	Herniation		Flexion		Extension	
										Begin	End	Begin	End
Torque Control													
										(°)	(°)	(°)	(°)
260	3	77033 (6025)	-1.53 (0.36)	21.17 (0.38)	-13.66 (2.30)	3	0	0	-4.50 (0.77)	6.18 (1.09)	8.19 (0.18)	-3.55 (1.42)	0.46 (0.53)
867	8	75670 (22286)	-1.61 (0.46)	27.23 (6.46)	-16.34 (3.76)	2	2 stage 2	4 stage 3	-7.80 (1.28)	11.69 (4.74)	10.98 (3.58)	-3.82 (3.60)	3.53 (3.66)
1472	5	84220 (4875)	-1.40 (0.32)	28.59 (0.63)	-11.86 (1.80)	1	0	4 stage 3	-7.86 (1.20)	16.12 (3.16)	12.58 (4.06)	-2.29 (1.04)	7.57 (2.80)
Angular Position Control													
										(N*m)	(N*m)	(N*m)	(N*m)
260	2	83700 (3818)	-1.60 (0.67)	24.63 (5.48)	-12.13 (2.30)	1	1 stage 2	0	-5.21 (2.12)	3.94 (0.92)	5.17 (0.95)	-1.95 (2.08)	-6.08 (4.83)
867	4	70550 (29477)	-1.28 (0.13)	22.13 (1.33)	-9.94 (3.24)	0	0	4 stage 4	-8.88 (2.48)	6.10 (1.40)	11.31 (2.33)	-4.02 (2.51)	-20.60 (2.94)
1472	4	34974 (9549)	-1.43 (0.31)	24.25 (1.59)	-12.32 (5.92)	0	0	3* stage 4	-11.18 (2.17)	11.21 (2.53)	20.10 (3.68)	-3.03 (1.85)	-31.59 (3.13)

* The fourth specimen was an end plate failure.

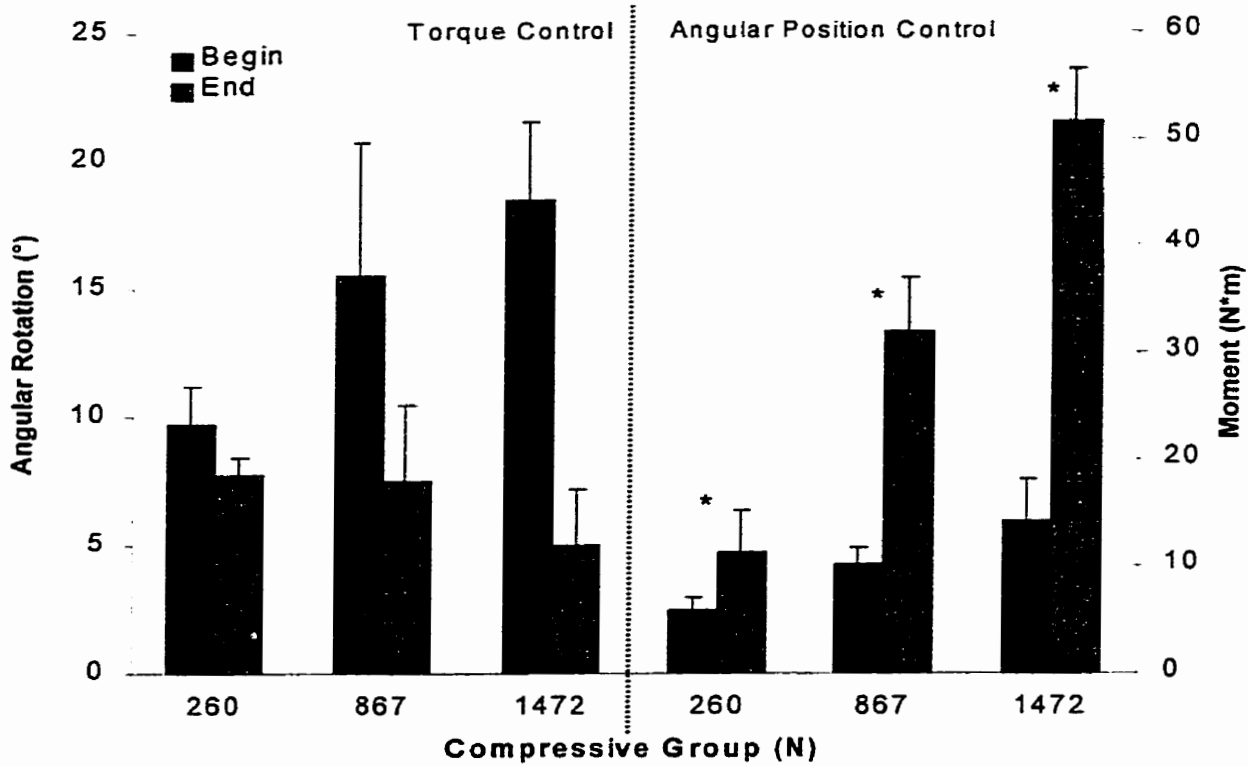


Figure 5.5: The total range (flexion peak - extension peak) of the angular position and torque control groups. Beginning versus end comparisons were significant for both torque and angular positional control ($P < 0.0001$). Comparisons of axial compressive load that were different within each control method ($P < 0.05$) are indicated with the same symbol.

Increased axial compressive load demonstrated an increasing trend in axial deformation. The amount of axial creep was compared across the six groupings (Table 5.1). There were no significant differences between any compression loads within the torque control condition. The positional control group demonstrated a trend of increased displacement with increased compressive load. Only the 260N versus 1472N compressive load conditions within positional control were significantly different ($P < 0.01$).

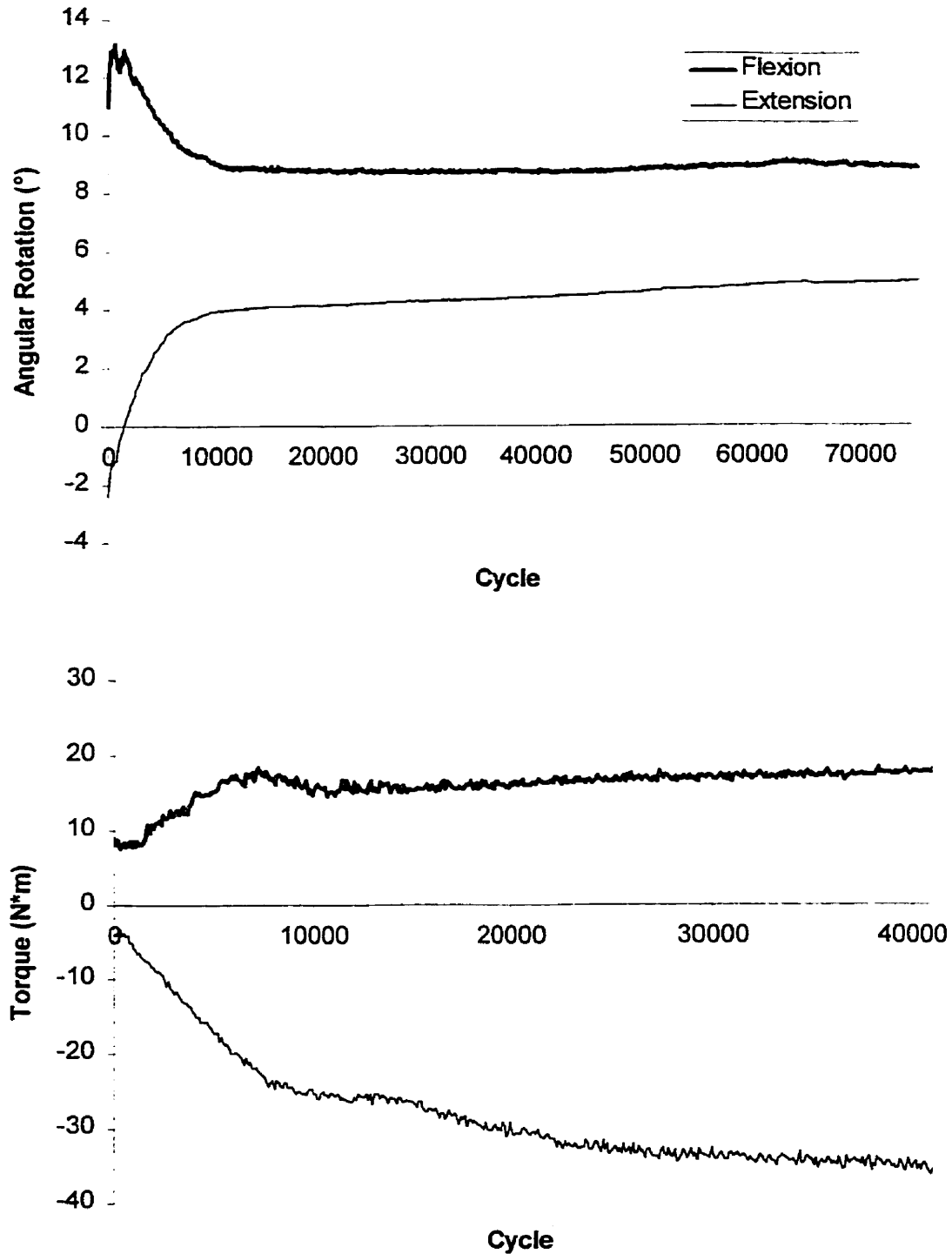


Figure 5.6: Time series for two specimens. **Upper)** Torque control specimen loaded at +11 and -5 N*m with a compressive load of 1472N showing the decreased angular rotations with a constant torque application. **Lower)** Angular positional control specimen loaded at +14° and -2.5° with a compressive load of 1472N showing the increased torque required to maintain the same angular rotations.

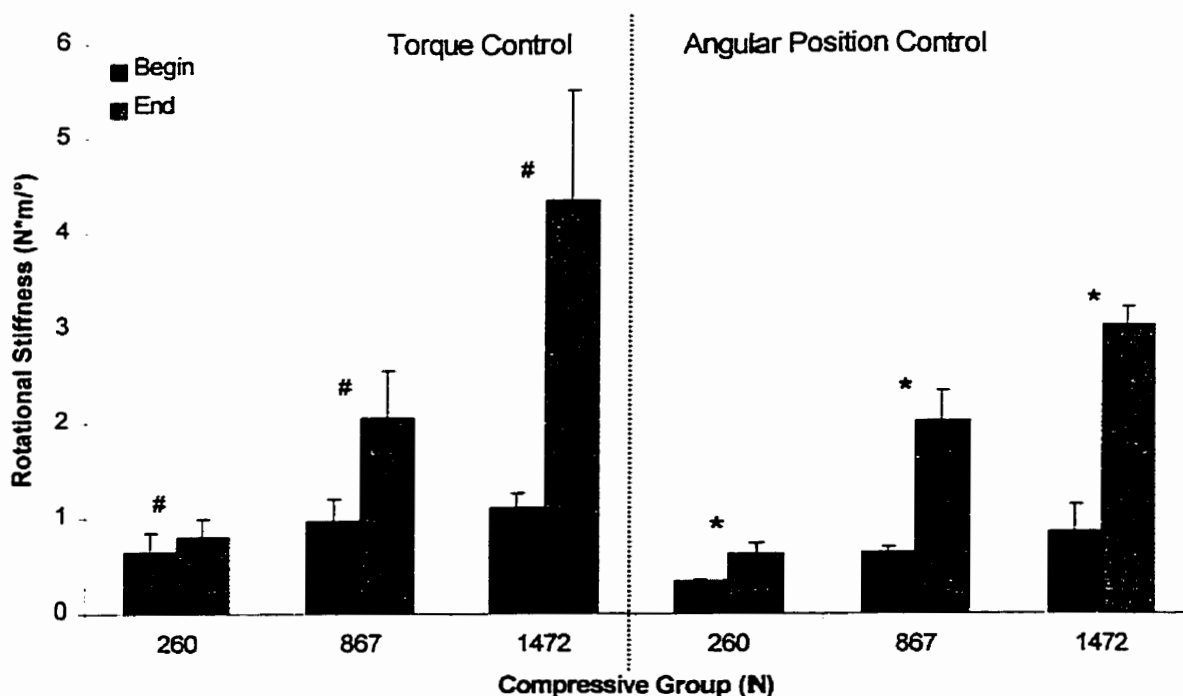


Figure 5.7: Mean rotational stiffness (+ 1SD). Beginning versus end comparisons were significant for both torque and angular positional control ($P < 0.0001$). Comparisons of axial compressive load that were different within each control method ($P < 0.05$) are indicated with the same symbol.

The dynamic test had no significant affect on the flexion moments in the pre vs post ROM test, however the extension moments were increased (Figure 5.8). The extension moments required to produce the same angular rotation for the position control group were significantly altered ($P < 0.014$) by the dynamic testing (Figure 5.8). Both the positional and torque control groups exhibited increased joint torque with increased compressive load to achieve the same joint flexion ($P < 0.0118$ and $P < 0.0066$ respectively) and extension ($P < 0.0001$ and $P < 0.0002$ respectively) (Figure 5.8). Post hoc comparisons revealed that all possible pairs within control were significantly different to a level of at least $P < 0.009$ (Figure 5.8).

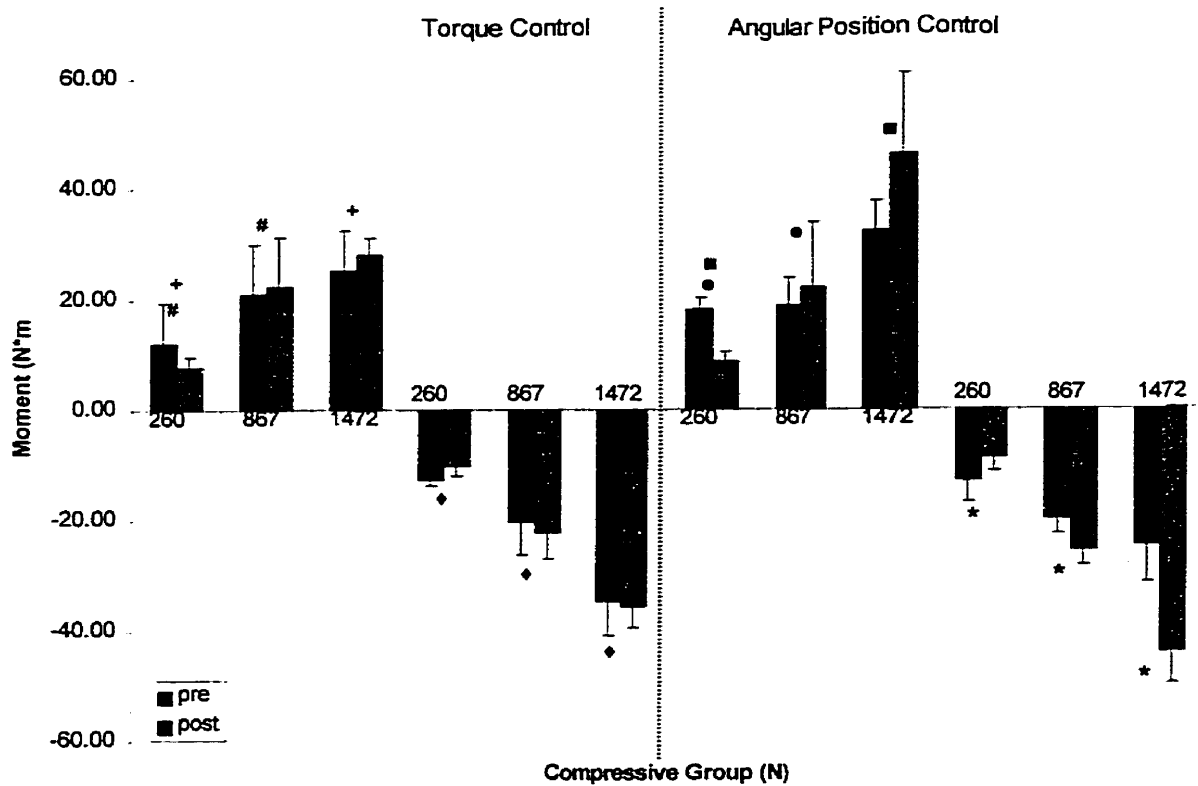


Figure 5.8: The flexion and extension moments from the range of motion test. Only the pre-post comparison of extension moments within angular positional control were significant ($P < 0.014$). Comparisons of axial compressive load that were different within each control method ($P < 0.05$) are indicated with the same symbol.

DISCUSSION

Low magnitude joint forces, highly repetitive motions, and modest flexion/extension moments resulted in disc herniations. Increased magnitudes of axial compressive force resulted in more frequent and more severe disc injuries. Specimens tested using angular position control produced more consistent injuries than specimens loaded under torque control. There is no doubt that disc herniation is a cumulative process that can result with modest forces if sufficient flexion/extension cycles are applied.

The magnitude of compression applied to the specimens modulated the potential for disc injury. Specimens within the 260N condition had only 1 of 5 specimens that demonstrated any disc injury, a tracking tear which had not reached the outer boundary of the annulus. The remaining 4 specimens had nucleus pulposus that were wholly intact and gelatinous after 86,400 cycles of loading. Goel et al. (1988) also found that specimens loaded under low moment with very small compressive loads applied did not demonstrate failures after 9600 cycles. Increasing the magnitude of compressive load resulted in increased rates of disc injury. The loading of specimens using positional control at the 867N and 1472N compression levels resulted in full herniations with extrusion of nuclear material into the spinal canal (stage 4 (Adams & Hutton. 1985)). In contrast, the specimens loaded at the same compressive magnitudes in torque control mode only generated stage 3 (Adams & Hutton. 1985) herniations which created tracking tears, posterior accumulation of nuclear material, as well as delamination but no extrusion through the external boundary of the annulus. The prevalence of herniations obtained in this study can partially be attributed to the use of only specimens with Grade 1 (Galante. 1967) intervertebral discs which have been shown to herniate more readily than more degenerated discs (Adams & Hutton. 1982).

The comparison of using load controlled versus position controlled testing has been argued extensively (Goel, Wilder, Pope, & Edwards. 1995). Regardless of the control method used, increases in stiffness were found for all test groups, which generates the following question; which method replicates the in-vivo loading scenario? A manual materials handling worker who lifts from floor to waist height repeatedly throughout the duration of their shift will be used as an example. Over the duration of the shift, the worker modifies spine posture due to

fatigue. At the initiation of the shift the worker was lifting with a bent knee squat lift, holding the load close to the body. As fatigue ensues, the worker starts lifting with a stooped fully flexed spine by the end of the shift. This would expose the spine to increased force and moment magnitudes as well as increased angular rotations. Both torque control and angular position control loading expose the in-vitro specimen to a constant magnitude of repeated testing. However, the decreased rotations experienced by a specimen under torque control would be less damaging and less representative of an in-vivo loading task than the increased torques exerted on a specimen when tested in angular positional control.

The angular stiffness of all specimens increased as the specimens progressed through the loading trials. An increased stiffness of specimens during repeated dynamic testing was also found by other researchers who examined compression-flexion (Goel, Voo, Weinstein, Liu, Okuma, & Njus. 1988; Yoganandan, Cusick, Pintar, Droese, & Reinartz. 1994) and in axial compression (Hansson, Keller, & Spengler. 1987) loading. The application of compressive loading in concert with repeated flexion/extension movements resulted in substantial loss of disc/specimen height. This loss of disc height would increase facet contact and would alter the center of rotation of the motion segment. While the center of rotation was not examined in this study, the axial creep of the specimens would result in contact points (the anterior portion of the end plate and the facet tips) which would likely become the points of rotation for flexion and extension respectively. Since these points have migrated from the center of the disc to extremes opposite the passive structures being stretched during rotation, this appears to be a mechanism to explain an increased rotational stiffness during prolonged cyclic loading.

Several limitations define the context of this work. The testing conditions were limited to flexion extension motions of the porcine motion segments. While the spine moves with six degrees of freedom the largest motion present is in the sagittal plane (flexion/extension) which will provide the greatest strain to the intervertebral discs and other passive structures. Further, the use of porcine material to replicate postures and loads present in human loading has been questioned. The porcine cervical spine provides a reasonable analogue (Yingling, Callaghan, & McGill. 1998) of the human lumbar spine. Anatomical (Oxland, Panjabi, Southern, & Duranceau. 1991), geometrical, and functional characteristics (Yingling, Callaghan, & McGill. 1998) were found to be very similar to the human lumbar spine. Stiffness and fatigue resistance of human lumbar motion segments in repeated loading have been shown to be affected by: age; disc degeneration; and bone mineral content (Hansson, Keller, & Spengler. 1987). While it would be preferable to use human tissue, the availability of a uniform quality of material (even spines of the same age can have different degeneration) is not possible. The porcine material used in this study was obtained from animals where mass, diet, age, and physical activity level was controlled. The average bending moment (156 N*m) and flexion angle (20°) (Osvalder, Neumann, Lovsund, & Nordwall. 1990) at failure of human motion segments were far stiffer than the porcine motion segments used in this study (61 N*m and 39° for 1 specimen). The entire comparison of the porcine cervical spine as a model for the human lumbar spine is presented in Appendix A. The number of cycles applied to an in-vitro structure must provide a realistic accumulation of in-vivo loading. Brinckmann et al. (1988) used a limit of 5000 cycles which they claimed represented an accumulation of industrial loading occurring in less than two weeks. The magnitude of loading examined ranged from 20 to 70% of the compressive strength

of the specimen. The defense of using a two week cutoff was that repair of bone micro fractures in-vivo would not occur within this amount of time (Brinckmann, Biggemann, & Hilweg. 1988). The proteoglycan turnover has been shown to take 500 days in dogs (Urban, Holm, & Maroudas. 1978) and the collagen production to take even longer (Adams & Hutton. 1982; Porter, Adams, & Hutton. 1989). The only repair/modification mechanism that would alter the results in-vivo would appear to be rest/sleep which would allow the resorption of fluid into the nucleus pulposus and the annulus. In contrast the compressive loads examined in this study were approximately 3 to 16% of the maximum compressive strength (Yingling, Callaghan, & McGill. 1997). The moments (average of 14% of max) or rotations (average of 35% in flexion and 10% in extension of max) applied were also selected to load the specimens in the low level range which would not require straining the joints past their toe region. This loading scenario was chosen to be representative of low load repetitive tasks. Therefore, the number of cycles allowed in this study was set to a maximum of 86,400 which required a testing period of 24 hours. Prolonged testing has been previously employed by other researchers, Hardy et al. (1958) tested specimens for as long as 5 weeks (> 1 million cycles) and Gordon et al. (1991) tested to a maximum of 70,000 cycles over a 13 hour period.

The notion that disc herniation is a progressive phenomenon where final extrusion of material appears to occur on the n^{th} load cycle analogous to "the straw that broke the camels back" is consistent with the lack of a clear indicator of when disc injury occurred. All variables recorded were examined for the full time course of testing. No acute or sudden changes were present to indicate a mechanical failure of the test specimen. Sequential x-rays of several specimens were taken which revealed a progression of injury. Disc injury initiation and breach of

the outer annular boundary were identified from the sequential x-rays and these cycle numbers were then used to examine the recorded displacements and forces. There were no changes evident in any of the corresponding time series around the cycles identified from the x-rays. There were two potential methods for determining if injury had occurred. The axial creep end point in the angular positional groups (867N and 1472N) which yielded more consistent and severe injuries had greater axial deformation (non-significant). The second test that could be useful in determining injuries was the ROM test. The angular position groups (867N and 1472N) resulted in larger changes in the post ROM test than the corresponding torque control groups, particularly the extension moments. Both methods will require further examination paired with documentation of injuries (x-ray) to determine if they could indicate the occurrence of disc injury.

This study has shown that disc injuries and herniations can be developed during highly repetitive low magnitude compression with modest moments and flexion/extension motions. With increased magnitudes of compressive load there was a corresponding increase in the number of disc injuries documented. This finding supports the in-vivo observation that cumulative compression and cumulative moment have been linked to increased probability of reporting back pain (Norman, Wells, Neumann, et al. 1998). This work confirms the occurrence of herniation with repetitive flexion/extension motions but low applied forces and moments.

Chapter VI

Summary

The series of research studies that comprises this thesis have contributed several issues to the field of biomechanics and the knowledge of the functioning of the lumbar spine. The gait study revealed that tissue loading during walking was below levels generated by many specific back rehabilitation tasks presented in the back exercises study of chapter IV (Callaghan, Gunning, & McGill. 1998) and for abdominal exercises (Axler & McGill. 1995), suggesting that walking would be a wise choice for general back exercise and rehabilitation programs. Based on the average body mass of the participants in the study, walking normally the peak compressive joint loading would be 1670 N. Even the simplest specific back exercise (Callaghan, Gunning, & McGill. 1998) (single leg extension from a kneeling position) surpasses this magnitude of loading. The mild muscle activation levels provide aerobic conditioning which has been suggested to increase muscular endurance (Nutter. 1988). This is an important conditioning concern since a lack of isometric endurance has been shown to be an indicator of potential for developing low back pain (Luoto, Heliövaara, Hurri, & Alaranta. 1995). Walking would be beneficial as an initial aerobic conditioning exercise for several reasons. The first being the low

levels of loading, spine motions, and muscular activation should present low risk of injury. Second, the aerobic benefits realized will be more substantial for injured or untrained individuals with reduced benefits as the level of fitness of the participant increases. Holm and Nachemson (1983) demonstrated that spinal motion increased the nutrition to the intervertebral disc indicating that slower walking (which produced a more constant or "static" load and motion profile of the spine) would not be as beneficial as faster walking with a normal arm swinging motion. The back exercises examined provide a range of joint loading and muscle activity levels. The tasks included exercises that ranged from those suitable for the majority of patients who need increased endurance and strength enhancement to activities that required very high muscular activity levels and resulted in substantial joint loads suggesting that their use is unwise. The examination of the time varying responses during sitting revealed that some individuals assume a wide range of postures which they alternate throughout the duration of sitting. This is in contrast to the classification of sitting as the adoption of a single static posture. The forces experienced by the lumbar spine during sitting and standing fell well below any single exposure tissue tolerance value. However, the prolonged exposure that individuals sustain of these static loads could present a cumulative injury mechanism. Standing appears to be a good rest from sitting with respect to lumbar spine posture. Therefore used alternatively as a rest, standing could form a basis for injury prevention when designing work. However, there was little rest/change for muscular activation or joint loading when standing was compared with sitting. Combining activities such as walking with more "static" activities would provide a cyclic activity for joint loads, muscular activation, and spine postures.

The in-vitro examination of repeated loading on the spine revealed that disc injuries and herniations can be developed during highly repetitive low magnitude compression with modest moments and flexion/extension motions. Increased magnitudes of compressive load produced an increased number of intervertebral disc injuries. This finding could explain why tasks below tolerance values produce injuries and supports the in-vivo observation that cumulative compression and cumulative moment have been linked to increased probability of reporting back pain (Norman, Wells, Neumann, et al. 1998).

Table 6.1: A comparison of the compressive forces and flexion angles used for the in-vitro testing with the magnitudes that were calculated from the in-vivo studies of this thesis.

Parameter	In-Vitro	Gait	Sitting	Standing	Exercise
Compression (% of max)	3.25-18	33	18	12	23-60
Flexion Angle (% of max)	35	11	30-80	10	n/a

The parameters selected for the in-vitro testing were based upon both the in-vivo studies and normalization to known tissue tolerance magnitudes of the porcine cervical spine. The compression forces used for the in-vitro testing of porcine cervical spine motion segments were either below or very similar to the values estimated in the in-vivo studies (Table 6.1). The porcine cervical spines were normalized to previous compression testing on spines obtained from the same source (Callaghan & McGill. 1995; Yingling, Callaghan, & McGill. 1997). The in-vivo average compression across subjects was normalized to the regression equation reported by Jager et al. (1991). The in-vitro flexion angles were normalized to one specimen that was loaded to

failure in flexion. Each of the in-vivo studies had individual normalized ranges based on a full lumbar flexion calibration task. The magnitude of in-vitro flexion was larger than the flexion angles documented in-vivo, with the exception of the sitting study. However, the motion in sitting (prolonged flexion) was not representative of the repeated flexion/extension motions examined in-vitro.

In summary the following the individual studies of this thesis suggest the following:

Gait Study

Arm swing was found to reduce spine loads and muscle activation levels; this has been debated for years. Increased walking speed increased the magnitude of muscle activation levels, loads on the lumbar spine, and lumbar spine postures, but also resulted in less constant levels of these variables. The traditionally used rigid link segment model, that assumes rigidity, appears to not represent the way the body dampens heel strike as it propagates through the linkage to the lumbar region.

Sitting/Standing Study

Sitting resulted in higher lumbar spine compression than standing. Individual sitting profiles were discovered with half of the subjects sitting in a very constant position and the other half varying lumbar spine posture over a wide range during the two hour sitting period.

Extensor Exercise Study

High joint compression forces and muscular activation levels were discovered for some typically prescribed back exercises. A gradient of exercises was assessed which provided a range of demands from low to very high.

In-Vitro Repetitive Flexion/Extension Study

While it has been very difficult for previous studies reported in the literature to consistently produce intervertebral disc herniations, they were produced with repeated flexion/extension motions combined with low magnitude compressive loading.

Herniation is a progressive, marked by slow creep and loss of height, tracking of nuclear material from the inner annulus through to the outer annulus with the final extrusion of nuclear material with the Nth repetition, or in real life a rather benign event.

APPENDIX A

The Porcine Cervical Spine as a Model of the Human Lumbar Spine: An Anatomical, Geometrical and Functional Comparison

Vanessa R. Yingling, Jack P. Callaghan, and Stuart M. McGill

Journal of Spinal Disorders (In Press), 1998

ABSTRACT

Summary: Animal models for analysis of spine injury and orthopaedic disorders are commonplace given concerns over bone integrity, disc degeneration and controlled studies of identical specimens, matched for age, weight, physical activity and genetic background. Given this asset, the question is asked; "Is the porcine cervical spine a reasonable model of the human lumbar spine?". Three porcine cervical spines (C2-C7) were assessed for geometrical characteristics, with a larger cohort (N= 24) loaded to failure under either compressive or shear loading. Also, *in vivo* loading was estimated and compared between the human low back (biped) and the porcine neck (quadruped). Generally, the porcine vertebrae are smaller in all dimensions.

The porcine vertebrae have anterior processes unlike humans, however they possess similar ligamentous structure and facet joint orientation. Stiffness values (compression and shear) are similar and comparable injuries resulted from both applied compressive and shear loads. Given the scarcity of healthy, young human lumbar spines, porcine cervical spines may be a useful model for studying human lumbar injury due to the similarity of mechanical characteristics and the resulting injuries, particularly of the adolescent or young adult who has not experienced disc degeneration or calcified end plates.

INTRODUCTION

While much has been learned about spine injury from human cadaveric test specimens, there are many questions in spine research for which human specimens are not preferred. Young, healthy, human spines are extremely rare as typically donors are elderly and sick or were obtained from younger donors who were either sick or sustained substantial violent trauma. This is an important issue as failure patterns in the spine are a function of biological age, for example older discs will not herniate rendering them unsuitable to investigate herniation mechanics. Another important age-related change that occurs is calcification of the cartilaginous end plate observed in older specimens. Furthermore, study of the injury-repair process requires an *in vivo* animal model where several species have been utilized (e.g., rabbits (Smith & Walmsley. 1951), dogs (Key & Ford. 1948), sheep (Osti, Roberts-Vernon, & Fraser. 1990)) together with various trauma models (e.g., pigs (Oxland, Panjabi, Southern, & Duranceau. 1991)) and spine instrumentation models where bone integrity is important (bovine specimens (Allan, Russell,

Moreau, Raso, & Budney. 1990)). A final issue is one of experimental design and scientific control as it is virtually impossible to collect a population of similar human specimens.

However, control is possible using a homogeneous sampling of animal specimens, specifically control over genetic make-up, age, weight, physical activity levels and diet. Further, another advantage with animal tissue is that it is typically harvested from healthy animals. While controlled experiments are only possible using an animal model, the obvious liability is that of relevance for application to human mechanics and orthopaedics. Perhaps the real strength in using an animal model is found "not from the extent to which it mimics reality, but rather from the extent to which it facilitates the formulation and subsequent testing of hypotheses that lead to an improved understanding of that reality" (Krag. 1996). The critical issue addressed in this study was whether the porcine cervical spine is a reasonable analog for furthering our knowledge of injury mechanisms in the human lumbar spine.

The purpose of this study was to assess differences and similarities of the porcine cervical spine and the human lumbar spine given its use as a surrogate model. Porcine and human specimens were compared with respect to several parameters: anatomical; geometrical; and functional characteristics. Anatomical-geometrical parameters, load-deformation, and failure characteristics of porcine cervical vertebrae were collected in the laboratory. Human vertebral geometry and functional behavior were gathered from the literature. Finally, to address the issue of comparing a biped to a quadruped, analytical modeling was performed to assess whether loading experienced by the human lumbar spine is similar to the porcine cervical spine *in vivo*.

METHODS

Geometrical Measurements

Calipers were used to measure nine parameters of the porcine vertebrae (Figure A.1): four parameters of the vertebral body, the width and depth of both the upper and lower endplates (UEW, LEW, UED, LED); seven parameters of the posterior elements, the pedicle width (PEDW), pars height (PH), pars width (PW), spinal canal depth and width (SCD, SCW).

A specially designed gimbal (Figure A.2) was used to measure the two major angles of the facet joint (Figure A.1). The sagittal facet angle was defined as the orientation of the facet face with the sagittal plane and the transverse angle was defined as the orientation of the pars and facet face with the horizontal plane (Figure A.1). The vertebrae were oriented using two site lines and the angles were measured via protractors attached to the gimbal.

Endplate areas were determined using two methods. The endplates of both human and porcine vertebrae are often described as resembling an ellipse (Figure A.3). Therefore, the formula for the surface area of an ellipse ($\pi/4 * a * b$) (Hutton & Adams. 1982) was used to estimate the surface area of the endplate of a vertebral body. A second method utilized an electronic digitizing tablet (Summasketch 010, Summagraphics, Seymour, CT), which determined the area of the endplate from the digitized perimeter using an area integration algorithm. Scaled photographs of both upper and lower endplates were taken and digitized using the digitizing tablet.

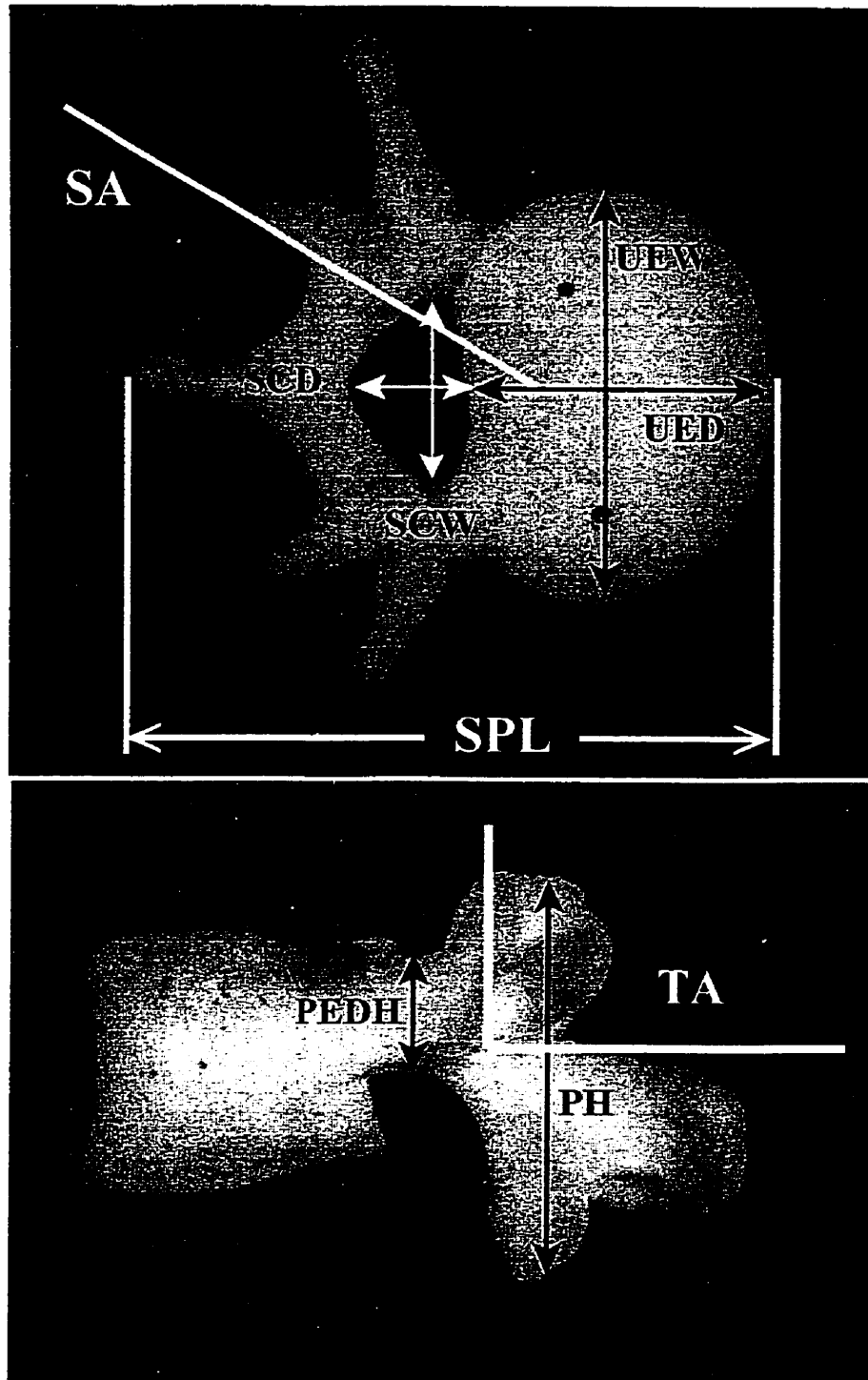


Figure A.1: Schematic top and side view of a human lumbar vertebra illustrating the measured parameters: width and depth of both upper and lower endplates (UEW, LEW, UED, LED), pedicle width (PEDW), pars height (PH), spinal canal depth and width (SCD, SCW), and the sagittal (SA) and transverse (TA) facet angles.

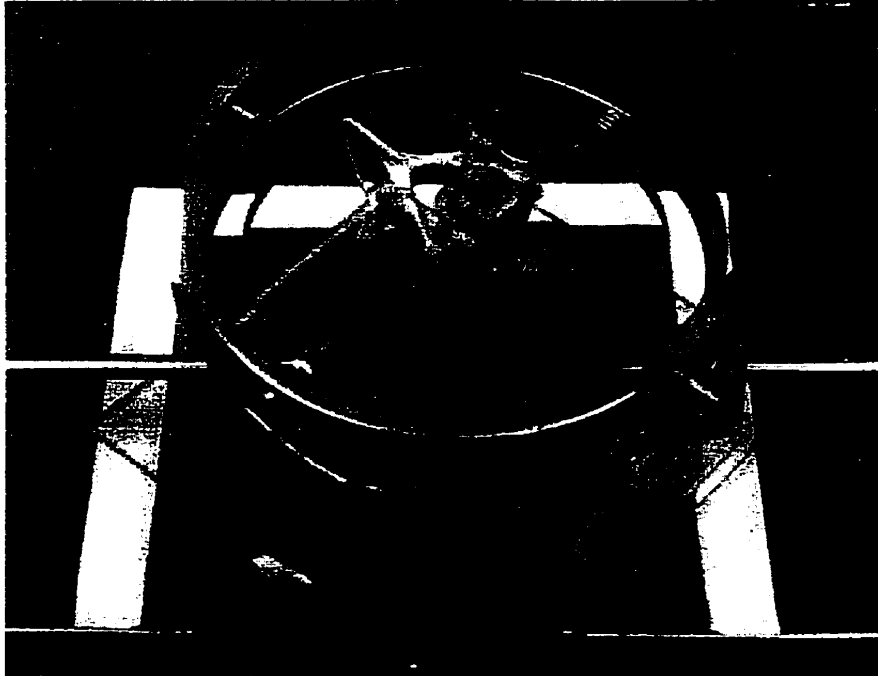


Figure A.2.: Angle measurement gimbal with three angular degrees of freedom and measurement.

Mechanical Properties

A servo-hydraulic dynamic testing machine (Instron Model 8511, Instron Canada Inc. Burlington, ON) was used to determine the mechanical properties of the porcine cervical motion segments under both shear (N=10) and compressive (N=14) loading. Similar methodological approaches were used for the compressive and shear tests, only the custom testing jigs differed between the two types of loading. For the compressive tests, each specimen consisted of three vertebrae to avoid the effects of the potting material on the "end" vertebrae. The specimens were mounted in stainless steel cups with the central vertebrae endplates parallel to the cups to avoid a bending moment during testing, and fixed with dental plaster (Denstone, Miles Inc. South Bend, IN. USA). A specially designed jig was used for the testing which applied only a compressive

load onto the specimens. A compressive preload of 300 N was applied for 15 minutes to the specimens to produce an equilibrium state in the creep response. The spines were then loaded to failure at different load rates, 100 N/s, 3000 N/s, 10,000 N/s 16,000 N/s. Each specimen was only tested once to failure. Failure was defined as a 3.125% drop in the compressive force applied to the specimens. The choice of the drop is important since too large a drop would not detect the first stages of failure (injury) and result in massive tissue destruction. Load deformation curves were sampled from 50-100 Hz and processed to obtain the mechanical parameters of the specimens which included the energy stored at failure, the deformation to failure, the ultimate compressive load at failure and the average stiffness of the specimen.

The specimens subjected to shear loading, which consisted of two vertebrae, were mounted into stainless steel cups using dental plaster with steel wire looped around the pedicles and the anterior processes to secure the specimens. A jig, compatible with the Instron machine, constrained the motion of one vertebral joint in pure shear. A compressive preload, 300 N, was applied to the motion segment through a calibrated spring mechanism. The spines were then loaded to failure.

Finally, the measured parameters and functional test values of the porcine cervical vertebrae were compared with values found in the literature on human thoracic and lumbar vertebrae. As well, an analytical model was used to assess loading on the quadruped porcine cervical spine and the human lumbar spine (the head-neck of an 80 kg pig was used to determine the modeling parameters needed for analysis).

RESULTS

Qualitatively, several structures of the porcine vertebrae appear to be somewhat similar to the human lumbar vertebrae (Figure A.3) with the exception of the anterior processes of the pig (which appear to have no significant mechanical role (Oxland, Panjabi, Southern, & Duranceau, 1991)). A comparison of the four vertebral body parameters from porcine specimens measured in this study to human values found in the literature demonstrate that both the endplate depth and width (Figure A.1) of the porcine specimens are on average 10 mm less than the human vertebrae (Table A.1). Consequently, the endplate areas are smaller in the porcine with an average area of 500 mm² likened to an average area of 1000 mm² for human lumbar vertebra (Table A.2). There was no statistical difference between the calculated endplate area using the ellipse formula and the area measured by the digitizing tablet suggesting that the ellipse seems to provide a good approximation of the shape of the vertebral endplate.

A comparison of the posterior elements of the porcine cervical vertebrae to the human lumbar vertebrae (Table A.3) demonstrated that the pars interarticularis, an important structure in resisting shear loads, is smaller in the porcine vertebrae. The pedicle of the vertebra, also a structure of the neural arch involved in resisting both applied shear loads and bending moments, compared well with values from human lumbar vertebrae (Table A.3). The spinal canal dimensions were similar to human lumbar vertebrae, but the spinal canal width (SCW) was smaller (Table A.3).

Table A.1: Human - Porcine comparison of vertebral body dimensions, mean (sd)

Variable	Porcine Vertebra C3-C7	Nissan & Gilad (1986) Human L1-L5 (Radiographs)	Cotterill et al.(1986) Human L3	White & Panjabi (1990) Human T12
Endplate Depth UED(mm)	22.28 (2.54)	L1: 33.5 (2.9)		32.8
		L2: 34.4 (2.9)		
		L3: 34.7 (2.7)	32.7 (6.1)	
		L4: 34.4 (2.7)		
		L5: 34.2 (2.7)		
(LED) (mm)	22.53 (2.67)	L1: 34.1 (2.9)		33.4
		L2: 34.7 (3.0)		
		L3: 34.6 (2.8)		
		L4: 34.9 (2.8)		
		L5: 33.9 (2.7)		

Table A.2: Comparison of upper endplate area (UEA) and lower endplate area (LEA) using both the formula of an ellipse and simograph, mean (sd).

Cervical spinal level	C3	C4	C5	C6	C7
UEA (mm ²) ellipse	501.72 (129.33)	572.23 (132.17)	580.91 (133.54)	570.03 (130.36)	534.79 (133.81)
UEA (mm ²) scanned	535.27 (136.28)	539.01 (127.00)	573.36 (132.08)	586.68 (144.50)	529.75 (102.02)
LEA (mm ²) ellipse formula	594.10 (133.06)	622.37 (139.72)	656.88 (146.81)	629.99 (150.55)	573.91 (159.21)
LEA (mm ²) scanned	649.01 (150.64)	558.83 (140.19)	598.37 (141.92)	597.21 (144.40)	567.65 (144.75)

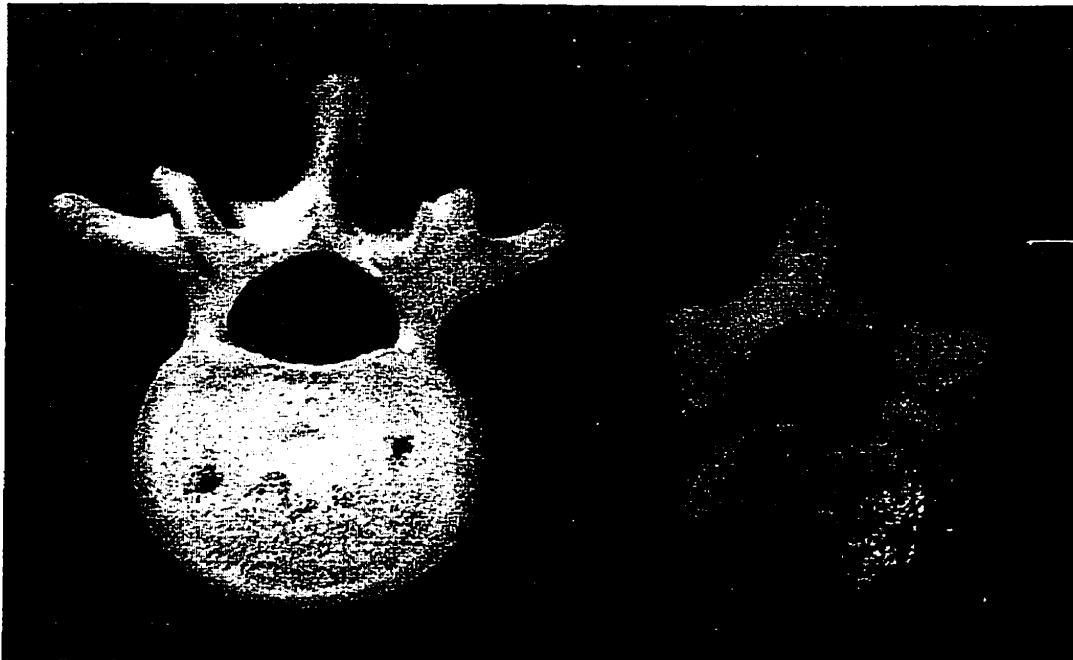


Figure A.3: Top view of a human lumbar vertebra and a porcine cervical vertebra (with anterior processes removed).

The facet joints of the human lumbar motion segments are oriented perpendicular to the vertebral body (transverse facet angle), which enables the facet joints to resist shear loading (Table A.3). A similar alignment was found for the porcine cervical vertebrae, the transverse facet angle was on average 81.2° (Table A.3). The facet faces are also angled approximately 45° from the sagittal plane (sagittal facet angle) (White & Panjabi. 1990) which permits the facets to resist torsional loading. The sagittal facet angle for porcine specimens was 45° (right) and 47.4° for the left (Table A.3).

The mechanical characteristics of porcine cervical vertebrae under applied shear loading appear to have similar values to human samples (Table A.4). Our data from porcine specimens and that from Cripton et al. (1995) on human specimens presented similar trends for anterior and posterior shear stiffness. Cripton et al. (1995) loaded under position control at rates 0.5 and 50.0 mm/s, but given the stiffness observed these translated to approximately 250 and 12500 N/s, respectively. Under destructive testing conditions, where vertebral rotation was constrained Cripton et al. (1995) found an ultimate load to failure of approximately 2500 N under anterior loading compared to an average of 1980 N (160 N) found in the porcine specimens from this study. Further, the fracture of the pars interarticularis below the facet face found through dissection and planar x-ray on porcine specimens compare to injuries found in human specimens following *in vitro* tests (Figure A.7) (Krypton, Berleman, Visarius, Begeman, Nolte, & Prasad. 1995).

Table A.3: Human - Porcine comparison of the posterior elements and the spinal canal dimensions, mean (sd).

Variable	Porcine		Cotterill et al. (1986)	White & Panjabi (1990)	Berry et al. (1987) Human L1-L5	
	Right	Left			Right	Left
Pedicule Width (PEDW) (mm)	8.67	8.91	8.4 (2.0)	8.8	L1: 7.0 (1.9)	L1: 6.9 (1.7)
	(1.21)	(.95)			L2: 7.4 (1.6)	L2: 7.5 (1.5)
					L3: 9.2 (1.3)	L3: 9.1 (1.6)
					L4: 10.3 (1.6)	L4: 10.4 (1.6)
					L5: 10.9 (3.4)	L5: 10.5 (2.9)
Pars Height (PH) (mm)	28.81	29.34	n.a.	n.a.	L1: 47.6 (3.7)	L1: 47.3 (3.7)
	(2.94)	(1.99)			L2: 45.2 (3.6)	L2: 44.8 (4.6)
					L3: 48 (3.2)	L3: 48.6 (3.3)
					L4: 48.5 (2.7)	L4: 49.1 (3.5)
					L5: 41.5 (4.4)	L5: 42.2 (3.7)
Pars Width (PW) (mm)	8.48	8.35	n.a.	n.a.		
	(.89)	(.92)				
Sagittal Facet Angle (degree)	45.0	47.4	57.8 (7.3)	45		n.a.
	(7.7)	(7.8)				
Transverse Facet Angle (degree)	81.2	81.7	87.2 (4.2)	90		n.a.
	(6.2)	(4.3)				
Spinal Canal Depth SCD	9.78		12.1 (1.5)	18.1	L1: 17.2 (1.3)	
	(1.68)				L2: 16.0 (2.6)	
					L3: 16.2 (2.6)	
					L4: 16.1 (1.5)	
					L5: 17.3 (2.9)	
Spinal Canal Width SCW (mm)	17.92		21.5 (1.7)	22.2	L1: 22.1 (2.3)	
	(1.84)				L2: 23.0 (2.3)	
					L3: 22.7 (1.7)	
					L4: 22.0 (1.8)	
					L5: 26.0 (2.5)	

Table A.4: Comparison of the mechanical properties of the human and porcine motion segments under shear loading, mean (sd)

Shear Loading	Human Lumbar Vertebrae Cripton et al. (1995)	Porcine Cervical Vertebrae
Anterior Stiffness N/mm	155	212 (42)
Anterior Loading Ultimate Load to Failure N	2500	1980 (160)
Posterior Stiffness N/mm	104	164 (24)



Figure A.7: Pars interarticularis injury resulting from *in vitro* shear loading of a porcine vertebra.

Compressive load tests under quasi-static and dynamic load rates have resulted in similar trends between human and porcine vertebrae (tolerance values for compressive tests on human and porcine vertebrae are shown in Table A.5). Injuries resulting from compressive loading using human and porcine motion segments were similar, endplate fractures were the common injury in both specimens (Figure A.4). Specifically, at lower load rates, stellate endplate fractures were recurrent, however, at higher load rates edge fractures of the vertebral bodies appeared (Figure A.6).



Figure A.4: Porcine endplate fracture resulting from compressive loading.

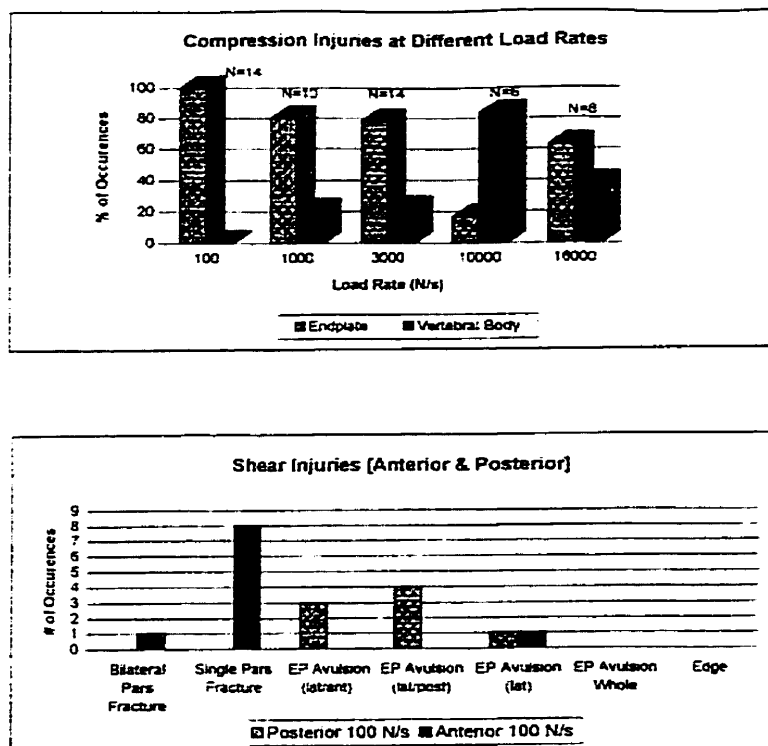


Figure A.6: Compressive and shear injuries resulting from *in vitro* testing of porcine vertebrae.

Table A.5: Comparison of the mechanical properties of the human and porcine motion segments under compressive loading, mean (sd)

Compressive Loading	Human Lumbar Vertebrae Genaidy et al. (1993) Porter et al. (1989) Jager et al. (1991)	Porcine Cervical Vertebrae Yingling et al. (1997)	
		Quasi-static	Dynamic
Stiffness N/mm	n.a.	1720 (280)	2780 (620)
Ultimate Compressive Load	4000 - 8000* 13954+ Female: 3970@ Male: 5810@	6750 (1180)	8890 (1440)

* Average values from a motion segment

+ Maximum value from one specimen

There are two final issues regarding the *in vivo* of loading between the two animals: the first is to compare the neck loads of a biped to an anatomically similar quadruped; the second is to compare the demands on the human lumbar spine and the porcine cervical spine. Upon first consideration, many would expect a biped neck to experience higher compressive loads than a quadruped given the upright orientation. This does not appear to be the case. The human neck supports the mass of the head, approximately 60 N of compression in an 80 kg person in upright standing. If one were to bend forward to simulate a quadruped posture and assuming the head center of mass to be cantilevered 7cm from the fulcrum of the C4-C5 joint, an extensor tissue moment arm of 2.32 cm (Moroney, Schultz, & Miller. 1988) then the compressive load increases approximately three-fold to 180 N. The point is that the head of a quadruped (horizontal spine orientation) increases the compressive load from a similar architecture orientated vertically (as in a biped). Now to compare the applied loads on a human lumbar spine to a pig cervical spine - in upright quiet standing and assuming an upper body mass of 40 kg, the human lumbar spine would experience approximately 400 N of compressive load. In contrast, during quiet standing the quadruped pig has the head/neck cantilevered in front of the body requiring an extensor moment for support (Figure A.5). Using the head-neck of an 80 kg pig the following measurements were obtained: a mass of 17.7 kg for the head to the C4-C5 segment, a center of mass residing 12.8 cm anterior of C4-C5, and an extensor moment arm of 12.9 cm (with a slight posterior shear orientation due to serratus ventralis cervicis and splenius). The resulting compressive load at C4-C5 would be 126 N (or approximately 31% of the human lumbar spine). This is a substantial load, but still smaller than the upright human lumbar static load. However, the pig has well developed extensor

muscles for uprooting food, which would impose much larger compressive forces on the cervical spine. This analysis helps to explain the functional similarity of the porcine cervical spine and the human lumbar spine as well as the greater need for compressive load bearing in the quadruped neck.

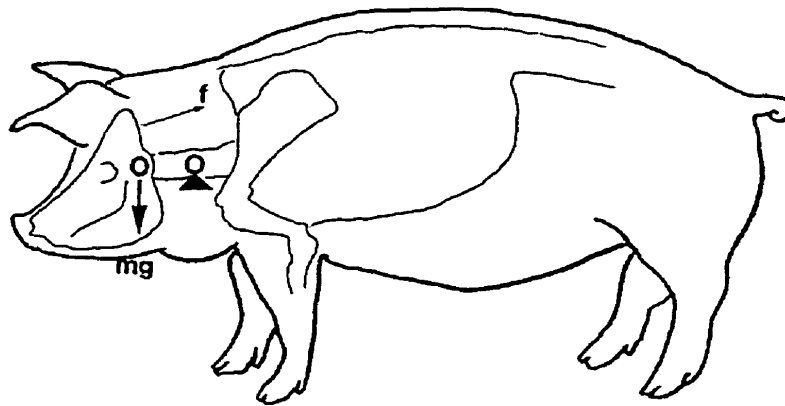


Figure A.5: The quadruped porcine must support the cantilevered head with an extensor moment creating approximately 126 N. of compressive load.

DISCUSSION

The current study assessed the structural and functional properties of porcine cervical vertebral motion segments and human lumbar vertebral motion segments and found them to share several parameters, although the porcine values appear to have to be scaled to replicate human values. Furthermore, given the similarity in the manner in which the specimens fail and are injured, it appears that human injury mechanisms and the spine's capacity to resist

different loading conditions may be investigated using a porcine model, particularly when a "younger" model is required.

Two main limitations should be realized for interpretation of the results of the current study. First, the number of porcine spines used for the quantitative geometry comparison was small (N=3 spines, 18 vertebrae), however, the repeatability of the porcine dimensions (see the small variance about the mean in Tables A.1 and A.3) indicated that a larger sample size was not necessary. Second, the porcine vertebrae were harvested from a homogeneous population and were compared to human tissue which was acquired from a variable and uncontrolled population. The human specimens varied in age, gender, race and disease state at the time of death. These factors have been found to affect the tolerance of the spine. Additionally, geometric differences and pedicle inclination have been found to differ between different racial populations (Cheung, Ruan, Chan, & Fang. 1994).

Oxland et. al. (1991) described qualitatively the similarities between porcine cervical vertebrae and human lumbar vertebrae. They determined that the facets shared a similar orientation and there was a "consistency" of the posterior interspinous and supraspinous ligaments. Furthermore, Sikoryn and Hukins (1990) reported similarities between the human and porcine ligamentum flavum after dissection. The maximum stress found in porcine ligamentum flavum, 2.6 -3.0 MPa (Sikoryn & Hukins. 1990) was somewhat lower than values found from human ligaments, 4.4 MPa (Krenz & Troup. 1973). The porcine vertebrae were characterized by ossification centers as determined through x-ray, which were similar to a child or adolescent spine (Oxland, Panjabi, Southern, & Duranceau. 1991). Furthermore, the porcine spine was shown to be preferable over young bovine spines for testing of spinal fracture

fixation devices since failure at end-plate was more readily observed in bovine spines (Allan, Russell, Moreau, Raso, & Budney. 1990).

The ultimate compressive strength of the spine has been found to be affected by the age, race, gender, body weight, level of disc degeneration, bone density and physical activity of the specimen donor together with the testing protocol reported. These factors compromise the direct comparison of tolerance values between porcine and human vertebrae, although geometrical similarities, the trends in the mechanical properties, and the injury mechanisms will be compared here. The alignment of the facet joints and the elliptical shape of the vertebral body and endplate are similar between the species. Researchers (Hutton, Cyron, & Stott. 1979; Kazarian & Graves. 1977) using human specimens found increases in the stiffness and the ultimate compressive loads of lumbar vertebrae and decreases in the deformation to failure between quasi-static and dynamic compressive loading tests. Kazarian et al. (1977) using three deformation rates (0.21, 21, 2100 in/min) found the ultimate compressive load to increase, (8.76 kN, 12.1 kN, 14.9 kN). The stiffness also increased with loading rate (2966 N/mm, 4234 N/mm, 5360 N/mm), respectively. A study using porcine cervical vertebrae by Yingling and colleagues (1997) found similar trends to the human tests; the stiffness increased from 1700 N/mm to 3000 N/mm with an increase in load rate from 100 N/s to 16,000 N/s. The maximum compressive load also increased from 7000 N to 9700 N.

Common compressive injuries resulting from *in vitro* compressive loading of human tissue are endplate failures or stellate fractures (two or more cracks running from the center of the endplate to the periphery (Brinckmann, Biggemann, & Hilweg. 1989). As the compressive load is applied to the joint, and pressure in the gelatinous nucleus increases, the annulus and the

endplates begin to bulge, the fracture occurs when the pressure of the endplate on the cancellous bone exceeds its tolerance. The stellate fractures are sometimes accompanied by an intrusion of nuclear gel into the trabecular bone. These injuries are difficult to detect *in vivo* and are typically documented post-mortem or using laminograms. These same stellate fractures are commonly found in porcine spines after compressive loading (Figure A.4) (see Tsai et al. (1997) who made similar observations).

A second type of injury due to compressive loading found in humans (Brinckmann, Biggemann, & Hilweg. 1989), and in porcine spines, are edge fractures of the vertebral body. These are wedge-like fractures at the edge of the vertebral body similar to a bone avulsion injury in a bone-ligament-bone complex. These fractures were more prevalent during higher load rate compressive testing of porcine material (Figure A.6). At higher load rates (but not impacts) the bony attachment of the annulus to the cortical vertebral body is weaker than the collagenous fibers of the annulus and the annulus-bone interface ruptures resulting in an edge fracture.

Shear loading results primarily in injuries to the pars interarticularis. A typical fracture originates at the posterior facing aspect of the superior facet below the facet face and on the anterior portion of the inferior facet above the facet face (Krypton, Berleman, Visarius, Begeman, Nolte, & Prasad. 1995). The thought that genetic factors predisposed individuals to pars defects which resulted in fractures was reexamined by Krenz & Troup. (1973). However, mechanical factors are currently thought to be associated with fractures of the pars interarticularis. An applied shear load to the intervertebral joint introduces a bending moment on the pars interarticularis and the pedicles. The porcine pars fractures found *in vitro* were

located in the same location as injuries described in human vertebrae. Pars injuries are not only found *in vitro*, injuries found *in vivo* on cricket bowlers are typically pars interarticularis defects. The study of 22 bowlers resulted in 6 bilateral and 6 unilateral pars defects being detected (Hardcastle, Annear, Foster, et al. 1992). Injuries found *in vivo* in clinical assessments of spondylolisthesis patients also suggest injuries of the pars interarticularis (Grobler, Novotny, Wilder, Frymoyer, & Pope. 1994; Newman. 1963). As well, a study of skeletons from Alaskan natives verified that every second skeleton showed one or more defective neural arches (Stewart. 1953). The defects were considered defects of the neural arch but did not specify whether they were defects to the pedicle or to the pars interarticularis. Porcine *in vitro* shear testing also resulted in annular avulsions, a tearing of the endplate from the vertebral body. Cripton et. al. (1995) reported avulsion injuries on human vertebrae after *in vitro* testing.

In conclusion, while it is acknowledged that human spines are preferable to answer many questions, the unavailability of young, healthy, matched specimens is a reality. The porcine cervical vertebral motion segment may be a useful model in research investigating injury mechanics of the human lumbar spine when a "young" disc and endplate is desired. However, clearly, observations and conclusions obtained from a porcine model must be within the limitations of non-human material and be scaled to match human magnitudes.

APPENDIX B

**Analysis of the loads transferred loads to the
spinal motion segment during in vitro testing**

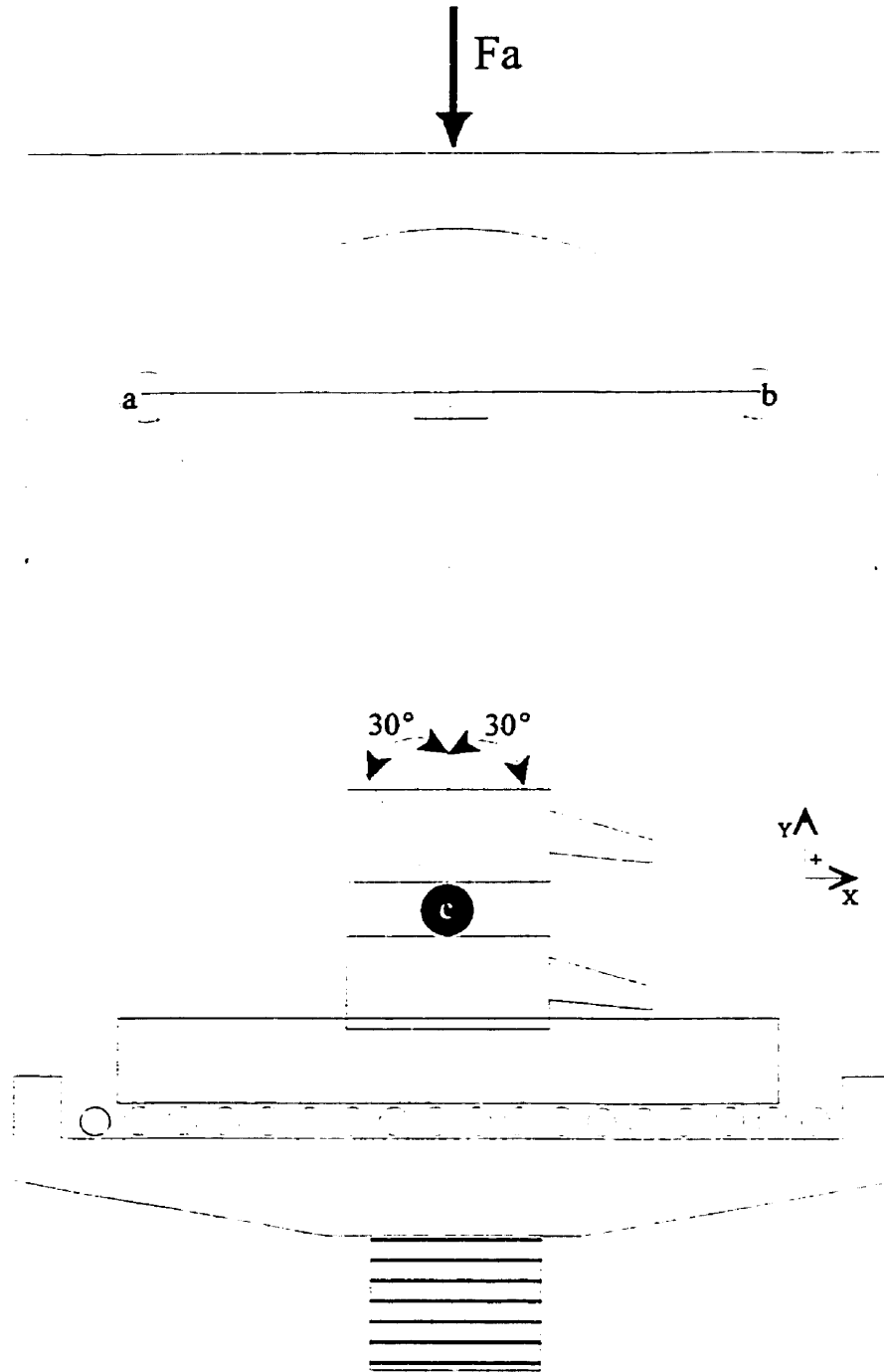


Figure B.1: The spherical seat of the flexion/extension jig used in the repeated in vitro testing. Points a and b were the roller bearing which only transmitted normal forces. F_a was the compressive force applied by the Instron test frame. The lower vertebra was mounted to a cup which freely translated on an X-Y table.

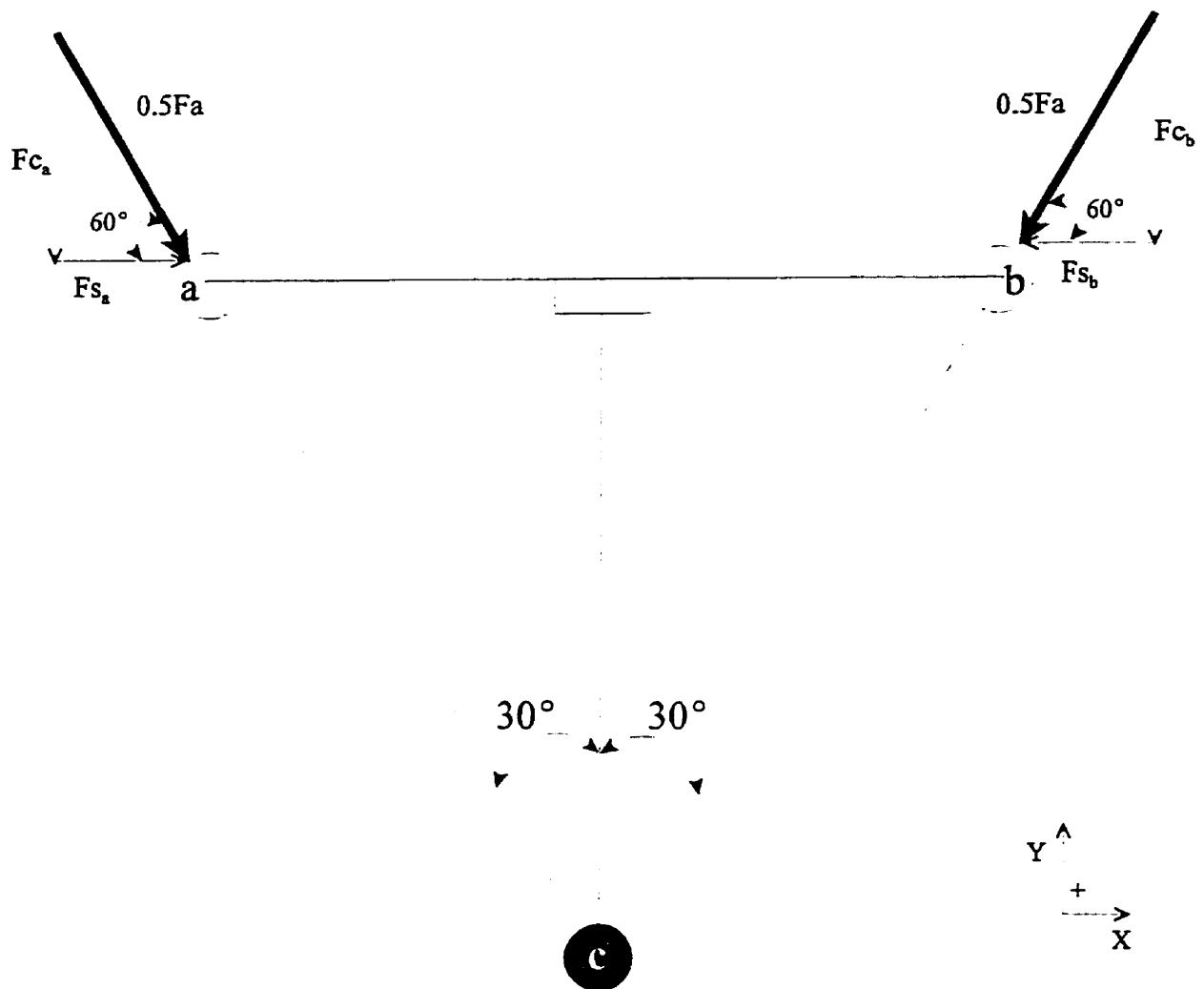


Figure B.2: Decomposition of the normal forces on the roller bearings into x and y components.

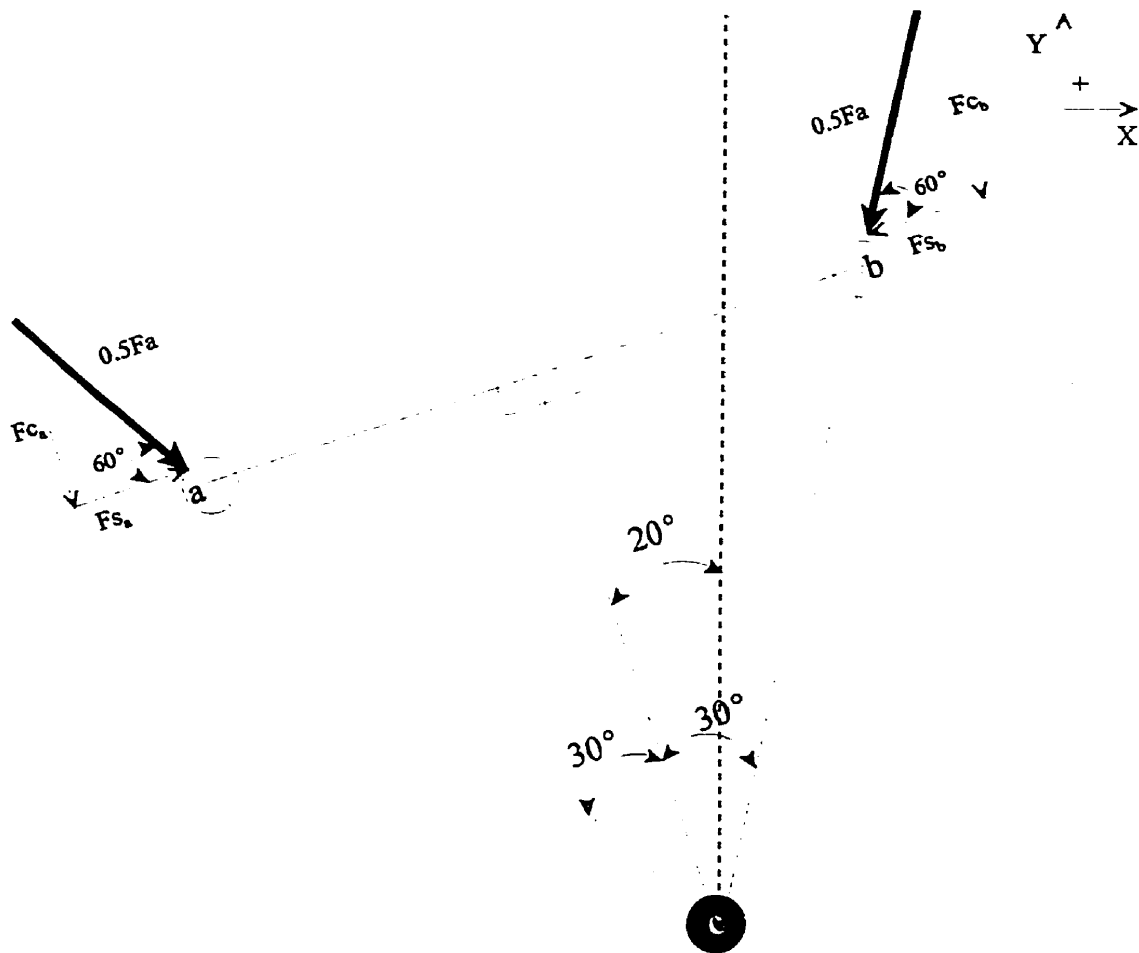


Figure B.3: Rotation of the specimen by 20° to demonstrate the invariable relationship between the axial applied compressive force and the force transmitted at point c .

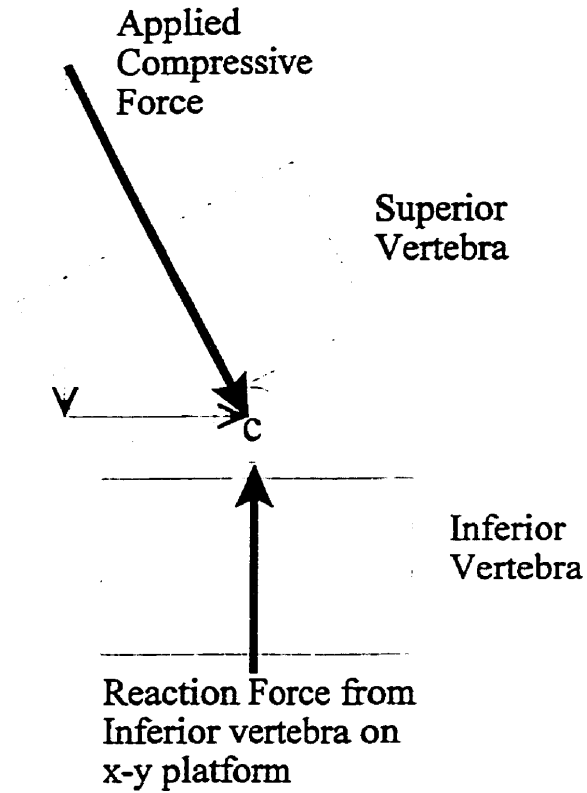


Figure B.4: The forces experienced by the motion segment.

A sagittal and simplified planar view of the loading apparatus is presented in figure B.1 to demonstrate the compressive forces applied to the specimen. The applied compressive force was assumed to be equally carried by the roller bearings that make contact with the spherical seat (figure B.2). The spherical contact surface will only transmit forces normal to the surface, which will result in canceling out any shear forces regardless of the angle of rotation (figure B.3). Therefore regardless of the angle of the cup, the invariable relationship of the angle of the roller bearings that only transmit a normal force insure that the force applied by the Instron will be purely compressive on the superior vertebra (figure B.4).

$$F_{s_a} = 0.5 * F_a * \cos(60^\circ)$$

$$F_{s_b} = 0.5 * F_a * \cos(60^\circ)$$

This demonstrates that the shear force at point a will always be equal and opposite to the shear force at point b (figures B.2 and B.3.).

$$F_{c_a} = 0.5 * F_a * \sin(60^\circ)$$

$$F_{c_b} = 0.5 * F_a * \sin(60^\circ)$$

Therefore compressive force on the superior vertebra will always be 0.866 of the Force applied by the Instron (F_a).

In Figure B.1 it can be seen that the lower vertebra is rigidly fixed to a cup that rests on an X-Y platform. If an assumption of negligible friction in the X-Y platform was made this cup would only transmit normal forces to the lower vertebra. This would only expose the lower vertebra to compressive forces. The shear forces that are applied due to the superior vertebra being angled with respect to the upper vertebra will result in a translation of the lower cup.

While this is a simplified analysis, which does not examine lateral forces or any moments that would be carried by the jig, it is merely intended to demonstrate the idea behind the conception of the design.

REFERENCES

- Adams, M.A., & Hutton, W.C. (1981). Is there compressive loading on the apophyseal joints of the lumbar spine in erect posture? In I.A.F. Stokes (Ed.), *Mechanical factors and the skeleton*. (pp. 23-24). London: John Libbey.
- Adams, M.A., & Hutton, W.C. (1982). Prolapsed intervertebral disc: A hyperflexion injury. *Spine*, 7, 184-191.
- Adams, M.A., & Hutton, W.C. (1983). The effect of fatigue on the lumbar intervertebral disc. *Journal of Bone and Joint Surgery (B)*, 65, 199-203.
- Adams, M.A., & Hutton, W.C. (1985). Gradual disc prolapse. *Spine*, 10, 524-531.
- Adams, M.A., & Hutton, W.C. (1986). Has the lumbar spine a margin of safety in forward bending. *Clinical Biomechanics*, 1, 3-6.
- Adams, M.A., Hutton, W.C., & Stott, J.R.R. (1980). The resistance to flexion of the lumbar intervertebral joint. *Spine*, 5, 245-253.
- Adams, M.A., McNally, D.S., Chinn, H., & Dolan, P. (1994). Posture and the compressive strength of the lumbar spine. *Clinical Biomechanics*, 9, 5-14.
- Allan, D.G., Russell, G.G., Moreau, M.J., Raso, V.J., & Budney, D. (1990). Vertebral end-plate failure in porcine and bovine models of spinal fracture instrumentation. *Journal of Orthopaedic Research*, #8, 154-156.

- Althoff, I., Brinckmann, P., Frobin, W., Sandover, J., & Burton, K. (1992). An improved method of stature measurements for quantitative determination of spinal loading - application to sitting postures and whole body vibration. *Spine*, *17*, 682-693.
- Andersson, G.B.J., Murphy, R.W., Örtengren, R., & Nachemson, A. (1979). The influence of backrest inclination and lumbar support on lumbar lordosis. *Spine*, *4*, 52-58.
- Axler, C. T. and McGill, S. M. (1995). Abdominal exercises: searching for the optimal muscle challenge with minimal spine loading. Stanford: Stanford University. 115p. Nineteenth Annual Meeting of the American Society of Biomechanics.
- Battie, M.C., Bigos, S.J., Fisher, L.D., Spengler, D.M., Hansson, T.M., Nachemson, A.L., & Wortley, M.D. (1990). The role of spinal flexibility in back pain complaints within industry: a prospective study. *Spine*, *15*, 768-773.
- Berry, J.L., Moran, J.M., Berg, W.S., & Steffee, A.D. (1987). A morphometric study of human lumbar and selected thoracic vertebrae. *Spine*, *12*, 362-367.
- Biering-Sorensen, F. (1984). Physical measurements as risk indicators for low-back trouble over a one-year period. *Spine*, *9*, 106-119.
- Brinckmann, P., Biggemann, M., & Hilweg, D. (1988). Fatigue fracture of human lumbar vertebrae. *Clinical Biomechanics*, *3 Suppl 1*, s1-s23
- Brinckmann, P., Biggemann, M., & Hilweg, D. (1989). Prediction of the compressive strength of human lumbar vertebrae. *Clinical Biomechanics*, *4, Suppl 2*, s1-s27

- Brinckmann, P., & Porter, R.W. (1994). A laboratory model of lumbar disc protrusion - Fissure and Fragment. *Spine*, *19*, 228-235.
- Buckwalter, J.A. (1995). Spine update: Aging and degeneration of the human intervertebral disc. *Spine*, *20*, 1307-1314.
- Burton, A.K., Tillotson, K.M., & Troup, J.D.G. (1989). Variation in lumbar sagittal mobility with low back trouble. *Spine*, *14*, 584-590.
- Callaghan, J.P., Gunning, J.L., & McGill, S.M. (1998). The relationship between lumbar spine load and muscle activity during extensor exercises. *Physical Therapy*, *78*, 8-18.
- Callaghan, J.P., & McGill, S.M. (1995). Frozen storage increases the ultimate compressive load of porcine vertebrae. *Journal of Orthopaedic Research*, *13*, 809-812.
- Callaghan, J. P., Patla, A. E., and McGill, S. M. (1996). An examination of rigid link segment models for gait analysis. Vancouver: Simon Fraser University. 216p. Proceedings of the Ninth Biennial Conference and Symposia of the Canadian Society for Biomechanics.
- Callaghan, J.P., Patla, A.E., & McGill, S.M. (1998). Low back three-dimensional joint forces, kinematics, and kinetics during walking. *Clinical Biomechanics*, *In Press*,
- Cappozzo, A. (1983). The forces and couples in the human trunk during level walking. *Journal of Biomechanics*, *16*, 265-277.

Cappozzo, A. (1984). Compressive loads in the lumbar vertebral column during normal level walking. *Journal of Orthopaedic Research*, 1, 292-301.

Cavanaugh, J.M. (1995). Neural mechanisms of lumbar pain. *Spine*, 20, 1804-1809.

Cavanaugh, J.M., Kallakuri, S., & Özaktay, A.C. (1995). Innervation of the rabbit lumbar intervertebral disc and posterior longitudinal ligament. *Spine*, 20, 2080-2085.

Chaffin, D.B., & Andersson, G.B.J. (1990). *Occupational Biomechanics*. New York: John Wiley & Sons Inc.

Cheung, K.M.C., Ruan, D., Chan, F.L., & Fang, D. (1994). Computed tomographic osteometry of asian lumbar pedicles. *Spine*, 19, 1495-1498.

Cholewicki, J., & McGill, S.M. (1996). Mechanical stability of the in vivo lumbar spine: Implications for injury and chronic low back pain. *Clinical Biomechanics*, 11, 1-15.

Cholewicki, J., McGill, S.M., & Norman, R.W. (1991). Lumbar spine loads during the lifting of extremely heavy weights. *Medicine and Science in Sports and Exercise*, 23, 1179-1186.

Cotterill, P.C., Kostuik, J.P., D'Angelo, G., Fernie, G.R., & Maki, B.E. (1986). An anatomical comparison of the human and bovine thoracolumbar spine. *J.Orthop.Res.*, 4, 298-303.

Cromwell, R., Schultz, A.B., Beck, R., & Warwick, D. (1989). Loads on the lumbar trunk during level walking. *Journal of Orthopaedic Research*, 7, 371-377.

Elftman, H. (1939). The function of the arms in walking. *Human Biology*, 11, 529-535.

Farfan, H.F., Huberdeau, R.M., & Dubow, H.I. (1972). Lumbar intervertebral disc degeneration: The influence of geometrical features on the pattern of disc degeneration - A post mortem study. *Journal of Bone and Joint Surgery (Am.)*, 54A, 492-510.

Flint, M.M. (1965). Abdominal muscle involvement during performance of various forms of sit-up exercises: electromyographic study. *American Journal of Physical Medicine*, 44, 224-234.

Galante, J.O. (1967). Tensile properties of the human lumbar annulus fibrosus. *Acta Orthop Scand, Suppl # 100*, 5-91.

Genaidy, A.M., Waly, S.M., Khalil, T.M., & Hidalgo, J. (1993). Spinal compression tolerance limits for the design of manual material handling operations in the workplace. *Ergonomics*, 36, 415-434.

Goel, V.K., Voo, L.M., Weinstein, J.N., Liu, Y.K., Okuma, T., & Njus, G.O. (1988). Response of the ligamentous lumbar spine to cyclic bending loads. *Spine*, 13, 294-300.

Goel, V.K., & Weinstein, J.N. (1990). *Biomechanics of the spine: Clinical and surgical perspective*. Boca Raton: CRC Press.

Goel, V.K., Wilder, D.G., Pope, M.H., & Edwards, W.T. (1995). Controversy: Biomechanical testing of the spine: Load-controlled versus displacement-controlled analysis. *Spine*, 20, 2354-2357.

Gordon, S.J., Yang, K.H., Mayer, P.J., Mace, A.H.Jr., Kish, V.L., & Radin, E.L. (1991). Mechanism of disc rupture - a preliminary report. *Spine*, 16, 450-456.

Grobler, L.J., Novotny, J.E., Wilder, D.G., Frymoyer, J.W., & Pope, M.H. (1994). L4-5 isthmic spondylolisthesis. *Spine*, 19, 222-227.

Gunzburg, R., Parkinson, R., Moore, R., Cantraine, F., Hutton, W.C., Vernon-Roberts, B., & Fraser, R. (1992). A cadaveric study comparing discography, magnetic resonance imaging, histology, and mechanical behavior of the human lumbar disc. *Spine*, 17, 417-423.

Hadler, N.M. (1997). Back pain in the workplace. What you lift or how you lift matters far less than whether you lift or when [editorial]. *Spine*, 22, 935-940.

Hagberg, M., Silverstein, B.A., Wells, R.P., Smith, M.J., Hendrick, H.W., Carayon, P., & Perusse, M. (1995). *Work related musculoskeletal disorders (WMSDs): A reference book for prevention*. Bristol, PA: Taylor & Francis.

Halpern, A.A., & Bleck, E.E. (1979). Sit-up exercises: an electromyographic study. *Clinical Orthopaedics and Related Research*, 145, 172-178.

Hansson, T.H., Keller, T.S., & Spengler, D.M. (1987). Mechanical behavior of the human lumbar spine. II. Fatigue strength during dynamic compressive loading. *Journal of Orthopaedic Research*, 5, 479-487.

Hardcastle, P., Annear, P., Foster, D.H., Chakera, T.M., McCormick, C., Khangure, M., & Burnett, A. (1992). Spinal abnormalities in young fast bowlers. *Journal of Bone and Joint Surgery (B)*, 74, 421-425.

Hardy, W.G., Lissner, H.R., Webster, J.E., & Gurdjian, E.S. (1958). Repeated loading tests of the lumbar spine. *Surgical Forum*, 9, 690-695.

Hilkka, R., Mattsson, T., Zitting, A., Wickstrom, G., Hanninen, K., & Waris, P. (1990). Radiographically detectable degenerative changes of lumbar spine among concrete reinforcement workers and house painters. *Spine*, 15, 114-119.

Holm, S., & Nachemson, A. (1983). Variations in the nutrition of the canine intervertebral disc induced by motion. *Spine*, 8, 866-874.

Holmes, A.D., Hukins, D.W.L., & Freemont, A.J. (1993). End-plate displacement during compression of lumbar vertebra-disc-vertebra segments and the mechanism of failure. *Spine*, 18, 128-135.

Hutton, W.C., & Adams, M.A. (1982). Can the lumbar spine be crushed in heavy lifting? *Spine*, 7, 586-590.

Hutton, W.C., Cyron, B.M., & Stott, J.R.R. (1979). The compressive strength of lumbar vertebrae. *Journal of Anatomy*, 129, 753-758.

Jager, M., Luttmann, A., & Laurig, W. (1991). Lumbar load during one-handed bricklaying. *International Journal of Industrial Ergonomics*, 8, 261-277.

Jette, M., Sidney, K., & Cicutti, N. (1984). A critical analysis of sit-ups: a case for the partial curl-ups as a test of muscular endurance. *Can J Phys Ed Rec*, *Sept-Oct*, 4-9.

Jian, Y., Winter, D.A., Ishac, M.G., & Gilchrist, L. (1993). Trajectory of the body COG and COP during initiation and termination of gait. *Gait and Posture*, *1*, 9-22.

Jonsson, B. (1978). Kinesiology: with special reference to electromyographic kinesiology. In W.A. Cobb & H. Duija (Eds.), *Contemporary clinical neurophysiology*. Amsterdam: Elsevier Science Publishers.

Kazarian, L., & Graves, G.A. (1977). Compressive strength characteristics of the human vertebral centrum. *Spine*, *2*, 1-14.

Keegan, J.J. (1953). Alterations of the lumbar curve related to posture and seating. *Journal of Bone and Joint Surgery (Am.)*, *35A*, 589-603.

Keller, T.S., Spengler, D.M., & Hansson, T.H. (1987). Mechanical behavior of the human lumbar spine. I. Creep analysis during static compressive loading. *Journal of Orthopaedic Research*, *5*, 467-478.

Key, J.A., & Ford, L.T. (1948). Experimental intervertebral-disc lesions. *Journal of Bone and Joint Surgery (Am.)*, *30A*, 621-630.

Khoo, B.C.C., Goh, J.C.H., & Bose, K. (1995). A biomechanical model to determine lumbosacral loads during single stance phase in normal gait. *Medical Engineering and Physics*, *17*, 27-35.

Knutsson, B., Kindh, K., & Telhag, H. (1966). Sitting-an electromyographic and mechanical study. *Acta Physiologica Scandinavica*, 37, 415-428.

Koes, B.W., Bouter, L.M., Beckerman, H., van der Heijden, G., & Knipschild, P. (1991). Physiotherapy exercises and back pain: a blinded review. *Brit Med J*, 302, 1572-1576.

Krag, M.H. (1996). Animal models for human disc degeneration. In J. Weinstein & S.L. Gordon (Eds.), *Low Back Pain*. Illinois: AAOS.

Krenz, J., & Troup, J.D.G. (1973). The structure of the pars interarticularis of the lower lumbar vertebrae and its relation to the etiology of spondylolysis. *Journal of Bone and Joint Surgery (B)*, 55-B, 735-741.

Krypton, P., Berleman, U., Visarius, H., Begeman, P. C., Nolte, L. P., and Prasad, P. (1995). Response of the lumbar spine due to shear loading. Detroit: Wayne State University. Proceeding of the Centers for Disease Control on Injury Prevention through Biomechanics.

Kumar, S. (1990). Cumulative load as a risk factor for back pain. *Spine*, 15, 1311-1316.

Kumar, S., Dufresne, R.M., & Van Schoor, T. (1995a). Human trunk strength profile in flexion and extension. *Spine*, 20, 160-168.

Kumar, S., Dufresne, R.M., & Van Schoor, T. (1995b). Human trunk strength profile in lateral flexion and axial rotation. *Spine*, 20, 169-177.

Liu, Y.K., Njus, G., Buckwalter, J.A., & Wakano, K. (1983). Fatigue response of lumbar intervertebral joints under axial cyclic loading. *Spine*, 8, 857-865.

Luoto, S., Heliövaara, M., Hurri, H., & Alaranta, H. (1995). Static back endurance and the risk of low-back pain. *Clinical Biomechanics*, 10, 323-324.

MacIntosh, J.E., & Bogduk, N. (1987). The morphology of the lumbar erector spinae. *Spine*, 12, 658-668.

MacIntosh, J.E., Valencia, F., Bogduk, N., & Munro, R.R. (1986). The morphology of the human lumbar multifidus. *Clinical Biomechanics*, 1, 196-204.

MacKinnon, C.D., & Winter, D.A. (1993). Control of whole body balance in the frontal plane during human walking. *Journal of Biomechanics*, 26, 633-644.

Malmivaara, A., Hakkinen, U., Aro, T., Heinrichs, M., Koskenniemi, L., Kuosma, E., Lappi, S., Palheimo, R., Servo, C., Vaaranen, V., & Hernberg, S. (1995). The treatment of acute low back pain - bed rest, exercises, or ordinary activity? *The New England Journal of Medicine*, 332, 351-355.

Marras, W.S., & Granata, K.P. (1997). Changes in trunk dynamics and spine loading during repeated trunk exertions. *Spine*, 22, 2564-2570.

Marras, W.S., Lavender, S.A., Leurgans, S.E., Rajulu, S.L., Allread, W.G., Fathallah, F.A., & Ferguson, S.A. (1993). The role of dynamic three-dimensional trunk motion in occupationally-related low back disorders: The effect of workplace factors, trunk position, and trunk motion characteristics on risk of injury. *Spine*, *18*, 617-628.

McGill, S.M. (1991). Electromyographic activity of the abdominal and low back musculature during the generation of isometric and dynamic axial trunk torque: implications for lumbar mechanics. *Journal of Orthopaedic Research*, *9*, 91-103.

McGill, S.M. (1992). A myoelectrically based dynamic three-dimensional model to predict loads on lumbar spine tissues during lateral bending. *Journal of Biomechanics*, *25*, 395-414.

McGill, S.M., Juker, D., & Kropf, P. (1996). Appropriately placed surface EMG electrodes reflect deep muscle activity (psoas, quadratus lumborum, abdominal wall) in the lumbar spine. *Journal of Biomechanics*, *29*, 1503-1507.

McGill, S.M., & Norman, R.W. (1985). Dynamically and statically determined low back moments during lifting. *Journal of Biomechanics*, *18*, 877-885.

McGill, S.M., & Norman, R.W. (1986). Partitioning of the L4/L5 dynamic moment into disc, ligamentous, and muscular components during lifting. *Spine*, *11*, 666-677.

McGill, S. M., Norman, R. W., Yingling, V. R., Wells, R. P., and Neumann, P. (1998). Shear happens! Suggested guidelines for ergonomists to reduce the risk of low back injury from shear loading. 30th Annual Conference of the Human Factors Association of Canada.

- McGregor, A.H., McCarthy, I.D., & Hughes, S.P. (1995). Motion characteristics of the lumbar spine in the normal population. *Spine*, 20, 2421-2428.
- McQuade, K.J., Turner, J.A., & Buchner, D.M. (1988). Physical fitness and chronic low back pain: An analysis of the relationships among fitness, functional limitations, and depression. *Clinical Orthopaedics and Related Research*, 233, 198-204.
- Mody, G.M., & Cassim, B. (1997). Rheumatologic manifestations of malignancy. *Curr. Opin. Rheumatol.*, 9, 75-79.
- Moroney, S.P., Schultz, A.B., & Miller, J.A.A. (1988). Analysis and measurement of neck loads. *Journal of Orthopaedic Research*, 6, 713-720.
- Nachemson, A. (1966). The load on the lumbar disks in different positions of the body. *Clinical Orthopaedics*, 45, 107-112.
- Nachemson, A., & Morris, J.M. (1964). In vivo measurements of intradiscal pressure. *Journal of Bone and Joint Surgery (Am.)*, 46A, 1077-1080.
- Nachemson, A.L. (1966). The load on lumbar disks in different positions of the body. *Clinical Orthopaedics and Related Research*, 45, 107-122.
- Nakata, M., Hagner, L.-M., & Jonsson, B. (1992). Perceived musculoskeletal discomfort and electromyography during repetitive light work. *Journal of Electromyography and Kinesiology*, 2, 103-111.

Neumann, P., Norman, R. W., and Wells, R. P. (1995). EMG-based estimates of peak and prolonged exposure of the low back to forces and moments during occupational tasks.

Jyväskylä, Finland: University of Jyväskylä. 670p. XVth Congress of the International Society of Biomechanics.

Newman, P.H. (1963). The etiology of spondylolisthesis. *Journal of Bone and Joint Surgery (B)*, 45-B, 39-59.

Nissan, M., & Gilad, I. (1986). Dimensions of human lumbar vertebrae in the sagittal plane. *Journal of Biomechanics*, 19, 753-758.

Norman, R.W., Wells, R.P., Neumann, P., Frank, J., Shannon, H.S., Kerr, M.S., & Ontario Universities Back Pain Study (OUBPS) Group. (1998). A comparison of peak vs cumulative physical work exposure risk factors for the reporting of low back pain in the automotive industry. *Clinical Biomechanics*, 13, 561-573.

Nutter, P. (1988). Aerobic exercise in the treatment and prevention of low back pain. *State Art Rev Occup Med*, 3, 137-145.

Osti, O.L., Roberts-Vernon, B., & Fraser, R.D. (1990). Anulus tears and intervertebral disc degeneration: An experimental study using an animal model. *Spine*, 15, 762-766.

Osvolder, A.L., Neumann, P., Lovsund, P., & Nordwall, A. (1990). Ultimate strength of the lumbar spine in flexion—an in vitro study. *J.Biomech.*, 23, 453-460.

Oxland, T.R., Panjabi, M.M., Southern, E.P., & Duranceau, J.S. (1991). An anatomic basis for spinal instability: a porcine trauma model. *Journal of Orthopaedic Research*, 9, 452-462.

Panjabi, M.M., Duranceau, J.S., Oxland, T.R., & Bowen, C.E. (1989). Multidirectional instabilities of traumatic cervical spine injuries in a porcine model. *Spine*, 14, 1111-1115.

Panjabi, M.M., Goel, V.K., & Takata, K. (1982). Physiologic strains in the lumbar spinal ligaments: an in vitro biomechanical study. *Spine*, 7, 192-203.

Pearcy, M.J., Portek, I., & Shepherd, J. (1984). Three-dimensional x-ray analysis of normal movement in the lumbar spine. *Spine*, 9, 294-297.

Phillips, P.E. (1997). Viral arthritis. *Curr.Opin.Rheumatol.*, 9, 337-344.

Pope, M.H., Andersson, G.B.J., & Chaffin, D.B. (1991). The workplace. In M.H. Pope, G.B.J. Andersson, J.W. Frymoyer, & D.B. Chaffin (Eds.), *Occupational low back pain: Assessment, treatment and prevention*. (pp. 117-131). St Louis: Mosby Year Book.

Porter, R.W., Adams, M.A., & Hutton, W.C. (1989). Physical activity and strength of the lumbar spine. *Spine*, 14, 201-203.

Potvin, J.R., McGill, S.M., & Norman, R.W. (1991). Trunk muscle and lumbar ligament contributions to dynamic lifts with varying degrees of trunk flexion. *Spine*, 16, 1099-1107.

Potvin, J. R. and Norman, R. W. (1992). Can fatigue compromise lifting safety? Chicago: 513p. Proceedings of the Second North American Congress on Biomechanics.

Punnett, L., Fine, L.J., Keyserling, W.M., Herrin, G.D., & Chaffin, D.B. (1991). Back disorders and nonneutral trunk postures of automobile assembly workers. *Scand J Work Environ Health, 17*, 337-346.

Rossignol, M., Stock, S., Patry, L., & Armstrong, B. (1997). Carpal tunnel syndrome: what is attributable to work? The Montreal study. *Occup. Environ. Med., 54*, 519-523.

Rowe, P.J., & White, M. (1996). Three dimensional, lumbar spinal kinematics during gait, following mild musculo-skeletal low back pain in nurses. *Gait and Posture, 4*, 242-251.

Saal, J.A., & Saal, J.S. (1989). Nonoperative treatment of herniated lumbar intervertebral disc with radiculopathy: An outcome study. *Spine, 14*, 431-437.

Samii, K., Cassinotti, P., de Freudenreich, J., Gallopin, Y., Le Fort, D., & Stalder, H. (1996). Acute bilateral carpal tunnel syndrome associated with human parvovirus B19 infection. *Clin. Infect. Dis., 22*, 162-164.

Sikoryn, T.A., & Hukins, D.W.L. (1990). Mechanism of failure of the ligamentum flavum of the spine during in vitro tensile tests. *Journal of Orthopaedic Research, 8*, 586-591.

Smeathers, J.E. (1984). Some time dependent properties of the intervertebral joint when under compression. *Engineering in Medicine, 13*, 83-87.

Smeathers, J.E., & Joanes, D.N. (1988). Dynamic compressive properties of human lumbar intervertebral joints: A comparison between fresh and thawed specimens. *Journal of Biomechanics, 21*, 425-433.

Smidt, G.L., McQuade, K., Wei, S.-H., & Barakatt, E. (1995). Sacroiliac kinematics for reciprocal straddle positions. *Spine*, 20, 1047-1054.

Smith, J.W., & Walmsley, R. (1951). Experimental incision on the intervertebral disc. *Journal of Bone and Joint Surgery (Am.)*, 33, 612-625.

Stewart, T.D. (1953). The age incidence of neural-arch defects in alaskan natives, considered from the standpoint of etiology. *Journal of Bone and Joint Surgery (Am.)*, 35-A, 937-950.

Sutarno, C.G., & McGill, S.M. (1995). Isovelocity investigation of the lengthening behaviour of the erector spinae muscles. *European Journal of Applied Physiology*, 70, 146-153.

Tanaka, M., Nakahara, S., & Inoue, H. (1993). A pathologic study of discs in the elderly: Separation between the cartilaginous endplate and the vertebral body. *Spine*, 18, 1456-1462.

Thorstensson, A., Carlson, H., Zomlefer, R., & Nilsson, J. (1982). Lumbar back muscle activity in relation to movements during locomotion in man. *Acta Physiologica Scandinavica*, 116, 13-20.

Thorstensson, A., Nilsson, J., Carlson, H., & Zomlefer, R. (1984). Trunk movements in human locomotion. *Acta Physiologica Scandinavica*, 121, 9-22.

Tsai, K.-H., Chang, G.-L., & Lin, R.-M. (1997). Differences in mechanical response between fractured and non-fractured spines under high-speed impact. *Clinical Biomechanics*, 12, 445-451.

Urban, J.P.G., Holm, S., & Maroudas, A. (1978). Diffusion of small solutes into the intervertebral disc: An in vivo study. *Biorheology*, 15, 203-223.

Veiersted, K.B., Westgaard, R.H., & Andersen, P. (1990). Pattern of muscle activity during stereotyped work and its relation to muscle pain. *Int.Arch.Occup.Environ.Health*, 62, 31-41.

Vernon-Roberts, B., & Pirie, C.J. (1973). Healing trabecular microfractures in the bodies of lumbar vertebrae. *Annals of the Rheumatic Diseases*, 32, 406-412.

Videman, T., Nurminen, M., & Troup, J.D.G. (1990). Lumbar spinal pathology in cadaveric material in relation to history of back pain, occupation, and physical loading. *Spine*, 15, 728-740.

Vincent, W.J., & Britten, S.D. (1980). Evaluation of the curl-up - a substitute for the bent knee sit-up. *Journal of Physical Education and Recreation*, February, 74-75.

Walters, C.E., & Partridge, M.J. (1957). Electromyographic study of the differential action of the abdominal muscles during exercise. *American Journal of Physical Medicine*, 36, 259-268.

White, A.A.I., & Panjabi, M.M. (1990). Physical properties and functional biomechanics of the spine. In Anonymous, *Clinical biomechanics of the spine*. (pp. 1-83). Philadelphia: J.B.Lippincott Company.

Whittle, M.W., & Levine, D.F. (1995). Sagittal plane motion of the lumbar spine during normal gait. *Gait and Posture*, 3, 82-82.

Wilder, D.G., & Pope, M.H. (1996). Epidemiological and aetiological aspects of low back pain in vibration environments - an update. *Clinical Biomechanics*, 11, 61-73.

Wilder, D.G., Pope, M.H., & Frymoyer, J.W. (1988). The biomechanics of lumbar disc herniation and the effect of overload and instability. *Journal of Spinal Disorders*, 1, 16-32.

Winter, D.A. (1990). *Biomechanics and motor control of human movement*. Toronto: Wiley and Sons, Inc.

Winter, D.A. (1991). *The biomechanics and motor control of human gait: Normal, elderly and pathological*. Waterloo, ON, CANADA: University of Waterloo Press.

Yeadon, M.R., & Morlock, M. (1989). The appropriate use of regression equations for the estimation of the segmental inertia parameters. *Journal of Biomechanics*, 22, 683-690.

Yingling, V.R., Callaghan, J.P., & McGill, S.M. (1997). Dynamic loading affects the mechanical properties and failure site of porcine spines. *Clinical Biomechanics*, 15, 301-305.

Yingling, V.R., Callaghan, J.P., & McGill, S.M. (1998). The porcine cervical spine a reasonable model of the human lumbar spine: An anatomical, geometrical and functional comparison. *Journal of Spinal Disorders*, Submitted,

Yingling, V.R., & McGill, S.M. (1998). Injuries to the lumbar spine during anterior and posterior shear loading. *Spine*,

Yoganandan, N., Cusick, J.F., Pintar, F.A., Droese, K., & Reinartz, J. (1994). Cyclic compression-flexion loading of the human lumbar spine. *Spine*, *19*, 784-790.

Zdeblick, T.A. (1995). The treatment of degenerative lumbar disorders: A critical review of the literature. *Spine*, *20*, 126-137.